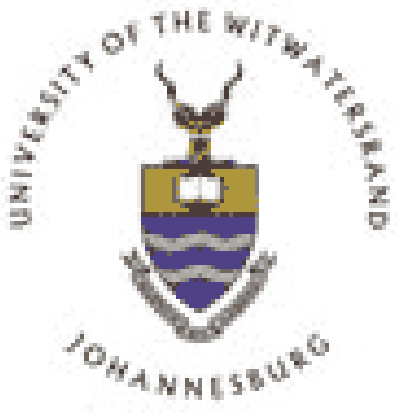

MOLECULAR EVALUATION OF RIBOSOMAL PROTEIN L9 AND LIPOIC ACID SYNTHETASE GENES AND IN LUNG AND APOPTOSIS

RAESIBE PAULINAH MPHAHLELE

A dissertation submitted to the Faculty of Science, University of the Witwatersrand, Johannesburg, South Africa, in fulfillment of the degree of Master of Science.

Johannesburg, South Africa, 2011

DECLARATION

I Raesibe Paulinah Mphahlele, declare that the dissertation "Molecular Evaluation of Ribosomal Protein L9 and Lipoic Acid Synthetase genes in Lung Cancer and Apoptosis" is my own original work and that all the sources that I have used have been indicated by complete references. This dissertation is being submitted in fulfillment for the degree of Master of Science at the University of the Witwatersrand, Johannesburg, South Africa.

_____

Raesibe Paulinah Mphahlele

Date:_____

Meetings

1. Molecular evaluation of Lipoic Acid Synthetase Gene in lung cancer. Raesibe Mphahlele[1], Zodwa Dlamini[2] and Raymond Motadi[3]. University of the Witwatersrand, RSA. **2006 97th Annual American Association for Cancer Research international meeting**, **Washinton DC, USA**.
2. Molecular evaluation of Ribosomal Protein L9 Gene (RPL9) in lung cancer. Zodwa Dlamini, Raesibe Mphahlele. Faculty of Health Sciences, University of the Witwatersrand, RSA. **2006 97th Annual American Association for Cancer Research international meeting, Washinton DC, USA.**
3. Molecular evaluation of Lipoic Acid Synthetase Gene in lung cancer. Raesibe Mphahlele[1], Zodwa Dlamini[2] and Raymond Motadi[3]. University of the Witwatersrand, RSA. **2006 XXth SASBMB Conference, Durban, RSA.**
4. Expression analysis of the Ribosomal Protein L9 (RPL9) in lung tumors. Z. Dlamini. Faculty of Health Sciences, University of the Witwatersrand, RSA. **2006 XXth SASBMB Conference, Durban, RSA.**

ABSTRACT

Background: A human ribosomal protein L9 (RPL9) encodes a protein that is a component of the 60S subunit. RPL9 is located on chromosome 4p14 and is approximately 5.5 kb in length and contains 8 exons. The message for human RPL9 is 712 nucleotides long. Some of the functions of RPL9 documented so far include the crucial involvement of the gene product in cell proliferation and protein biosynthesis. Lipoic acid synthetase (LIAS) is a 1.73 kb gene also located at chromosome 4p14. Alternative splicing occurs at these locus and two transcript variants encoding distinct isoforms have been identified but in this study the results represents both isoforms together. The protein encoded by LIAS gene belongs to the biotin and lipoic acid synthetases family and localizes in the mitochondrion. Function of lipoic acid synthetase is not yet well documented. Some studies have attempted to characterise its function by looking at the biological pathways at which LIAS gene product plays a crucial role, for example the biosynthesis of alpha-lipoic acid. Alpha lipoic acid is a natural antioxidant and it is also naturally-occurring enzyme co-factor found in a number of multi-enzyme complexes regulating oxidative metabolism.

Motivation for study: RPL9 and LIAS were previously found to be mutated in CHO (Chinese Hamster Ovary) cell lines and these mutant lines had gained resistance to apoptosis.

Aim: The main objective of this study was to evaluate the expression pattern of RPL9 and LIAS in lung cancer and to characterise their role in apoptosis and also to determine if the expression pattern of this genes varies between normal and diseased state of the tissue.

Methods: In Situ hybridization, quantitative Real Time PCR, TUNEL and Bio-informatics have been employed in order to attain the objectives of this study.

Results: In Situ hybridization showed that RPL9 localises in the cytoplasm and it is up-regulated in lung cancer relative to normal lung. LIAS localises in the cytoplasm and it is also up-regulated in lung cancer. The expression of RPL9 was relatively higher than that of

LIAS determined by the intensity of localisation. Quantitative real time PCR confirmed the up-regulation of RPL9 and LIAS in lung cancer. RPL9 and LIAS were found to be up-regulated 8 and 4 fold respectively in lung A549 lung adenocarcinoma relative to MRC5 normal lung fibroblast cell lines. TUNEL showed the highest DNA fragmentation in adenocarcinoma, followed by squamous cell lung carcinoma then large cell lung carcinoma which is the same pattern observed in RPL9 and LIAS mRNA localisation by In Situ hybridization.

To further characterise the role of RPL9 and LIAS in human, Bio-informatics tools were used and the results revealed that RPL9 is highly conserved through evolution, up-to 100 % identical to chimpanzee and 98 % to mouse. LIAS was found to be 91 % identical to rat and 90 % identical to mouse. It has been documented that the rate of conservation of a gene in evolution is believed to be correlated with its biological importance and its number of protein–protein interactions.

Conclusion: All these discoveries coupled with resistance to apoptosis of CHO cell line in which RPL9 and LIAS were found to be mutated following promoter-trap mutagenesis, strongly suggests that RPL9 might be playing a role in cell cycle and apoptosis. RPL9 has been highly conserved through evolution. Manipulation of this gene can lead to greater biological discoveries in cancer research and the elevated expression of RPL9 can be used as a molecular marker for early detection of cancer.

DEDICATIONS

I dedicate this work to my daughter Rorisang whom I left when she was very young to pursue this degree and to my mother who utterly stood in and not replaced me but helped raise my child with so much love.

ACKNOWLEDGEMENTS

- My heartfelt admiration and gratitude goes to my supervisors Prof Dlamini and Prof Hosie for encouraging and supporting me throughout the research.

- To Prof D.J.G Rees from the department of Biochemistry, University of the Western Cape for granting the project making this study possible

- To the National Health Laboratory Service, department of Pathology for providing with the tissue sections.

- To Dr. M Ntwasa from the School of Molecular and Cell Biology for the use of the Zeiss microscope camera and AxioCam software.

- To my colleagues for their support and making it such a pleasant time. I am utterly grateful to Raymond Motadi for his support in all my experiments that required cultured cells making this study possible.

- To my family and friends, mainly my mother and my father who stood by me encouraging me to follow my dreams. My sincere gratitude to my two brothers and three sisters who made my daughter's stay at home a warm and fun place to be.

- To the University of the Witwatersrand, National Research Foundation (NRF), Medical Research Council (MRC), University Research Council (URC) for funding provided making this study possible.

TABLE OF CONTENTS

Declaration ii

Meetings iii

Abstract iv

Dedications vi

Acknowledgements vii

Table of contents ix

List of figures xv

Abbreviations xvii

1. Literature Review 1

1.1. Apoptosis 1

1.1.1. Two major apoptosis pathways 2

1.1.1.1. Extrinsic/Death Receptor pathway 2

1.1.1.1.1. Fas signalling pathway 3

1.1.1.1.2. TNFR signalling pathway 5

1.1.1.1.3. TRAIL signalling pathway 5

1.1.1.2. Intrinsic- mitochondria activated- pathway 7

1.1.2. Genetic regulation of apoptosis by tumour suppressor genes 9

1.1.2.1. P53 9

1.1.2.2. Retinoblastoma (Rb) 9

1.2. Cell cycle 12

1.2.1. Regulation of cell cycle 12

1.2.1.1. Cyclin dependent kinases 12

1.3. Cancer 13

1.4. Lung Cancer 15

1.4.1. Pathophysiology 16

1.4.1.1. SCLC 16

1.4.1.2. NSCLC 17

1.4.1.2.1. Squamous Cell Carcinoma 17

1.4.1.2.2. Adenocarcinoma 18

1.4.1.2.3. Large-cell carcinoma 19

1.4.2. Prognosis 19

1.4.3. Aetiology 22

1.4.3.1. Tobacco smoking 22

1.4.3.2. Asbestos 23

1.4.3.3. Genetic alterations 24

1.4.3.3.1. Oncogenes 24

1.4.3.3.1.1. Ras 24

1.4.3.3.1.2. c-Myc 25

1.4.3.3.1.3. EGFR 26

1.4.3.3.2. Tumour suppressor genes 27

1.4.3.3.2.1. P53 27

1.4.3.3.2.2. Retinoblastoma (Rb) protein 28

1.4.3.3.2.3. Tumour suppressor genes at

chromosome region 3p 28

1.4.3.3.3. Apoptosis genes 29

1.4.3.3.3.1. Fas 29

1.4.3.3.3.2. BCL-2 29

1.4.4. Lung cancer and apoptosis 30

1.5. Lipoic Acid Synthetase 31

1.5.1. LIAS and apoptosis 33

1.6. Ribosomal Protein L9 33

1.6.1. RPL9 and apoptosis 34

Main Objective 35

Rationale 35

2. Materials and Methods 36

2.1. Sample collection 36

2.2. Preparation of Competent Cells 36

2.3. In Situ Hybridization 37

2.3.1. RNA isolation 38

2.3.2. Formaldehyde agarose gel electrophoresis 40

2.3.3. Reverse transcription- Polymerase Chain Reaction 41

2.3.4. Primers design and synthesis 42

2.3.5. Polymerase Chain Reaction 43

2.3.6. Agarose gel electrophoresis for DNA 44

2.3.7. Cloning 45

2.3.7.1 Ligation 45

2.3.7.2. Transformation 46

2.3.8. Colony Polymerase Chain Reaction 47

2.3.9. Plasmid DNA extraction 47

2.3.10. Sequencing 49

2.3.11. Linearization of clones 49

2.3.12. Purification of DNA from Agarose Gel 50

2.3.13. Digoxygenin (DIG) Probe Labelling 52

2.3.14. Estimation of probe concentration 54

2.3.15. Procedure for In Situ Hybridization 56

2.3.15.1. Pre-hybridization treatment of sections 56

2.3.15.2. Hybridization 57

2.3.15.3. Post-Hybridization 58

2.3.15.3.1. Colorimetric Detection 58

2.3.15.3.2. Fluorescent Detection 59

2.4. Real Time Polymerase Chain Reaction 60

2.4.1. Optimisation of primers 63

2.4.2. Standard curve generation 64

2.4.3. Relative quantitative Real Time Polymerase Chain Reaction 66

2.5. TUNEL 67

2.5.1. Controls 68

2.6. Bioinformatics 69

2.6.1. Gene Conservation 69

3. Results 70

3.1. Expression of LIAS and RPL9 in human lung cancer 70

3.1.1. In Situ hybridization 70

3.1.1.1. RNA extraction 70

3.1.1.2. Polymerase Chain Reaction 70

3.1.1.3. Cloning of RPL9 and LIAS into p-GEM T Easy 72

3.1.1.4. Colony PCR 72

3.1.1.5. Plasmid DNA extraction and sequencing 73

3.1.1.6. Linearisation of clones and DIG labeling of probes 76

3.1.1.7. Ribosomal Protein L9 and Lipoic Acid Synthetase genes localisation 77

3.2. Real Time Polymerase Chain Reaction 86

3.2.1. Assessment of assay efficiency and optimisation using standard curves 86

3.2.2. Melting curves for RPL9 and LIAS 90

3.2.3. Relative Quantitative Real Time Polymerase reaction of RPL9 and LIAS expression normalised against unit mass 93

3.3. TUNEL 97

3.4. Bioinformatics 100

3.4.1. Gene Conservation 100

3.4.1.1. Lipoic Acid Synthetase CLUSTALW 2.0.3 multiple sequence alignment 100

3.4.1.2. Ribosomal Protein L9 CLUSTALW 2.0.3 multiple sequence alignment 102

3.4.2. Bioinformatics gene Interaction 104

4. Discussion 106

4.1. Lung cancer 106

4.2. In Situ Hybridization 107

4.3. Real Time Polymerase Chain Reaction 108

4.4. Bioinformatics 110

4.5. TUNEL 112

5. Conclusion 114

6. References 116

Appendix 1: Reagents and Solutions 129

LIST OF FIGURES

Figure 1-1. Models for Apoptosis signalling Death Factors

Figure 1-2. Intrinsic apoptotic pathway triggered by p53

Figure 1-3. Activation of p21 by p53 in response to DNA damage

Figure 1-4. Cell cycle arrest by p35

Figure 3-1: Polymerase Chain Reaction

Figure 3-2: Colony Polymerase Chain Reaction

Figure 3-3. Sequence alignment of RPL9 and LIAS genes

Figure 3-4: Plasmid DNA extraction

Figure 3-5: Restriction digestion RPL9 clone

Figure 3-6: Restriction digestion of LIAS clone

Figure 3-7: Localisation of RPL9 mRNA in Squamous Cell Lung Carcinoma

Figure 3-8: Localisation of RPL9 mRNA in Small Cell Lung Carcinoma

Figure 3-9: Localisation of RPL9 mRNA in Large Cell Lung Carcinoma

Figure 3-10: Localisation of RPL9 mRNA in Lung Adenocarcinoma

Figure 3-11: Localisation of LIAS in Squamous Cell Lung Carcinoma

Figure 3-12: Localisation of LIAS mRNA in Lung Adenocarcinoma

Figure 3-13: Localisation of LIAS mRNA in Small Cell Lung Carcinoma

Figure 3-14: RPL9 standard curve to assess the efficiency of the reaction assay.

Figure 3-15: LIAS standard curve generated to assess the efficiency of the reaction assay

Figure 3-16: Annealing temperature optimization and melting curve to analyse the specificity of RPL9 primers

Figure3-17: Annealing temperature optimization and melting curve to analyse the specificity of LIAS primers

Figure 3-18: Quantification curve for LIAS

Figure 3-19: Quantification curve for RPL9

Figure 3-20: Apoptosis detection by TUNEL in lung cancer

Figure 3-21: CLUSTALW 2.0.3 multiple sequence alignment for LIAS

Figure 3-22: CLUSTALW 2.0.3 multiple sequence alignment for RPL9

ABBREVIATIONS

%	- Percent
°C	– Degree Celsius
µ	- micro
aa	- Amino acid
$A_{260/280}$	- Absorbance at 260 nm or 280 nm
A549	– Human Epithelial Cell Lung Carcinoma Cell Line
Acinis	– Apoptotic Chromatin Condensation Inducer in the Nucleus
ADP	– Adenosine Diphosphate
AP	- Alkaline phosphatase
Apaf	– Apoptosis Activating Factor
APO	- Apoptosis-Mediating Surface Antigen Fas
Arg	- Arginine
ATP	– Adenosine Triphosphate
ATPase	- Adenosine Triphosphate
B	- Beta
Bad	– Bcl-2-Antagonist of Cell Death Protein
Bax	– Bcl-Associated X Protein
BCIP	– 5-Bromo-4-Chloro-3-Indolyl Phosphate
Bcl	– B-Cell Lymphoma/Leukaemia
BH	– Bcl-2 Homology
Bid	– Bcl-2-Interacting Domain Death Agonist
bp	– base pair

BSA – Bovine Serum Albumin

$CaCL_2$ – Calcium Chloride

CAD - Caspase-Activated DNase (ADP-Ribose)

CARD - Caspase Recruitment Domain

Caspases – Cysteinyl Aspartate-Specific Proteases

Cdc - Cell Division Cycle

cDNA – complementary Deoxy-ribonucleic Acid

CDK - Cyclin-Dependent Kinase

CDK4 - Cyclin-Dependent Kinase 4

CDKI - Cyclin-Dependent Kinase Inhibitors

cm^3 – Cubis Centimetre

CoA - Coenzyme A

cRNA – complementary – RiboNucleic Acid

C_T – Threshold Cycle

Da – Daltons

dATP - Deoxyadenine Triphosphate

dCTP - Deoxyvytosine Triphosphate

DD – Death Domain

DDT – dithiotretiol

DED – Death Effector Domain

DEPC – Diethyl Pyrocarbonate

DF – Dilution Factor

dGTP - Deoxyguanine Triphosphate

DIG – Digoxigenin

DISC – Death Inducing Signalling Complex

DMEM - Dulbecco's Modified Eagle Media

DNA – Deoxy-ribonucleic Acid

DNase – Deoxyribonuclease

dNTP – Deoxyribonucleotide Triphosphate

DcR – Decoy Receptor

DR – Death Receptor

ds – Double Stranded

dsDNA – double stranded Deoxy-ribonucleic Acid

dTTP - Deoxythymine Triphosphate

dUTP – Deoxyuridine Triphosphate

E – Efficiency

EDTA – Ethylenediamine Tetra Acetic Acid

EGFR – Epidermal Growth Factor Receptor

FADD – Fas-Associated Death Domain

Fas – Fibroblast-Associated

FasL – Fibroblast-Associated Ligand

FITC – Fluorescein Isothiocyanate

Fig – figure

g – Gram

H&E – Haematoxylin and Eosin

H_2O – Water

HCl	– Hydrochloric Acid
H&E	- Haematoxylin and Eosin
Hr	– hour
Hrs	– hours
I	- One
IAP	- Inhibitors of Apoptosis Protein
Ig	- Immunoglobulin
II	- Two
III	- Three
IPTG	– Isopropyl-β-D-Thiogalactopyranoside
IV	- Four
K	- Kappa
k	– Kilo
KAc	- Potassium Acetate
l	– Litre
L	- Litre
LB	– Luria Bertani
LIAS	– Lipoic Acid Synthetase
LiCL	– Lithium Chloride
m	– milli
M	– Molar
mg	- Milligram
$MgCl_2$	– Magnesium Chloride

min – minutes

ml – millilitres

$MnCl_2$ – Manganese Chloride

MOPS - 3-[N-Morpholino] Propane Sulfonic Acid

mRNA – messenger Ribonucleic Acid

NaCl – Sodium Chloride

NADH – Nicotinamide Adenine Dinucleotide Hydrogenase

NaOH - Sodium Hydroxide

NBT – Nitroblue Tetrazolium

NCBI – National Centre for Biomedical Information

NF – Nuclear Factor

nm - Nanometre

p53 - Tumour suppressor protein 53

PBS – Phosphate Buffer Saline

PCR – Polymerase Chain Reaction

PFA – Paraformaldehyde

pH - Hydrogen Ion Concentration

qRT-PCR – quantitative Real Time Polymerase Chain Reaction

Raf - Riboflacin-Aldehyde Forming Enzyme

Rb – Retinoblastoma

RNA – Ribonucleic Acid

RNase – Ribonuclease

RPL9 – Ribosomal Protein L9

RPM – Revolutions per Minute

RT – Room Temperature

RT-PCR – Real Time Polymerase Chain Reaction

S - Second

S - DNA Synthesis Phase

SDS - Sodium Dodecyl Sulphate

sdH_2O – Sterile Distilled Water

SSC – Sodium Chloride and Sodium Citrate

TBE – Tris-Borate/EDTA

TBS – Tris Buffer Saline

TE – Tris-HCL/EDTA

Tm – Melting Temperature

TNB – Tri-Sodium Blocking

TNF – Tumour Necrosis Factor

TNFR – TNF Receptor

TRADD – TNFR-I-Associated Death Domain

TRAIL – TNF-Related Apoptosis Inducing Ligand

Tris – Tris (Hydroxymethyl) Aminomethane

Tween 20 – Polyethylene Sorbitan Monolaurat

TYM – Trptone Yeast Extract $MgCL_2$

UV – Ultra Violet

VEGF - Vascular Endothelial Growth Factor

v/v - Volume/Volume

WHO – World Health Organisation

w/v - Weight/Volume

α – Alpha

β – Beta

1. Literature Review

1.1. Apoptosis

For every cell there is time to live and time to die. There are two major mechanisms by which cells die, apoptosis and necrosis (Kroemer, et al., 2009). In necrosis cell death is uncontrollable and lead to lysis of cells, inflammatory responses and detrimental health problems. Contrary to necrosis, apoptosis is a genetically controlled mechanism essential for the maintenance of tissue homeostasis, proper development and the elimination of unwanted cells by allowing a cell to self-degrade hence is also called programmed cell death. Apoptosis is shown to occur in a predictable manner during development and also to serve as a major mechanism for removal of unwanted and potentially dangerous cells such as virus-infected cells, self-reactive lymphocytes, tumour cells, aged cells and cells with DNA damage that cannot be repaired (Lockshin and Zakeri, 2001).

Upon receiving specific stimuli instructing the cell to undergo apoptosis, a number of morphological and biochemical changes occur in the cell, including cell shrinkage, chromatin condensation, nuclear fragmentation, membrane blebbing and loss of adhesion (Kroemer *et al.*, 2009; Kerr *et al*., 1972). A family of proteins known as caspases are activated in early stages of apoptosis. These proteins cleave key cellular substrates that are required for normal cellular functioning such as structural proteins and nuclear proteins. The caspases can also activate other degradative enzymes such as DNases, which begin to cleave DNA in the nucleus. The result of these biochemical changes is appearance of morphological changes in the cell. Typically cytoplasm begins to shrink. Nuclear condense following the breakdown of chromatin and nuclear structural proteins.

Cells continue to shrink, packaging themselves in a form that allows for recognition and clearance by macrophages. (Baehrecke, 2002; Martin *et al*., 1995).

1.1.1. Two major apoptosis pathways

Although cell death can be triggered by vast array of stimuli, the manner by which all apoptotic signals engage the cell death machinery falls under two broad categories, one beginning at the level of cell surface, death receptor (the extrinsic pathway), the other is mediated by mitochondrial (the intrinsic pathway) (Kiechle and Zhang, 2002).

1.1.1.1. Extrinsic/Death Receptor pathway

In the death receptor pathway, apoptosis induction involves the engagement of a set of ligands and their corresponding receptors and then transmission of the apoptotic signal in the cytoplasm by a number of caspases (Yusuke *et al.,* 2010). There are a number of ligand-receptor systems and target caspases involved in apoptosis. These death-inducing receptors belong to the tumour necrosis factor (TNF) superfamily. The most well characterised death receptors are Fas, TNF-R1, TRAIL-R1 and TRAIL-R2 receptors, all of which are characterised by a cysteine-rich extracellular "death domain" (Ashkenazi and Dixit, 2008). The ligands that activate these receptors are structurally related molecules that belong to the TNF genes superfamily; fas ligand (FasL) bind to Fas, TNFα and lymphotoxinα bind to TNF-R1 and TRAIL bind to TRAIL-R1 and TRAIL-R2 (Igney and Krammer, 2002; Debatin and Krammer, 2004).

When a ligand binds to the death receptor, the receptor becomes trimerised and activated. The activated receptor recruits a death domain containing adaptor and a pro-caspase 8 molecule through protein-protein interaction to form a death inducing signalling complex (DISC). Fas associated death domain (FADD) is directly recruited into the DISC during Fas-mediated apoptosis, while TNF-induced apoptosis involves both FADD and TRADD (TNF Receptor-Associated Death Domain) (Kischkel, *et al.,* 2000). Recruitment of pro-caspase 8 to the DISC activates caspase 8 by oligomerisation-induced autocatalytic processing which results in activation of downstream caspases, such as caspase 3, 6 and 7, and induction of apoptosis (Ashkenazi and Dixit, 1998; Ashkenazi and Dixit, 2008).

1.1.1.1.1. Fas signalling pathway

Fas, a cell surface receptor plays a crucial role in apoptosis signalling in many cell types. Fas is expressed on the surface of cell membranes in a variety of normal tissue cells and malignant cells including lung cancer cells whereas the expression of FasL is restricted to the cells within the immune system, such as activated T cells and natural killer cells. Fas is ubiquitously expressed in various tissues with abundant expression in the thymus, liver, heart and kidney. Fas is also predominantly expressed in activated T lymphocytes and natural killer cells (Kitaura *et al.,* 2002). This receptor interacts with its natural ligand (FasL), a member of the tumour necrosis factor superfamily, to initiates the death signal cascades which results in apoptotic cell death. Upon FasL binding, juxtaposition of the Death Domain (DD) allows interaction with the DD containing adaptor protein FADD. FADD is a 26 kDa cytoplasmic protein that contain a C-terminal DD and a homologous Death Effector Domain (DED). Fas ligation results in DISC assembly commencing

within minutes of ligand binding and localizing initially FADD and then caspase 8 to the receptor complex. Caspase 8 has two C-terminal DED that display homology to and can interact with DED of FADD (Kischkel *et al*., 2000). Caspase 8 is produced as a zymogen, activated first by removal of a pro-domain then by limited cleavage at an aspartate residue to separate the large 20 kDa active protease subunit from the smaller 10 kDa subunit. This caspase can process downstream pro-caspases as well as its own procaspase precursor. Caspase activation proceeds in a hierarchical manner until activation of the executor caspases such as caspase 3, 6 and 7, result in apoptosis. The effector caspases are responsible for proteolytic cleavage of various cellular substances leading to the distinctive DNA fragmentation that marks apoptosis (Salvesen and Dixit, 1999).

Reduced expression of Fas and/or increased expression of FasL have been detected in many types of human cancers including lung cancer and appear to be a feature of malignant phenotype suggesting that the Fas/FasL system play an important role in cancer formation. There is strong evidence demonstrating that decreased expression of Fas may protect transformed cells from elimination by anti-tumour immune response, but elevated expression of FasL may increase the ability of tumour cells to counterattack the immune system by killing Fas sensitive lymphocytes and therefore contribute to cancer development. Since FasL expressed on T-lymphocytes can induce apoptosis in Fas-expressing lung cancer cells, the Fas/FasL system plays an important role in the cell-mediated cytotoxic reactions against lung cancer. Commonly used chemotherapy drugs have been shown to induce Fas expression on lung cancer cells and apoptosis of lung cancer cells (Volm and Rittgen, 2000).

1.1.1.1.2. TNFR signalling pathway

In contrast to Fas, TNF-R1 only signals for cell death in certain circumstances, for example, when protein synthesis is blocked. In most scenarios, TNF-R1 instead induces the transcription and activation of inflammatory genes suggesting that TNF-R1 signalling provides a mechanism to suppress the apoptotic stimulus (Kischkel, *et al.,* 2000).

1.1.1.1.3. TRAIL signalling pathway

Tumour necrosis factor-related apoptosis-inducing ligand (TRAIL) is a potential anticancer drug that promotes apoptosis specifically in tumour cells. TRAIL seems to induce apoptosis only in cancer cells and not in normal tissue and this includes lung cancer cells (Yanase *et al.,* 2005; Ashkenazi *et al.,* 1999). TRAIL triggers apoptosis through interaction with death receptor DR4 and DR5. In contrast to other members of TNF superfamily, TRAIL is expressed constitutively in many tissues which suggest the existence of physiological mechanism that can protect many normal cell types from induction of apoptosis specifically by TRAIL. One of such mechanism may involve expression of antagonistic decoy receptors that can compete with TRAIL-R1 (DR4) and TRAIL-R2 (DR5) for ligand binding; TRAIL binds with 3 such decoys: TRAIL-R3 (DcR1), TRAIL-R4 (DcR2) and TRAIL-R5 (osteoprotegerin) (Yusuke *et al.,* 2010; Ashkenazi *et al.,* 1999).

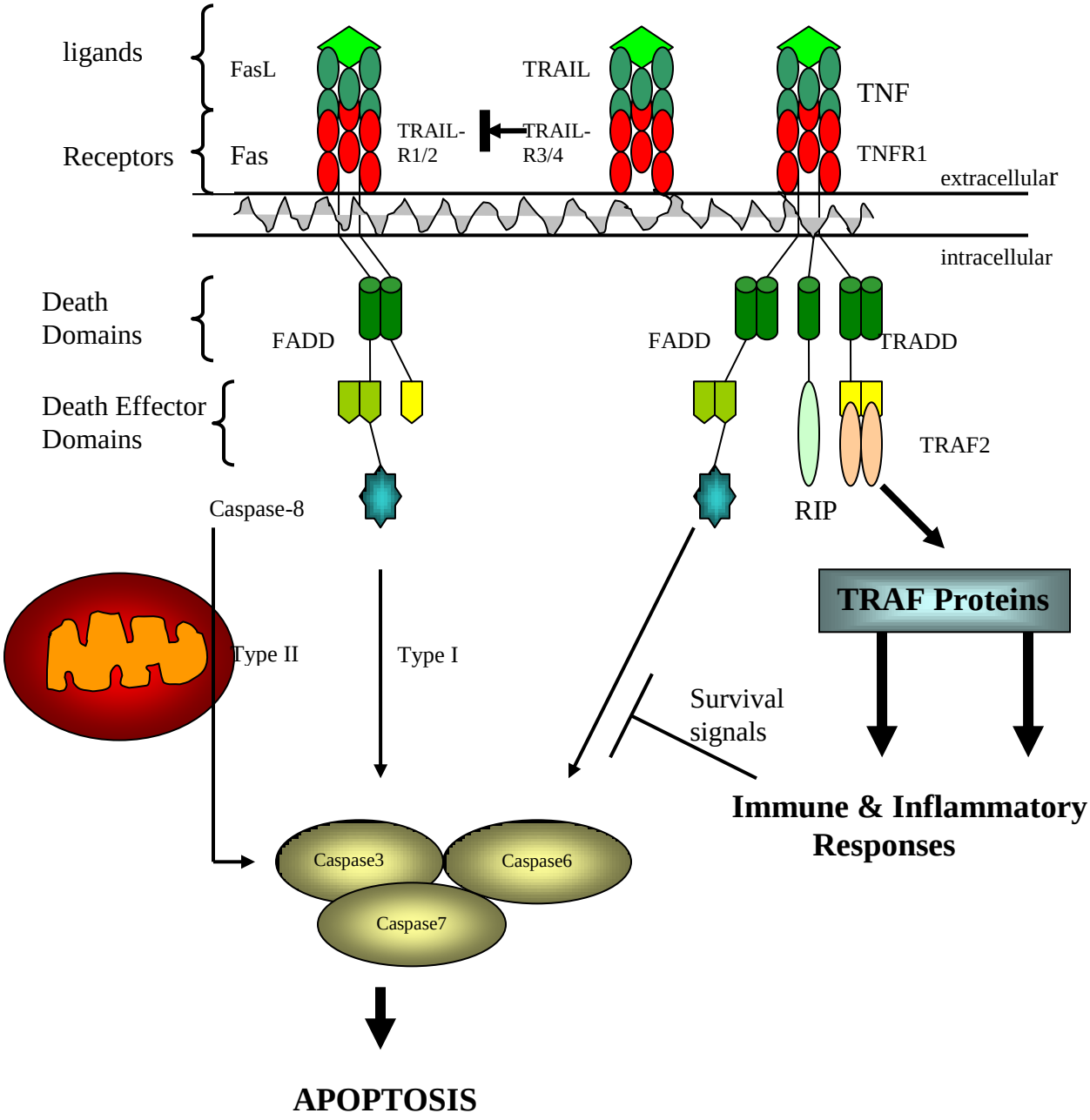

Figure 1-1. Models for Apoptosis signalling Death Factors. Binding of FasL to Fas induces trimerisation of Fas receptor, which recruits caspase-8 via FADD adaptor. Trimerised TNFR1 due to TNF binding recruits TRADD, which then recruits FADD in one pathway to activate caspase-8. In another pathway, RIP binds to TRADD and transduces an apoptotic signal through the death domain.

1.1.1.2. Intrinsic- mitochondria activated- pathway

The intrinsic cell death pathway is initiated as a response to multiple stress signals and depends on alterations involving the mitochondria ultimately leading to mitochondrial dysfunction. The Bcl-2 family members play a vital role in intrinsic pathway. The Bcl-2 family of proteins contains both the pro- and anti-apoptotic molecules and the ratio between two subsets help determine the susceptibility of a cell signal (Vo and Letai, 2010). Bcl-2 family members possess up to four conserved Bcl-2 homology (BH) domains designated BH1, BH2, BH3 and BH4. Many of the anti-apoptotic members display sequences conserved in all four domains while the pro-apoptotic members display less sequence conservation of the BH4 domain. Pro- and anti-apoptotic Bcl-2 members localise to separate subcellular compartments in the absence of a death signal. Anti-apoptotic members are intergral membrane proteins found in the mitochondria, endoplasmic reticulum or nuclear membrane (Hockenbery 2010; Hsu *et al.*, 1997).

Triggering of mitochondrial cell death pathway results in release of pro-apoptotic proteins from the mitochondrial intermembrane space into the cytosol. Signals from the internal sensors are propagated to the mitochondria via pro-apoptotic Bcl-2 subfamily members (BH3 only), such as Bid, to oligomerize Bax and Bak, which are outer mitochondrial membrane proteins that promote the release of cytochrome c. Cytochrome c oligomerizes Apaf1 and recruits pro-caspase-9 (forming the apoptosome), which results in proteolytic conversion of pro-caspase-9 to an active enzyme. Caspase-9 then converts pro-caspase-3 to its active form, which, with other executioner caspases, such as caspase-7 stimulate the apoptotic signal pathway (Saelens et al., 2004; Gross *et al.*, 1998).

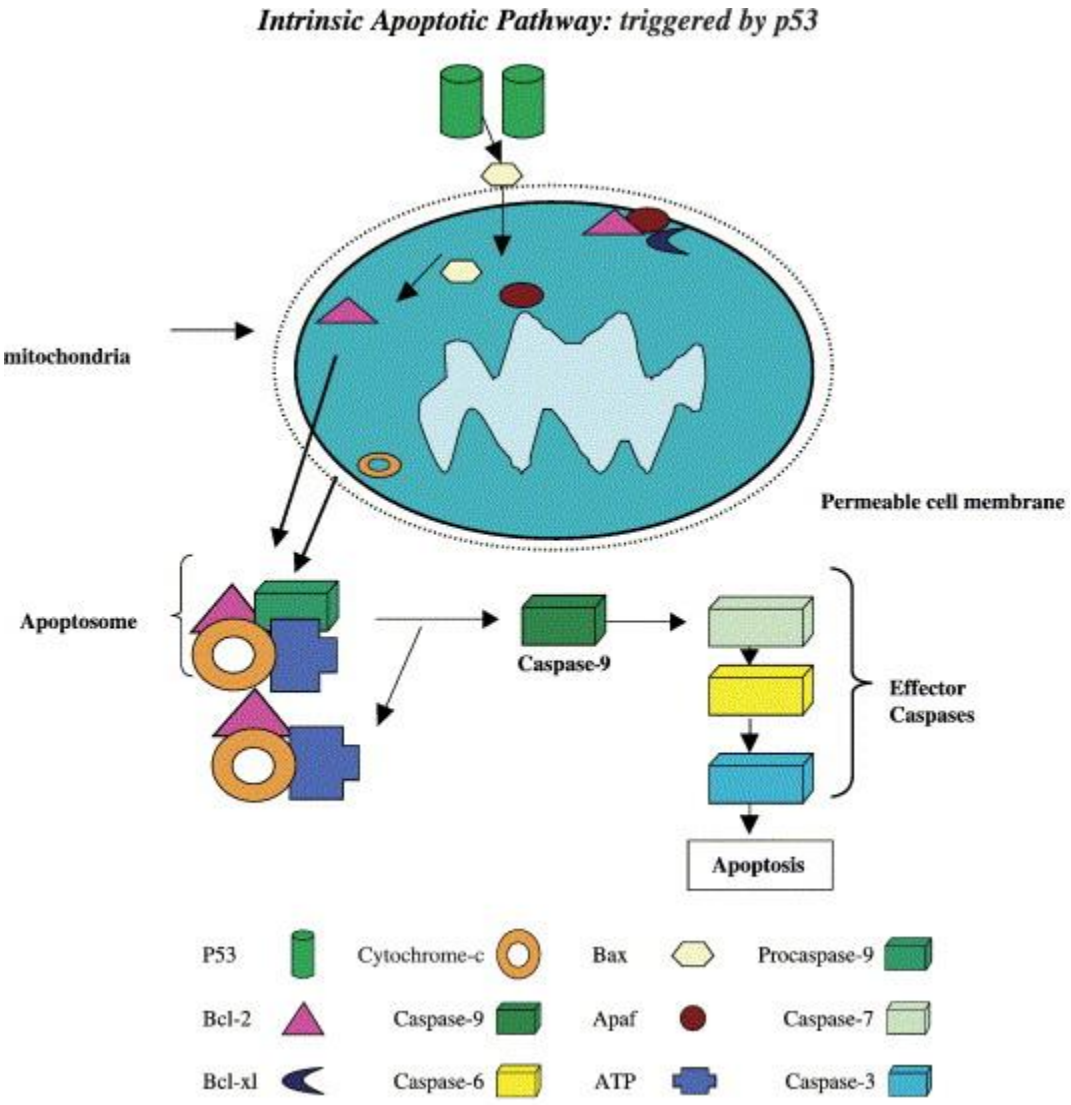

Figure 1-2. Intrinsic apoptotic pathway triggered by p53. The intrinsic apoptotic pathway is initiated by internal sensors such as p53 that monitor cellular stresses such as viral infection via activation of BH3 domain−only members of the Bcl-2 family. Activated BH3-only proteins are thought to mediate the assembly of pro-apoptotic members of the Bcl-2 family resulting in the release of factors such as cytochrome c which after entry into the cytosol stimulates the formation of a complex called apoptosome, leading to caspase-9 activity ant then resulting stimulation of apoptotic signal pathway (McCabe and Dlamini, 2005).

1.1.2. Genetic regulation of apoptosis by tumour suppressor genes

1.1.2.1. P53

P53 is a tumour suppressor gene which monitors stress and directs the cell towards an appropriate response. Upon activation, p53 induces either G1 cell cycle arrest or apoptosis. For these reason, p53 is called "the guardian of the genome" (Levie, 1997; Rusan and Peifer, 2008, Tommasi *et al.*, 2008). The p53 protein prevents a cell from completing the cell cycle if its DNA is damaged or the cell has suffered other types of damage. It does this by binding to a transcriptional factor called E2F. This prevents E2F from binding to the promoters of proto-oncogenes such as c-fos. Transcription c-fos is needed for mitosis, so blocking the transcription factor needed to turn on these genes prevents cell division. If the damage is minor, p53 halts the cell cycle hence cell division until the damage is repaired. If the damage is major and cannot be repaired, p53 triggers the cell to commit suicide by apoptosis as illustrated in Fig 1-3.

P53 also prevent a cell from completing the cycle in response to DNA damage by inducing expression of a series of cdk inhibitors, p21, p27, and p57 which function to maintain retinoblastoma protein (Rb) in its unphosphorylated state even in the face of mitogenic stimulation. This control is released once the cell has effectively repaired its damaged DNA (Colman *et al.*, 2000)

1.1.2.2. Retinoblastoma (Rb)

Retinoblastoma protein was the first protein to be identified as a tumour suppressor in humans in a study that demonstrated that loss of function of the protein leads to retinoblastoma in children (Friend *et al.*, 1986). Additionally pRb's functional loss has

also been implicated in other malignancies such as ovarian cancer (Armes *et al.*, 2005, Li *et al.*, 2007d, Masamha and Benbrook, 2009), head and neck squamous cell carcinoma (Golam Sabbir *et al.*, 2006) and soft-tissue sarcoma (Polsky *et al.*, 2006, Pereira *et al.*, 2009). These suggest that pRb loss plays a pivotal role in cancer progression.

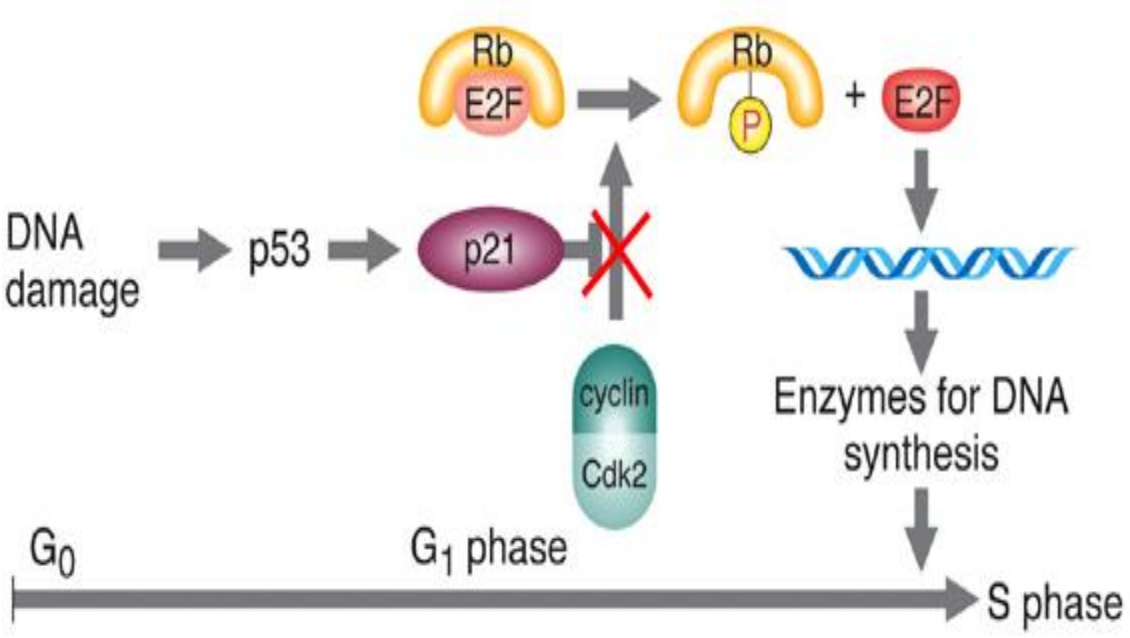

Figure 1-3. Activation of p21 by p53 in response to DNA damage. In response to DNA damage, p53 activate p21 to inhibit the release of transcription factor E2F from Rb by cyclin/cdk2. This stops the expression of enzymes essential for DNA replication and thus halt the cell from continuing with cell cycle. This allows time for DNA to be repaired and failure to repair DNA will lead to cell death by apoptosis triggered by p53. http://www.nature.com/nrc/journal/v6/n1/full/nrc1780.html

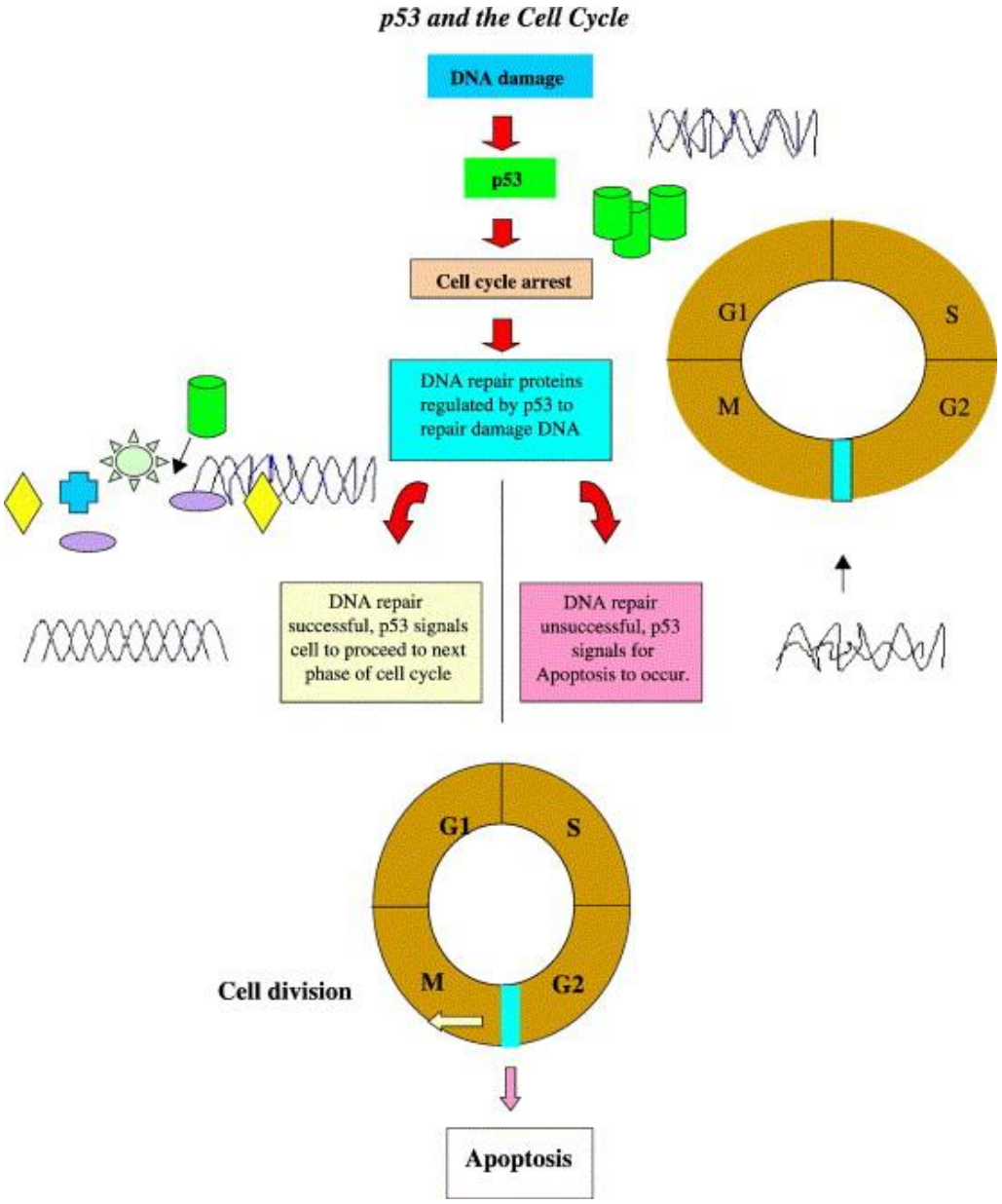

Figure 1-4. Cell cycle arrest by p35. P53 induce cell cycle arrest to allow time for DNA to be repaired. If the damage is too severe and cannot be repaired, then p53 triggers cell death by apoptosis. (McCabe and Dlamini, 2005)

1.2. Cell cycle

The cell cycle is the set of events that are responsible for duplication of the cell. Eukaryotic cell cycle consists of the two most important phases, S-phase and the M-phase. At S-phase, DNA is replicated and proteins are synthesized. During this stage every double-helical DNA molecule is duplicated, making two strands of DNA that are exactly identical. At the M-phase the replicated material is segregated into two daughter nuclei. Between S and M phase there are two gaps, G1 prior to S-phase and G2 prior to M-phase. G1 is the growth phase of the cell and preparation of chromosomes for replication occur at these phase. G2 is the preparation phase for mitosis. Following M-phase is the cytokinesis phase.The actual cell division takes place in the cytokinesis and is the phase when the physical division of the cell's cytoplasm into two daughter cells takes place. Each daughter cell receives about half the contents of the original cell including one copy of the DNA (Nurse, 1994; Manuel and Sergio, 1997).

1.2.1. Regulation of cell cycle

1.2.1.1. Cyclin dependent kinases

To allow for normal growth and development, the passage of the cell through the cell cycle is regulated by highly coordinated and tightly controlled checkpoints at G1/S transition and G2/M transition. These processes make use of cytoplasmic proteins. Among the main players are cyclins and cyclin-dependent kinases (Cdk). Cyclins include a G1-phase cyclin (cyclin D), S-phase cyclin (cyclin E and D) and mitotic cyclins (cyclin A and B). In animal cell at least eight (cdk1-cdk8) cyclin dependent kinases have been discovered although only M-phase cdk1, G1 cdk4 and cdk6, and S-phase cdk2 play a role

in cell cycle regulation. (Nigg, 1995). Cdk levels in the cell remain fairly stable, but each must bind the appropriate cyclin, whose levels fluctuate with the stages of the cell, in order to be activated. A cyclin joins with an appropriate cdk to form a complex. If for some reason the cell detects some problem with a continuation of a cycle, the activation of a cyclin-cdk complex is not completed. If no defect is detected, the cyclin-cdk complex is activated by phosphorylation and these lead to the activation of a transcription factor by the removal of an inhibitor of the transcription factor. The transcription factor then turns on the transcription of specific genes necessary for the next cell cycle step (Manuel and Sergio, 1997).

1.3. Cancer

Cell cycle is strictly regulated by mechanisms described previously in order to maintain the tissue homeostasis. Failure of these regulatory mechanisms can lead to uncontrolled proliferation of cells leading to formation of tumours. Tumours can either be non-cancerous (benign) or cancerous (malignant). Benign tumours may grow causing discomfort due to bleeding, but they do not spread to other parts of the body and generally are not life threatening. Malignant tumours spread into other areas of the body and destroy normal tissue. This uncontrolled proliferation of cells that tend to invade surrounding tissues and metastasize to other organs is termed cancer (De Stefani *et al*., 2005).

A number of factors are involved in cancer development, among them is age, carcinogens, genetic make-up and day-to-day environment. These factors lead to accumulation of genetic mutations that cause cells to be non-responsive to the regulatory

mechanisms. This includes: point mutations which cause amino acid substitutions, frame-shift mutations or mutations to stop codons which either trunscate or scramble it's sequence. These mutations have two distinctive consequences, they allow the inappropriate expression or activation of genes, or conversely, they result in the functional activation of the gene or its protein product.

Mutations with two basic functions are selected by cells developing cancer, mutations which increase the activity of a certain protein they code for; this class of genes are called oncogenes, or mutations which inactivate gene function in the case of genes classed as tumour suppressor genes. Oncogenes are involved in signalling pathways which stimulate proliferation, while most tumour suppressor genes code for proteins which normally act as checkpoints to cell proliferation or cell death (Ames *et al.,* 1993; Armes *et al.*, 2005).

Chemical damage to DNA itself is not mutagenic, it requires proliferation. DNA replication and subsequent cell division is necessary to convert chemical damage to an inheritable change in DNA, which is defined or referred to as mutation (Ames *et al.*, 1993). To most effectively reduce the probability of mutations, the genome should be damage free before the onset of replication. To achieve this and to also ensure that a cell has all the nutritional support required for the synthesis of the new DNA strands, mammalian cells have devised elaborate checkpoints to prevent premature entry into the division cycle.

1.4. Lung Cancer

Lung cancer is the global most important leading cause of cancer deaths (Wingo *et al.*, 1995) with wide geographic variations in risk. Tobacco smoking is the main cause of lung cancer with a positive linear relationship between the probability of getting the cancer and dose-response relationship (years and amount smoked). Lung cancer has a lower incidence than other types of cancers (breast, colon, prostate and cervical) but it is more lethal with a 5 year survival of less than 10% (Parkin *et al.*, 2005). Like all cells of the body, lungs cells divide and reproduce at a controlled rate to repair worn-out or injured tissues and allow for normal growth. Lung cancer develops when cells inside the lungs multiply at an uncontrollable rate. As cancer cells break away from the primary (original) tumour in the lung and spread through the blood and lymph systems, they form secondary (metastatic) tumours. Lung cancer can spread to any organ in the body, e.g. brain, liver, etc. Most often secondary tumours will develop in the brain, bone, liver and bone marrow. Secondary tumours are referred to as metastatic lung cancer rather than brain or liver cancer to indicate that they are part of a single disease originating in the lungs and are not new cancers starting in these organs (De Stefani *et al*. 2005). Since previously more men than women were smoking, lung cancer used to be more prevalent in men than in women. But because currently just as many women as men are smoking, incidence of lung cancer in women is just as high as in men. This is due to the fact that, though there are other risk factors associated with the development of lung cancer, smoking is the major aetiological factor.

1.4.1. Pathophysiology

Lung cancers are divided into two major groups, which make up more than 90% of all lung cancer cases; small cell lung cancer (SCLC) and non-small cell lung cancer (NSCLC). SCLC as opposed to NSCLC is characterized by relatively high sensitivity to treatment with anticancer drugs and irradiation. The way non-small cell lung cancer spreads and its treatment is very different from that of small cell lung cancer. Sometimes a lung tumour contains more than one type of cancerous cell. Because of the different types of lung cancers and different ways they may respond to treatment, it is very important to identify the cell types so that the best treatment can be given. In addition to the two main types of lung cancer, other tumours can occur in the lung. Some of these are non-cancerous (benign). Most are slow-growing tumours that are called typical carcinoid tumours. They are generally cured by surgery. Although some typical carcinoid tumours can spread, they usually have a better prognosis than small cell or non-small cell lung cancer (Franklin, 2000).

1.4.1.1. SCLC

SCLC makes up about 20% to 25% of all lung cancer cases. The identified cells include oat cell, intermediate cell (cells which have many sides and are spindle shaped) and combined cell (small cell combined with other types of cancer). Small cell lung cancer is most often found in the bronchial submucosa and is more likely to have spread at the time of diagnosis than other types of lung cancer. Small cell lung cancer is separated from other cell types due to its rapid growth rate. Symptoms are of brief duration prior to diagnosis (Friedman *et al.*, 1965)

1.4.1.2. NSCLC

NSCLC is a heterogeneous aggregate of at least 3 distinct histologies of lung cancer including squamous carcinoma, adenocarcinoma, and large cell carcinoma. These histologies are often classified together because, when localized, all have the potential for cure with surgical resection. Systemic chemotherapy can produce objective partial responses and palliation of symptoms for short durations in patients with advanced disease. Local control can be achieved with radiation in a large number of patients with unresectable disease, but cure is seen only in a small minority of patients. At diagnosis, patients with NSCLC can be divided into 3 groups that reflect the extent of disease and treatment approach. The first group of patients has tumours that are surgically resectable. This is the group with the best prognosis, depending on a variety of tumour and host factors. Patients with resectable disease who have medical contraindications to surgery can be considered for curative radiation therapy. The second group includes patients with either locally or regionally advanced lung cancer who have a diverse natural history. This group is treated with radiation therapy or, more commonly, with radiation therapy in combination with chemotherapy or other therapy modalities. The final group of patients have distant metastases found at the time of diagnosis. This group can be treated with radiation therapy or chemotherapy for palliation of symptoms from the primary tumour (Albain *et al*, 1991).

1.4.1.2.1. Squamous Cell Carcinoma

Squamous cell carcinoma accounts for over 30% of lung cancers. Squamous cell carcinoma usually starts in the large bronchi and very often stays in the chest, without

spreading for longer periods of time than other types of lung cancer. Because of its central location and the tendency of these cells to exfoliate, squamous cell carcinoma can be detected on cytologic examination at an early stage. With time these tumours tend to cause bronchial obstruction and atelectasis or pneumonia. They also tend to remain localised. Of all the subtypes of NSCLC, the sguamous cell lung carcinoma has the strongest association with smoking. Pathologically, it is characterised by visible keratinisation with prominent desmosomes and intercellular bridges. Increased secretion of a parathyroid-like hormone in squamous cell lung carcinoma has led to this subtype's association with hypercalcemia (Ihde, 1991)

1.4.1.2.2. Adenocarcinoma

Adenocarcinomas is the most common form of cancer worldwide accounting for 35% of all lung cancers and have cube or column-shaped cells. These tumours are often found along the outer edges of the lungs and under the lining of the bronchi. New studies are under way to examine reasons for the increase in the rate of adenocarcinoma (Franklin, 2000). The increased rate of adenocarcinoma could be associated with increased smoking incidences because the tumours often originate from scars that contain entrapped bronchial epithelium which are mostly caused by smoking. Even with smoking cessation, the risk remains elevated because the injury incurred in the airways cannot be reversed (Damjanov, 1996)

1.4.1.2.3. Large-cell carcinoma

This type of cancer accounts for about 10% - 15% of lung cancers. It may appear in any part of the lung, and it tends to grow and spread quickly resulting in a poor prognosis. Where a poorly differentiated tumour has none of the defining features of small cell lung carcinoma, squamous cell lung carcinoma or adenocarcinoma, it may be classified as large cell lung carcinoma: that is, where the cells of the lesion are not-columnar in shape, do not contain mucous, do not show squamous differentiation, and do not have neuroendocrine properties or small cell characteristics. Tumours tend to consist of large cells with abundant cytoplasm, large nuclei and prominent nucleoli and they may occur peripherally or centrally. Variants of large cell carcinoma include clear cell carcinoma, giant cell carcinoma and large cell neuroendocrine carcinoma (Ihde, 1991)

1.4.2. Prognosis

The most important prognosis factor in lung cancer is the stage of the disease. Determination of stage has important therapeutic and prognosis implications, hence careful initial diagnostic evaluation to define location and extent of primary and metastatic tumour involvement is critical for the appropriate care for the patient. The TNM staging system for lung cancer has been developed and it is important as it provides a consistent reproducible description of the extent of anatomic involvement, consistency in patient treatments and it provides the basis of epidemiological and biological studies. This is achieved by defining the characteristics of primary tumour (T), regional lymph node involvement (N), and metastasis (M) (Table 1.1) (Mountain, 1997; Omar *et al.*, 1999).

TABLE 1.1: TNM staging of lung cancer

Primary tumour (T)

Tx Tumour proven by the presence of malignant cells in brochopulmonary secretions but not visualised roentgenographically or bronchoscopically or any tumour that cannot be assessed, as in pre-treatment staging

T0 No evidence of primary tumour

Tis Carcinoma in situ

T1 Tumour ≤ 3.0 cm in greatest dimension, surrounded by lung or visceral pleura, and without evidence of invasion to a lobar bronchus at bronchoscopy

T2 Tumour > 3.0 cm in greatest dimension or tumour of any size that either invades the visceral pleura or has associated atelectasis or obstructive pneumonitis extending to the hilar region (but involving less than the entire lung). At bronchoscopy, the proximal extend of demonstrate tumour must be within a lobar bronchus or at least 2.0 cm distal to the carina.

T3 Tumour of any size with a direct extension into the chest wall (including superior sulcus tumours), diaphragm or mediastinal pleura or pericardium without involving the heart, great vessels, trachea, oesophagus, or vertebral body; or tumour in the bronchus within 2 cm of, but not involving the carina.

T4 Tumour of any size with invasion of the mediastinum or involving the heart, great vessels, trachea, oesophagus, vertebral body, or carina; or presence of

malignant pleural effusion.

Regional lymph nodes (N)

Nx	Regional lymph nodes cannot be assessed
N0	No demonstrable metastasis to regional lymph nodes
N1	Metastasis to lymph nodes in the epibronchial and/or ipsilateral hilar region, including direct extension.
N2	Metastasis to ipsilateral mediastinal and subcarinal lymph nodes.
N3	Metastasis to contralateral mediastinal, contralateral hilar, ipsilateral or contralateral scalene, or supraclavicular lymph nodes

---

Distant metastasis (M)

Mx	Distant metastasis cannot be assessed
M0	No distant metastasis
M1	Distant metastasis

Stage grouping

Occult carcinoma	Tx	N0	M0
Stage 0	Tis	N0	M0
Stage 1A	T1	N0	M0
Stage 1B	T2	N0	M0
Stage IIA	T1	N1	M0

Stage IIB	T2	N1	M0
	T3	N0	M0
Stage IIIA	T3	N1	M0
	T1-3	N2	M0
Stage IIIB	Any T	N3	M0
	T4	Any N	M0
Stage IV	Any T	Any N	M1

Omar *et al.,* 1999

1.4.3. Aetiology

Lung cancer has a multifactorial aetiology and is a complex multi-step process. epidemic of lung cancer is directly attributed to cigarette smoking and there needs to be major efforts to prevent initiation and aid with cessation of smoking. Recently it has been clear that smoking leads to persistent genetic damage of the respiratory tract which implicates smoking as a core risk factor for the development of lung cancer (Wynder and Graham, 1950)

1.4.3.1. Tobacco smoking

There has been overwhelming evidence that the epidemic of lung cancer is directly attributable to tobacco smoking (Doll and Hill, 1950; Wynder and Graham, 1950). Experimental studies have shown that painting of rabbit skin with cigarette tar induced

cancers, and some of the carcinogens present in tobacco smoke had been identified (Doll, 1998)

Tobacco smoking is a major risk factor of lung cancer with a contribution of 80-85% of lung cancer cases. Approximately one in ten lifetime smokers develop lung cancer suggesting individual differences in susceptibly to tobacco smoke. Genetic susceptibility to lung cancer may in part be determined by inter-individual variations in the genetic factors associated with cigarette smoking. Molecular biology has led growing interest in investigation of biological markers, which may increase/decrease predisposition to smoking–related carcinogenesis. Genetic differences are known for substances in tobacco smoke absorption, their metabolism and for their interactions with receptors (Kiyohara *et al.,* 2002).

Tobacco smoke contains tumour initiators, the most important of which are benzo[a]pyrene, promoters such as phenol derivatives, complete carcinogens and cocarcinogens. Benzo[a]pyrene which occur in amounts of 20 to 40 ng per cigarette forms adducts preferentially in the mutation hotspot of p53 gene (Denissenko *et al.*, 1996). These specific G:C to T:A transversion mutations contribute 38% of the p53 mutations in lung carcinoma and are not as abundant in other cancer types (Harris and Hollistein, 1993). Smoking increases the risk of all lung cancer types, especially small cell and squamous cell carcinoma (Morabia and Wynder, 1992).

1.4.3.2. Asbestos

Asbestos is a mineral made up of tiny fibres. When it is disturbed, it forms a dust. The fibres can be inhaled into the lungs. The most frequent occupational cause of cancer is

past exposure to asbestos (Oksa *et al*. 1997, Steenland *et al*. 1996). Furthermore, interaction between smoking and asbestos has produced a very high risk for lung cancer in those with both heavy smoke and asbestos exposures, estimated to be 50 times greater than that of the non-smoking, non-asbestos population (Steenland *et al*. 1996). Asbestos can cause chromosome loss and deletion which can lead to accumulation of proto-oncogenes or inactivation of tumour suppressor genes (Barrett *et al*. 1989). In lung carcinoma, frequency of p53 protein accumulation has been associated with clinical and histological asbestos exposure as well as with heavy tobacco smoking (Nuorva *et al*. 1994).

1.4.3.3. Genetic alterations

Lung cancer at molecular level is not well defined and it is believed that multiple genetic and molecular changes characterize lung cancer development (Johnson and Kelley, 1993). Though no gene directly related to lung cancer has been identified, tumour oncogenes, suppressor genes, and apoptotic genes are involved in the initiation of lung cancer.

1.4.3.3.1. Oncogenes

1.4.3.3.1.1. Ras

The Ras gene family mutations are found in approximately 20-30% of lung adenocarcinoma and 15-20% of all non-small cell lung carcinoma but very rarely in small cell lung carcinoma with K-ras mutations accounting for approximately 90% of Ras mutations in lung adenocarcinoma (Richardson and Johnson, 1993). K-ras and p21

proteins form a complex that lead to growth arrest, not proliferation (Kammouni *et al*., 2002)**.** The p21-Ras protein is able to bind to quanosine triphosphate (GTP) and has intrinsic GTPase activity, which hydrolyzes bound GTP to quanosine diphosphate (GDP). When bound to GTP, Ras protein is in its active configuration, which allows the transduction of a growth signal to the cell nucleus. When GTP is hydrolyzed, the molecule assumes its inactive configuration and the signal transduction falls silent. When a Ras gene is mutated, p21-Ras loose its capability to hydrolyze GTP and the molecule can no longer switch back to inactive configuration and this result in a continuous and inappropriate growth signal to the cell nucleus (Sekido *et al*., 1998).

Some studies showed that K-ras mutations are found in only 5-7% of lung tumours from non-smoking lung cancer patients. These results suggest that K-ras mutations were induced primarily by tobacco-smoke carcinogens. It has been suggested that such mutations occur in carcinogen-exposed cells during the mis-replication of a bulky DNA adducts formed between a carcinogen and guanine bases in the gene sequence. About 70% of K-ras mutations are G-T transversions with the substitution of the normal glycine with either cystein or valine and this mutations represent the type of DNA damage expected from bulky DNA adducts caused by polycyclic hydrocarbons and nitrosamines found in tobacco smoke (Slebos *et al*., 1991).

1.4.3.3.1.2. c-Myc

The c-myc gene has emerged as a central oncogenic switch in many human and animal cancers. The Myc oncogene family encodes group of nuclear phosphoproteins that play a role in cell growth and in the development of human tumours. c-Myc belongs to a family

of myc genes that includes B-myc, L-myc, and N-myc, however only c-myc, L-myc and N-myc have neoplastic potential. c-Myc affect cell cycle regulation, apoptosis, and metabolism positively, whereas it affects cellular differentiation and cell adhesion negatively. With deregulated c-myc in tumours, these coordinated activities presumably contribute to the neoplastic phenotypes. c-Myc appears to induce apoptosis by a wild type p53 dependent pathway. c-Myc might also be related to an activated Fas death pathway but using FADD knockout cells, other studies suggest that c-myc induced apoptosis is independent of Fas death pathway (Johnson *et al.,* 1996).

c-Myc has been reported to be more frequently activated in small cell lung carcinoma and non-small cell lung carcinoma. Gene amplification of myc family genes has been observed in 18% small cell lung carcinoma tumours and 31 % of small cell lung carcinoma cell lines. In non-small cell lung carcinoma amplification has been observed in 8% tumours and 20% cell lines (Johnson *et al.,* 1996). Myc amplification appears to occur more frequently in cell lines most derived from metastatic lesions than in primary tumours (Richardson and Johnson, 1993).

1.4.3.3.1.3. EGFR

EGFR belongs to broad family of receptor tyrosine kinases. These receptors have a common structure comprising an extracellular ligand binding domain, a transmembrane domain and an intracellular domain with tyrosine kinase activity for signal activation. Binding of a ligand such as epidermal growth factor causes EGFR to dimerize with itself or another member of EGFR family of receptors, leads to receptor linked tyrosine activation and results in a signalling cascade (Mendelsohn and Baselga, 2000). EGRF is

expressed on the exterior of normal and neoplastic cells. EGFR is frequently altered in epithelial tumours and its expression has been associated with advanced stage, poor prognosis, and/or resistance to therapy (Brabender *et al.*, 2001; Gupta and raina, 2010). EGFR over-expression has been associated with the pathogenesis, proliferation, invasion and metastasis of various solid tumours including NSCLC. EGFR is over-expressed in approximately 40% to 80% of documented cases of NSCLC and approximately 88% of intractable cases of NSCLC. Tumour over-expressing EGFR have a poor response to both chemotherapy and radiation therapy.

1.4.3.3.2. Tumour suppressor genes

Tumour suppressor genes suppress tumour formation by inhibiting apoptosis with their protein product. When mutated the mutant allele behave as recessive, that is, as long as the cell contain one normal allele, tumour suppression continues. There are a number of known tumour suppressor genes but p53 and Rb genes are the well studied.

1.4.3.3.2.1. P53

Mutation within the tumour suppressor p53 gene is one of the most common genetic alterations present in lung cancer. About 70% of small cell lung carcinoma and 50% of non-small cell lung carcinoma have mutations in one allele of p53 often accompanied with loss of the wild type allele (Brambilla, *et al*., 2003). Concerning non-small cell lung carcinoma, p53 mutations are more frequently found in squamous cell carcinomas than in adernocarcinomas and large cell carcinomas (Tammemagi, *et al*., 1999). Notably, the p53 mutational spectra of lung cancer show an excess of G:C to T:C transversion (Hainaut

and Pfeifer, 2001). Smoking has been shown to be associated with mutations in the p53 tumour suppressor genes, the most common genetic alterations detected in human cancers. Such mutations have been associated with a history of heavy tobacco use, but they have also been detected in non-smokers with lung cancer (Beckett, 1993).

1.4.3.3.2.2. Retinoblastoma (Rb) protein

Rb mutations together with loss of wild type allele have been demonstrated in lung cancer (Harbour *et al*., 1988; Horowitz *et al.,* 1990). Rb protein is abnormal in over 90% of small cell lung carcinomas and 15-30% non-small cell lung carcinomas. RB mutations in lung cancer include transaction by deletions, nonsense mutations or splicing abnormalities (Reissmann *et al.,* 1993).

Other evidence linking Rb with lung cancer development is suggested by the observation that germline carriers of an Rb mutation who were relatives of retinoblastoma patients were about 15 times more likely to develop lung cancer than the general population (Sanders *et al.,* 1989). The re-introduction of the wild type Rb gene suppressed the growth of SCLC cells (Ookawa *et al.,* 1993).

1.4.3.3.2.3. Tumour suppressor genes at chromosome region 3p

A cytogenetic deletion in chromosome 3 in lung cancer was first reported by Whang-Peng *et al.* The study comprised of 12 cell lines cultured from human small-cell lung cancer tissue and 2-day tumour culture specimens from three patients. Acquired chromosomal abnormality (deletion at 3p) has been found in at least one chromosome 3 in 100 percent of the specimens (Whang-Peng *et al.,* 1982).

At least three distinct 3p regions have been allelotypically identified suggesting that there are probably over three tumour suppressor genes located on 3p (Hibi *et al.,* 1992). One of the examples of tumour suppressor genes found at chromosome 3 is *FHIT*. *FHIT* is a candidate tumour suppressor gene on the basis of frequent loss of heterozygosity (LOH) in lung cancer and homozygous deletion in several lung cancer cell lines with most of the homozygously deletions found in NSCLC (Yanakisawa *et al.,* 1996). Frequent LOH of the *FHIT* gene was observed in lung cancer from 80% of smokers and 22% non-smokers, suggesting that *FHIT* may be a molecular target of tobacco smoke carcinogens (Sozzi *et al.,* 1997).

1.4.3.3.3. Apoptosis genes

1.4.3.3.3.1. Fas

Kawasaki and colleagues reported that the expression of Fas in lung cancer cell lines varied and that the difference was independent of the cell type. However in general, Fas expression in lung cancer is down-regulated and also in some case non-functional. A functional Fas-FasL co-expression was found in most lung cancer cell lines. It is not clear why these cells expressing both functional Fas and FasL don't trigger cell death by apoptosis, but it is suspected that, since these cells express Fas in low levels, they may escape from binding to FasL and therefore the subsequent cell death (Kawasaki et al., 2000).

1.4.3.3.3.2. BCL-2

Bcl-2 protects cells from apoptosis and thus may probably play a role in determining the response to chemotherapy through repression of apoptosis in cancer cells because most

chemotherapy drugs are designated to induce apoptosis (Ohmori *et al.*, 1993). Studies have shown that the frequency of Bcl-2 protein expression is much higher in small cell lung carcinoma than in non-small cell lung carcinoma (Jiang *et al.*, 1995). And this is contrary to previous studies that small cell lung carcinoma are usually much more sensitive to chemotherapy, which usually occurs by apoptosis than non-small cell lung carcinoma (Kaiser *et al.*, 1996). Similarly, a better survival of Bcl-2 positive cell lung cancer cases was observed in NSCLC and in addition, a longer survival was observed in patients whose SCLC tumours express Bcl-2 (Hagashiyama *et al.*, 1997). Thus the role of Bcl-2 in lung cancer seems to be complex and not well understood and that the suggestion that Bcl-2 may be converted to Bax-like death affectors caspase family of cysteine protease may be relevant.

1.4.4. Lung cancer and apoptosis

Apoptosis can be viewed as a form of programmed cell death that performs a vital role in sculpting tissues, organs and organisms. Defects in the regulation of cell death contribute to a number of human diseases, e.g. excessive down regulation of this process has been linked to cancer and viral infections, while excessive up-regulation causes autoimmune disorders and neurodegerative diseases such as Alzheimer's disease and ischaemic injury (Iwahashi *et al*, 1997)

It is well known that ectopic expression of tumour suppressor p53 augments apoptotic activity in human NSCLC cells incubated with chemotherapeutic agents (Gottliem and Oren, 1996). It has been previously reported that human NSCLC cells that have mutated

p53 showed significantly poorer response to intensive chemotherapy and able to induce drug resistance by interfering with the normal apoptotic pathway (Lai *et al*., 2000; Israels and Israels, 1999).

Tumour necrosis factors (TNFs) have emerged as one of the main host-derived mediators that, either alone or in combination, appear to mediate both antiproliferation and tumourigenic effects in malignant tumours. The TNF family is comprised of two cytokines, TNF-α (cachectin) and TNF-β (lymphotoxin-α), which are secreted by a wide variety of cells. TNFs bind with nearly identical affinities to distinct tumour necrosis factor receptors (TNFRs), TNFR-I and TNFR-II. The two cytokines have been reported as vital mediators of TNF-α in triggering apoptosis. The expression of TNFR-II can strongly induce TNF-α mediated cytotoxicity through TNFR-I in lung cancer cells. Although normal lung cancer cells express TNFR-I and -II, loss or downregulation of TNFRs occurs during the progression of lung cancers (Li-Feng *et al*., 2004). It had also been reported that retinoic acid modulate the expression of TNFR-I and –II in lung cancer cells and sensitise cells to TNF-induced apoptosis (Manna and Aggamal, 2000). These findings provide strong evidence that aberrant regulation of apoptosis can be linked to the development of lung cancer.

1.5. Lipoic Acid Synthetase

Lipoic acid synthetase (LIAS) is a 1.73 kb gene located at chromosome 4p14. Alternative splicing occurs at this locus omitting residues 1030-1137 corresponding to exon 10 of the full length gene, and two transcript variants encoding distinct isoforms have been identified. Variant two lacks exon 10 resulting in a shorter protein (isoform 2) that has a

distinct C-terminus, compared to isoform 1 which consist of 11 exons (Mantovani *et al*., 2003). The protein encoded by LIAS gene belongs to the biotin and lipoic acid synthetases family and localizes in the mitochondrion.

Though the function of lipoic acid synthetase is not yet well documented, some studies have attempted to characterise its function by looking at the biological pathways at which LIAS gene product plays a crucial role, one of which being biosynthesis of alpha-lipoic acid. Alpha-Lipoic acid is a naturally-occurring enzyme co-factor found in a number of multi-enzyme complexes regulating oxidative metabolism. Alpha lipoic acid is also a natural antioxidant that is often included in therapeutic drugs for treatment of diseases in which pro- and antioxidant balance is disrupted (diabetes, neurodegenerative diseases, Acquired Immune Deficiency Syndrome (AIDS)). Research has shown that in diabetic retinopathy, oxidative stress increase in the retina and retinal capillary cells undergo accelerated apoptosis. Alpha lipoic acid has shown to be very beneficial in the prevention of diabetic retinopathy by inhibiting the parameters of oxidative stress generated by high glucose concentrations (West, 2000).

Alpha lipoic acid has recently been the subject of research in HIV. NF-κB binds to HIV proviral gene material in the nucleus of HIV infected cells and activates HIV replication. Viral replication in turn, increases cellular levels of cytokines such as TNFα that promote production of free radicals and activation of NF-κB, initiating a viscous cycle of viral replication and free radical production (Pande and Ramos, 2003). Alpha lipoic acid appears to directly affect this cycle by completely blocking the activation of NF-κB (Kim *et al.*, 2007).

Lipoic acid is a crucial cofactor in the pyruvate dehydrogenase (PDH) and alpha - ketoglutarate dehydrogenase (KGDH) multienzyme complexes responsible for the production of acetyl-CoA in metabolic pathways (Busby et al., 1999; Yasuno and Wada, 2002).

1.5.1. LIAS and apoptosis

The function of LIAS in apoptosis is not yet well defined but some attempts have been made to define its function in apoptosis. It has been reported that alpha-lipoic acid has differential effects on the growth and viability of normal versus transformed cell lines. Alpha-lipoic acid induced apoptosis in human FaDu and Jurkat tumour cell lines and the mechanism of apoptosis was found to be independent of Fas-mediated signalling, as alpha-lipoic acid-treated Jurkat cell mutants deficient in Fas or FADD retained sensitivity to apoptosis. The differential selectivity of the pro-apoptotic effects of alpha-lipoic acid for transformed cells supports its potential use in the treatment of neoplastic disorders (Van de Mark *et. al*., 2003).

1.6. Ribosomal Protein L9

The eukaryotic ribosome is a complex structure with two subunits, large (60S) and small (40S) composed of four RNA molecules and as many as 80 different proteins. The human ribosomal protein L9 gene (RPL9) is approximately 5.5 kb in length and contains 8 exons. It is located on chromosome 4p14. The message for RPL9 is 712 nucleotides in length. This gene encodes a ribosomal protein that is a component of the 60S subunit. The protein localises in the cytoplasm. As is typical for genes encoding ribosomal

proteins, there are multiple processed pseudogenes of these genes dispersed through the genome (Mazuruk *et al*., 1996).

1.6.1. RPL9 and apoptosis

RPL9 has been highly conserved through evolution. The amino acid sequence of mouse and human RPL9 is 98% identical. For decades mouse have been used as human models in research hence the use of 6132A PRO mouse cells to investigate the effect of L9 to cancer. cDNA sequence of L9 from UV induced 6132A PRO tumour cells, differ from the normal sequence at one nucleotide: A instead of T. This mutation encodes histidine instead of leucine at position 47. Antigenic activity was found at high level in ribosomes isolated from 6132A-PRO cells. Reintroduction of the lost wild type L9 allele into 6132A-PRO variant suppressed the growth of tumour cells in vivo (Paul *et.al*. 1995). The highest expression levels of eukaryotic ribosomal protein genes have been observed in cells undergoing growth and development and that the level of expression declines as the tissue reaches developmental maturity (Williams and Sussex, 1995).

Main Objective

The purpose of this study was to establish the expression of the RPL9 (ribosomal protein gene) and LIAS (lipoic acid synthetase) genes in human lung cancer and to characterize their role in apoptosis and lung cancer and also to determine whether the expression levels of this two genes varies between the normal and the diseased state of the tissue.

Rationale

Since there is strong evidence that suggest that aberrant regulation of apoptosis can be linked to the development of cancer, the generation of well characterized mutants that are resistant to apoptosis can potentially provide useful tools to study the action and efficiency on known and novel drugs directed against cancer. The identification of such genes would provide novel targets for drug development to treat diseases such as cancer. Both LIAS and RPL9 genes were found mutated in CHO cell lines that gained resistance to apoptosis due to promoter-trap mutagenesis. The work was done at the University of the Western Cape, in Prof D.J.G Rees laboratory (unpublished). As already briefly indicated above the link between apoptosis and these two genes, it is imperative to further study the direct relationship between them and apoptosis in human cancers and in this case, human lung cancer.

2. Materials and Methods

2.1. Sample collection

Ethics clearance was obtained from Human Ethics Committee, University of the Witwatersrand, clearance number (M050308). The normal and cancerous lung tissue sections were obtained from National Health Laboratory Service, department of Pathology. Cancer cases provided were Adenorcarcinoma, Large cell carcinoma, Squamous cell carcinoma, Small cell carcinoma. Normal lung cell line (Fibroblast MRC-5) and lung adenorcacinoma (A549) cell lines (Highveld Biologicals, South Africa) were used for RNA extraction.

2.2. Preparation of Competent Cells

Normally *Escherichia coli* cells do not possess the ability to take up DNA from the environment. However, if their cell walls are altered, these bacterial cells become more likely to incorporate foreign DNA and thus these cells are said to be "competent". These cells can be made competent by chemical or physical treatment. Chemical treatment includes the calcium chloride method while physical treatment includes electoporation whereby the bacterial cell is shocked with 2500 V. In preparation of competent cells, cells in the log phase are used as they are undergoing rapid growth and become competent more easily than cells in any other growth stage.

Chemical treatment was used in order to make MC1061 *Escherichia coli* cells competent.

1. MC1061 cells were plated on Luria Bertani (LB) agar plates containing 10 mM Magenesium Chloride ($MgCl_2$). The plates were incubated at 37 °C overnight.
2. A single colony was added to 20 ml Tryptone Yeast Extract $MgCl_2$ (TYM) Broth in a 500 ml conical flask and grown at 37 °C overnight, shaking constantly at 300 rpm.

3. Following an overnight incuation, 1 ml of cells in the TYM Broth were added to 100 ml fresh TYM Broth in a 2 L conical flask. The cells were grown for a further 2-3 hours or until optical density at 550 nm lies between 0.4 and 0.6 at 37 °C hours with constant shaking at 300 rpm.
4. Thereafter, 400 ml of fresh TYM broth was added to the 2 L conical flask and cells allowed to grow for a further 2-3 hours or until optical density at 550 nm lies between 0.4 and 0.6 at 37 °C with constantly shaking at 300 rpm
5. Bacterial cells were rapidly cooled in ice water, shaking constantly after which they were centrifuged in two 125 ml propylene tubes at 3000 rpm for 10 minutes at 4 °C.
6. The supernatant was discarded and the pellet resuspended in 125 ml Tfb1. This solution was allowed to incubate for 30 minutes on ice after which the bacterial cells were centrifuged at 3000 rpm for 10 minutes at 4 °C.
7. The bacterial cells were gently resuspended in 80 ml Tfb2. 300 µl of the cells were aliquoted into 0.5 ml eppendorf tubes. The cells were then frozen on dry ice and stored at -70 °C for further use.

2.3. In Situ Hybridization

In situ hybridization is a technique used to view the location of nucleic acids in situ, i.e. in their native location in the cell or nucleus. For viewing the location of RNA in the cell, the tissue is gently fixed so as not to disrupt the double stranded DNA. Tissues are then hybridized to a chemically or radioactively labelled RNA or DNA probe that is complimentary (or anti-sense) to the desired mRNA of interest. The chemical or radioactive probe can then be detected in the tissue by antibodies to the chemical label or

by autoradiography. When using the chemically labelled probe the antibody may be fluorescently labelled (fluorescence) or can have an enzyme (colorimetric) associated with it that when exposed to substrate there is an emission of light at a specific wavelength or generates a coloured precipitate respectively so that localization in cells is easy. In this study both fluorescence and colorimetric methods were used.

2.3.1. RNA isolation

Total RNA was extracted using the Trizol^{TM}LS reagent method. The method can be divided into four stages, the disruption, homogenisation, phase separation and RNA precipitation stages. During the disruption stage the cell wall, plasma membrane of the cell and organelles found in the cell are disrupted allowing for the release of all the RNA contained in the sample. At homogenisation the viscosity of the cell lysates produced during disruption is reduced and the shearing of high molecular weight genomic DNA and other high molecular weight cellular components occurs using the TRIzol^{TM} LS Reagent. RNA is separated from the rest of the lysate using chloroform while RNA is isolated by RNA precipitation using isopropyl propanol

1. RNA was extracted from normal lung fibroblast cell line MRC5. The cells were cultured in a 25 cm^3 tissue culture plate in 10 % Foetal Bovine Serum (FBS)-Dulbecco's Modified Eagled Medium (DMEM) (Highveld Biologicals, California) until they were confluent.
2. The cells were grown in a monolayer that is attached on the culture plate and they were washed with PBS before RNA was extracted.
3. The cells were then homogenised by adding 2 ml Trizol^{TM}LS reagent (Invitrogen

Corporation, Life Technologie, Carlsbad, CA, USA) per 25 cm^3 of culture plate with vigorous shaking for 2 hours.
4. Cells were completely homogenised by passing the lysate through the pippet a several times.
5. The homogenate was split into two 1 ml and each 1ml was transferred to a 2 ml eppendorf tube. 1 ml of chloroform (Merck Chemicals (Pty) Ltd, Gauteng, South Africa) was added to each tube and vigorously vortexed for 30 seconds followed by incubation at RT for 10 minutes
6. The homogenate was then centrifuged at 4º C for 1 hour at 12000 rpm.
7. After centrifugation the combined top aqueous layer was transferred to a clean 2 ml eppendorf tube to which 1 ml isopropyl alcohol (Merck Chemicals (Pty) Ltd, Gauteng, South Africa) was added and mixed thoroughly by inverting the tube a several times and then incubated at 4 ºC for 30 minutes so as to precipitate the RNA
8. RNA was pelleted by spinning at 12000 rpm for 30 minutes at 4º C and immediately supernatant was discarded.
9. The RNA pellet was then washed with 1 ml 70 % ethanol by centrifuging the mixture at 12000 rpm for 5 minutes at 4 ˚C.
10. Supernatant was immediately discarded, pellet dried and re-suspended in 100 µl DEPC water and stored at -70 ºC
11. The quality of the RNA extracted was determined by formaldehyde agarose gel electrophoresis (Section 2.3.2.) and quantified spectrophotometrically

Quantification of RNA

$$[\text{RNA}] \text{ in } \mu g/\mu l = \frac{40X \text{ dilution factor } XOD}{1000}$$

2.3.2. Formaldehyde agarose gel electrophoresis

Quality of extracted RNA was analysed on 1 % (w/v) agarose gel. The gel was prepared by dissolving 1g agarose in 10 ml of 10 X 3-[N-morpholino] propane sulfonic acid (MOPS) (Fluka Chemie GmbH, Sigma-Aldrich Chemie, GmbH, Steinheim, Switzerland) and 84.6 ml sterile DEPC treated water. The gel was allowed to cool to 50 ºC prior to addition of 5.4 ml 37 % (v/v) formaldehyde (Riedel-de-Haën, Sigma Aldrich Laborchemikalien GmbH, Seelze) and 4 µl of 100 µg/ml ethidium bromide (Merck KGoA, Darmstadt, Germany). The gel was poured into a casting tray and allowed to set at room temperature. 10 µl RNA sample was mixed with freshly prepared formaldehyde gel loading buffer and the mixture was then heated at 65 ºC for 5 minutes to denature RNA and cooled on ice for 10 minutes before loading on the gel. Once the gel was completely set, the comb was carefully removed and the gel placed on electrophoresis tank. 1 XMOPS was added to the tank until the gel was completely submerged. RNA mixture was loaded into the wells and electrophoresed at 50V for 1 hour or until the loading dye reached three-quarters of the gel. After the run the gel was visualised and photographed using Universal Hood II UV transluminator (Bio-Rad Laboratories, Hercules, CA, Italy) and the QuantityOne-D-Analysis Software (Bio-Rad Laboratories, Hercules, CA, USA).

2.3.3. Reverse transcription- Polymerase Chain Reaction

Reverse transcription polymerase chain reaction is the most sensitive method for the detection of the low abundant mRNA often obtained from cell lines or limited tissue samples. mRNA was reverse transcribed into cDNA using ImProm-II Reverse Transcription system (Promega Corporation, Madison, WI, USA) and manufacturer's instructions were followed. The oligo-p$(dT)_{15}$ was used. Oligo-p$(dT)_{15}$ primer binds to the 3'-end poly (A) tail of mRNA and together with reverse transcriptase, mRNA is reverse transcribed into cDNA. Reaction volumes and concentrations are shown in table 2.1.

Table 2.1: cDNA synthesis cocktail

Reagents	Volumes per sample	Final concentration
5 X Reaction buffer	5 µl	1 X
25 mM $MgCl_2$	3 µl	3 mM
10 mM deoxyribonucleotide mix	2.5 µl	1 mM
Oligo-p$(dT)_{15}$	1 µl	
RNAse inhibitor	0.5 µl	
AMV Reverse Transcriptase	1 µl	
Sterile distilled water	X µl	
RNA sample	X µl	
Total volume	25 µl	-

X depends on the RNA concentration

Reverse transcriptase was added last to avoid degradation. The mixture was then briefly vortexed and centrifuged to collect the mixture at the bottom of the tube. The reaction was carried out under the following conditions.

25 ºC for 10 minutes

42 ºC for 60 minutes

75 ºC for 15 minutes

4 ºC for 10 minutes

cDNA was then stored at -20 ºC until used for Polymerase Chain Reaction (PCR).

2.3.4. Primers design and synthesis

Primers for RPL9 and LIAS were designed and synthesised at Inqaba Biotech (RSA). The primer sequences were confirmed using the NCBI BLAST search engene. Primers sequences, product sizes and annealing temperatures are shown in table.

Table 2.2: Primer sequences for RPL9 and LIAS

Gene	Primers Sequence	PCR amplicon size	Annealing Temperature (Tm)
LIAS	Forward taagactgcaagaaatcctcctcc Reverse cacaaggatttttggattcctttcc	190 bp	57 ºC
RPL9	Forward ctccgggttgacaaatggtgg Reverse cccattctcctggataacaacg	165 bp	61 ºC

2.3.5. Polymerase Chain Reaction

Polymerase chain reaction (PCR) is a three step technique that allow for amplification of minute DNA quantity into a significant quantity of the fragment of interest through repetitive cycle of DNA synthesis. The three PCR steps are denaturation in which case the temperature is taken up to as high as 94 ºC. At this temperature the two DNA strands separate (denature). The second step is annealing of primers to the templates (denatured DNA strands). The temperature is taken down specific for the set of primers used which is normally 5 ºC less than the melting temperature (Tm). The last step is polymerisation (elongation) of the annealed primer. DNA polymerase is used to synthesise a double stranded DNA by complementary base pairing with the DNA template. It is essential to use a thermo stable DNA polymerase that can withstand the harsh denaturation temperature and for this reason Taq polymerase is often used which elongate or polymerise at 72 ºC. After elongation the cycle starts again and production is exponential. The cDNA obtained through reverse transcription was used as a template using sequence specific primers for LIAS and RPL9. Master Mix from (Promega Corporation, Madison, WI, USA) was used and instructor's manual was followed. Reaction components and concentration are shown in table 2.3.

Table 2.3: Cocktail for Polymerase Chain Reaction

Reagent	**Volume**	**Final concentration**
Master Mix	12.5 µl	1 X
Forward Primer (10 ρmoles)	1 µl	0.4 ρmoles/ µl
Reverse Primer (10 ρmoles)	1 µl	0.4 ρmoles/ µl
25 mM $MgCl_2$	2.0 µl	2 mM

Sterile nuclease free water	*y*	
Template DNA	*x*	1 µg
Total volume	25 µl	

x and y – variable depending on cDNA concentration

The reaction was carried out under the following conditions depending on the gene of interest and primer set used.

95 ºC for 2 min

94 ºC for 30 sec

Tm -5 ºC for 30 sec } 35 cycles

72 ºC for 1 min

72 ºC for 10 min

4°C for ∞

2.3.6. Agarose gel electrophoresis for DNA

Agarose gel electrophoresis is a technique used for separation of nucleic acids according to size, charge and shape. Using a stain like ethidium bromide which intercalates between the bases of DNA and illuminate the gel under UV light, DNA fragments can be visualised. 0.8 % agarose gel was prepared by dissolving 0.8 g agarose in 100ml 1 X TBE buffer. Ethidium bromide to a final concentration of 1 µg/ml was added when the solution reaches 50 ºC and allowed to set in a gel-casting tray. The DNA samples were mixed with 1 X Orange-blue loading dye (Fermentas Life Sciences, Hanover, MD, USA). Generuler^{TM} 100 base pair DNA ladder was used (Fermentas Life Sciences, Hanover, MD, USA). The DNA samples and DNA molecular weight marker were loaded onto the

gel and run at 70 V in 1 X TBE buffer. The gel was allowed to run until the dye reached three quarters of the gel after which gel was viewed and image captured using a UV transluminator.

2.3.7. Cloning

Cloning is an umbrella term traditionally used to describe different processes for duplicating biological material. The different types of cloning are recombinant DNA technology or DNA cloning, reproductive cloning, and therapeutic cloning. Cloning technology used in this study was DNA cloning which is defined as a transfer of DNA fragment of interest from one organism to a self-replicating genetic element such as a bacterial plasmid. The DNA of interest can then be propagated in a foreign host cell. Cloning makes it easy to sequence DNA fragment of interest because cloned fragments can be prepared to obtain required DNA concentration for sequencing and other applications such as probe synthesis.

2.3.7.1 Ligation

PGEM-T-Easy vector allows for cloning of PCR products without purifying them. LigaFast™ Rapid Ligation System (Promega Corporation, Madison, WI, USA) was used to clone PCR products into pGEM-T-Easy vector for both sequencing and probe synthesis. Ligation mixture consisting of 3 ng PCR product and 10 ng pGEM-T-Easy vector was prepared and ligation was carried out by T4 DNA ligase. Background control (no insert) was also setup as well as a positive control supplied with the kit. The components were mixed and briefly centrifuged to collect everything at the bottom of the

tube. The ligation mixture was incubated at room temperature for a minimum of one hour. After the hour the ligation mixture was transformed into MC1061 *E. coli* cloning strain competent cells.

Table 2.4: Ligation

Reagents	Experimental Reaction	Negative Control Reaction	Positive Control Reaction
2 X ligation buffer	5 µl	5 µl	5 µl
PCR product	3 ng	-	3 ng
pGEM-T-Easy	10 ng	10 ng	10 ng
T4 ligase	1 µl	1 µl	1 µl
SdH_2O	Adjust to 10 µl	Adjust to 10 µl	Adjust to 10 µl
Total volume	10 µl	10 µl	10 µl

2.3.7.2. Transformation

E. coli competent cells were thawed on ice before use. 100 µl of these cells were added to ligation mixture set above. This was incubated for 30 minutes on ice. Immediately followed by incubation at 37 ºC for 5 minutes to heat shock the cells and then followed by incubation for 2 minutes on ice. 900 µl of Luria broth (LB) lacking ampicillin was added onto the mixture and incubated for one hour at 37 ºC to allow for the growth of cells. After the hour, transformation mix (100 µl) was plated on pre-warmed Luria agar plates containing ampicillin. The plates were then incubated at 37 ºC overnight.

Note: negative control was cells with no plasmid DNA transformed into them while positive control was supplied with the kit i.e. a DNA fragment that was assured to ligate to pGEM-T-Easy cloning vector. And the background control was cells transformed with pGEM-T-Easy vector with no insert to check if the vector was ligating to itself.

2.3.8. Colony Polymerase Chain Reaction

Colony PCR is a technique that uses PCR technology to identify and select cell colonies that have the correct plasmid insert. Instead of using purified DNA, colony mixed with water is used as a template for PCR reaction.

Aliquots of 10 µl of sterile distilled water were added into a set of 0.2 ml eppendorf tubes corresponding to a number of colonies to be screened. Each colony was mixed with sterile distilled water in its own eppendorf. 1 µl of each colony mix was used as a template for PCR reaction as tabulated on table 2.3. Sequence specific primers were used to find the insert of interest. At the end of PCR the results were analysed on 0.8 % agarose gel electrophoresis (Section 2.3.6). Colonies that showed the presence of the DNA fragment of the correct size was taken through to plasmid DNA extraction. The remainder of the 10 µl of colony mix was used to inoculate an overnight culture for plasmid DNA extraction.

2.3.9. Plasmid DNA extraction

In order to get a high quality DNA for subsequent experiment such as sequencing and probe synthesis, plasmid DNA was extracted using Promega WizardPlus® Miniprep

DNA Purification System (Promega Madison, WI, USA). Manufacturer's instructions were followed and the full protocol is outlined below.

Plasmid DNA extraction protocol
1. An overnight culture was prepared by inoculating 6 ml luria broth with ampicillin with a colony containing plasmid of interest overnight.
2. 6 ml of an overnight culture was centrifuged at 12 000 rpm for 8 minutes at RT.
3. Supernatant was carefully discarded and pellet resuspended in 250 µl Cell Resuspension Solution.
4. 250 µl Cell Lysis Solution was added to the cell suspension and tube inverted 4-5 times to mix
5. 10 µl Alkaline Protease Solution was added. The tube was inverted 4-5 times to mix followed by incubation at RT for 5 minutes.
6. 350 µl Neutralizing Solution was added and the tube inverted 4-5 times to mix.
7. The sample was centrifuged at 12 000 rpm for 10 minutes at RT.
8. Spin column was inserted into collection tube.
9. Cleared lysate was poured off into spin column assembly followed by centrifugation at 12 000 rpm for 1 minute at RT.
10. The flow through was discarded and spin column reinserted into the collection tube.
11. 750 µl Wash Solution (Ethanol added) was added followed by centrifugation at 12 000 rpm for 1 minute at RT.
12. The flow through was discarded and spin column reinserted into collection tube.

13. Step 11 was repeated with 250 µl Wash Solution and centrifuged for 2 minutes at RT
14. Spin column was inserted into a clean sterile 1.5 ml eppendorf tube.
15. Plasmid DNA was eluted into the eppendorf tube by adding 50 µl nuclease-free water to the spin column followed by centrifugation at top speed for 1 minute at RT.
16. Spin column was discarded and plasmid DNA stored at -20 ºC.
17. To determine if plasmid DNA was isolated the results were analysed agarose gel electrophoresis (Section 2.3.6)

2.3.10. Sequencing

Sequencing was done at Inqaba Biotech (Pretoria, RSA). Sequences were analyzed using CHROMAS, version 1.62 (Technelysium (Pty) Ltd, Australia) and BLAST tool from the National Centre for Biomedical Information (NICB) at URL: www.ncbi.nlm.nih.gov to compare the sequence obtained to a reference sequence Accession number

2.3.11. Linearization of clones

The first step of probe synthesis is linearization of clones with PstI and ApaI. PstI cuts the pGEM-T-Easy clone vector at the Sp6 side of the insert so that the T7 promoter can be used for in vitro transcription of the antisense probe. ApaI cuts pGEM-T-Easy vector at the T7 side of the insert and this allows for in vitro transcription of the sense probe using the Sp6 promoter. Restriction digestion setups are illustrated in table 2.5.

Table 2.5: Linearisation of clones

	PstI digest	ApaI digest
pGEM-T-Easy clone	10 µl	10 µl
10 X Buffer	2 µl	-
10 X Buffer	-	2 µl
PstI	3 µl	-
ApaI	-	3 µl
SdH_2O	15 µl	15 µl
Total volume	30 µl	30 µl

The reaction digestions were incubated at RT overnight and then the enzymes were inactivated by incubating the tubes at 65 ºC for 5 minutes. To check if the clones were completely linearised, 5 µl of the reaction was run on 0.8 % agarose gel electrophoresis. After verifying that the clones were completely linearised, the rest of the reaction digest was run on 0.8 % agarose gel (Section 2.3.6) and purified from the gel as described in section 2.3.12

2.3.12. Purification of DNA from Agarose Gel

Wizard SV gel and PCR clean-up system (Promega Corporation, Madison, WI, USA) was used to purify the linearized clones from agarose gel for probe labelling. Manufacturer's instructions were followed and the protocol is outlined below.

1. Linearized clone was electrophoresed on 0.8 % agarose gel
2. DNA band was visualised with a long wavelength UV light and excised out with a sharp sterile blade.
3. Gel slice was transferred to a weighed eppendorf and its mass calculated.
4. Gel slice was dissolved in 10 µl membrane binding solution for each 10 mg of the slice.
5. The gel slice mix was incubated at 65 ºC for 10 minutes or until the gel dissolved completely with occasional mixing.
6. Once dissolved, SV mini column was inserted into collection tube and dissolved gel poured into the SV mini column assembly and incubated at RT for 1 minute.
7. This was followed by centrifugation in a microfuge at 10 000 rpm for 1 minute at RT. The flow through was discarded and the mini column reinserted into the collection tube.
8. 700µl of membrane wash solution (ethanol added) was added to the mini column and followed by centrifugation at 10 000 rpm for 1 minute at RT.
9. Step was repeated with 500 µl membrane wash solution and centrifuged for 5 minutes at the same speed.
10. The SV mini column was carefully removed from the assembly making sure that the mini column did not touch the flow through.
11. SV mini column was then inserted into a sterile 1.5 ml sterile eppendorf.
12. 50 µl sterile DEPC treated water was added to the centre of the column and incubated at RT for 1 minute followed by centrifuged at 10 000 rpm

for 1 minute.
13. SV mini column was discarded and the DNA was quantitated spectrophotometrically and stored at -20 ºC for labelling.

2.3.13. Digoxygenin (DIG) Probe Labelling

Purified, linearized clones with RPL9 and LIAS inserts were used as templates for labelling of the sense and antisense cRNA probes. For the generation of the antisense probe, 2 µg of the PstI linearized clone was incubated with DIG dUTP and T7 RNA polymerase and for the generation of the sense probe, ApaI linearised clone was incubated with Sp6 RNA polymerase. The specificity of the labelling reaction was determined by generating a DIG labelling control RNA from DNA PSPT 18-Neo/Pvu II supplied with the kit. The reaction mixture of the DIG labelling of the sense, antisense and control RNA probes was generated by adding the reagents as tabulated in table 2.6. The reaction mixtures were PCR incubated at 37 ºC for two hours. After the incubation the reaction was stopped with 4 µl 0.2 M EDTA (pH 8.0). These were briefly mixed and pulse spun to collect everything at the bottom of the tube. 4.4 µl 4M Lithium chloride was added. 150 µl absolute ethanol was added to precipitate the labelled cRNA. This was briefly mixed and pulse spun to collect everything at the bottom of the tube. The reaction was then incubated at -20 ºC for 2 hours. After the incubation the precipitate was pelleted by centrifugation at 4 ºC for 15 minutes at 13 000 rpm. The supernatant was discarded and pellet washed with 200 µl cold 70 % ethanol by centrifuging at 13 000 rpm for 15 minutes at 4 ^{o}C after which the supernatant was carefully removed with a pipette to avoid losing the pellet. The pellet was then dried in a laminar flow for two hours. After two

hours the pellet was dissolved in 50 µl sterile DEPC treated water. The pellet was allowed to dissolve completely at 4 ºC for 1 hour. The DIG labelled cRNA transcripts were stored at -70 ºC in 10 µl aliquots.

Table 2.6: DIG labelling reaction mix

Reagent	Antisense cRNA	Sense cRNA	Control cRNA
LIAS (B) (2 µg)	10 µl	10 µl	-
LIAS (V1) (2 µg)	10 µl	10 µl	-
RPL9 (2 µg)	10 µl	10 µl	-
Control DNA PSPT 18-Neo/PvuII	-	-	
10X NTP labelling mix	2 µl	2 µl	-
10X Transcription buffer	2 µl	2 µl	2 µl
T7 RNA polymerase	2 µl	-	-
Sp6 RNA polymerase	-	2 µl	-
DEPC H_2O	4 µl	4 µl	
Total volume	20 µl	20 µl	

ADJUSTMENTS

RNAse inhibitor was not added as it requires high concentration of DDT (dithiotretiol) fro activity and DDT affects T7 and Sp6 activity.

DNAse was not used as it may not be RNAse free and also because it might leave too little DNA template to label.

2.3.14. Estimation of probe concentration

The concentration of anti-sense and sense probes was estimated by comparing the intensity of the spots with that of DIG labelled cRNA supplied with the kit. DIG user's guide (Roche Diagnostics, Germany) was used. Dilutions for labelled anti-sense, sense, DIG labelled cRNA to control DNA pSPT-18-Neo and control labelled cRNA supplied with kit were made as tabulated in table 2.7. Spot points corresponding to the number of probes and the number dilutions were marked lightly with a pencil on nylon membrane (Hybond). 1 µl of each dilution was spotted on the marked point on the membrane and allowed to air dry for 5 minutes at RT. The probes were fixed on the membrane by placing the membrane under UV light for 5 minutes. The membrane was washed with 1 X washing solution (Roche Diagnostics, Germany) while shaking for 5 minutes. The membrane was then incubated with 1 X blocking buffer to cover the membrane with shaking for 30 minutes (Roche Diagnostics, Germany). This was followed by incubating the membrane with Anti-DIG-Alkaline phosphatase (Roche Diagnostics, Germany) diluted in 1:10000 in 1 X blocking buffer for 30 minutes. The membrane was washed twice in 1X washing buffer to cover the membrane with shaking for 15 minutes for each wash. After washing, the membrane was incubated in 1 X detection buffer (Roche Diagnostics, Germany) with shaking for 2 minutes. The membrane was further incubated in NBT/BCIP (Roche Diagnostics, Germany) diluted in 1:50 detection buffer enough to cover the membrane while shaking. It was then allowed to develop overnight. The reaction was terminated in 50 ml TE buffer (pH 8.0) with shaking for 5 minutes. The membrane was air dried and probe concentrations estimated from that of the DIG labelled

cRNA provided with the kit by comparing the colour intensity of the spots that develop on the membrane.

Table 2.7. Dilutions for the estimation of the probe concentration

Dilution	DIG labelled cRNA	DIG labelled cRNA to the control DNA	Antisense and Sense probes
Initial Conc.	0.1 µg/µl	~50 ng/µl	
Dilution 1	1:5 1 µl + 4 µl SdH_2O		1:10 1 µl + 9 µl SdH_2O
Dilution 2	1:20 2 µl + 38 µl sdH_2O	1:5 2 µl + 38 µl sdH_2O	1:20 2 µl + 38 µl sdH_2O
Dilution 3	5 µl + 45 µl SdH_2O	5 µl + 45 µl SdH_2O	5 µl + 45 µl SdH_2O
Dilution 4	5 µl + 45 µl SdH_2O	5 µl + 45 µl SdH_2O	5 µl + 45 µl SdH_2O
Dilution 5	5 µl + 45 µl SdH_2O	5 µl + 45 µl SdH_2O	5 µl + 45 µl SdH_2O
Dilution 6	5 µl + 45 µl SdH_2O	5 µl + 45 µl SdH_2O	5 µl + 45 µl SdH_2O
Dilution 7	5 µl + 45 µl SdH_2O	5 µl + 45 µl SdH_2O	5 µl + 45 µl SdH_2O

For each dilution, the previous dilution was diluted in water to make the next dilution, i.e. dilution 3 = 5 µl dilution 2 plus 45 µl SdH_2O.

2.3.15. Procedure for In Situ Hybridization

This procedure can be divided into three major steps, pre-hybridization treatment of section, hybridization and post-hybridization. Pre-treatment is the step at which tissue sections are de-waxed and treated with various chemicals to reduce the background staining. Hybridization is the step at which the DIG labelled RNA bind to mRNA of interest in the tissue sections. Post-hybridization at which excess or unbound probe is washed off and probe bound to mRNA can be colorimetrically or fluorescently detected thus locating the gene at RNA level.

Two controls were used in this study. A negative control which was hybridization with the sense probe, thus allowing determining if localization was specific and if localization occurred when tissue sections were hybridized with anti-sense probe. The second control was the normal tissue section which is used to determine if there is any difference of expression in the cancer tissue section this being the main objective of the study.

2.3.15.1. Pre-hybridization treatment of sections

Prior to pre-treatment of sections, 0.5 % acetic anhydride and 4 % paraformaldehyde (PFA) in 100 mM phosphate buffer were freshly prepared and 1 X TBS chilled at 4 °C.

Tissue sections were de-waxed in fresh xylene (Saarchem, Merck Chemical (Pty) Ltd, Gauteng, South Africa) for 30 minutes (three changes of 10 minutes each) at RT. Tissue sections were then rehydrated in fresh absolute ethanol for 6 minutes which consisted of 2 changes of 3 minutes each at RT. This was followed by a further rehydration in 90 %,

70 %, 50 % ethanol and DEPC treated water for 3 minutes in each. Sections were fixed in freshly prepared 4 % PFA for 20 minutes at RT. They were then rinsed three times in fresh 1 X Tris Buffer Saline (TBS) consisting of 3 changes of 1 minute each at RT. Proteins were denatured in 0.1 M HCl for 10 minutes followed by rinsing 3 times in TBS which consisted of 3 changes of 1 minute each at RT. Non-specific binding was limited by incubating the section in 0.5 % Acetic Anhydride in 100 mM Tris (pH 8.0) for 10 minutes at RT. The sections were then rinsed 3 times in TBS (3 changes of 1 minute each). Cell membranes were permeabilized with 20 µg/ml Proteinase K (Roche Diagnostics, Germany) in 1 X TBS for 20 minutes The sections were rinsed 3 minutes in TBS (3 changes of 1 minute each) at RT. Proteinase K activity was terminate by incubating the sections in 4 °C TBS for 5 minutes. The sections were then dehydrated by incubating them in DEPC treated water, 50 %, 70 % and 90 % ethanol respectively for 1 minute in each. The sections were further dehydrated in absolute ethanol for 2 minutes (2 changes of 1 minute each) after which they were dried in chloroform for 10 minutes in fume cupboard. At this point the sections can be kept in a dry and dust free area.

2.3.15.2. Hybridization

In section 2.2.14 the minimal amount of both antisense and sense cRNA for LIAS and RPL9 probes that could be detected was 10 ρg. The dilutions were worked up to determine the concentration of the undiluted probes which was found to be 2 ng/µl.

1 µl of each probe (sense and anti-sense) was added to 900 µl of hybridization buffer. This was followed by boiling of the solution for 5 minutes and placed immediately on ice

for 2 minutes. Thereafter, 100 µl of the hybridization mix was placed on each slide and allowed to hybridize overnight in a humidity chamber at 55 ºC. To limit evaporation of hybridization mix, a solution of 5 X SSC (3M NaCl, 0.3 M Na-citrate, pH 7.0) buffer and 50 % formamide was prepared and poured into the hybridization chamber.

2.3.15.3. Post-Hybridization

After hybridization, sections were subjected to various concentrations of SSC to wash-off excess probe. Firstly the sections were washed in 2 X SSC for 30 minutes at 37 ºC in hybridization oven. Sections were further washed in 1 X SSC, 0.5 X SSC and 0.1 X SSC for 20 minutes each at 55 ºC. The slides were rinsed in TBS for 3 minutes consisting of 3 changes of 1 minute each at RT. Non-specific binding was blocked by incubating the sections with 100 µl of 1 X blocking solution to each slide in a humid chamber for 2 hrs at RT. The protocol here after varies depending on the detection method to be used.

2.3.15.3.1. Colorimetric Detection

DIG-labelled RNA probes that have hybridized to the target sequence can be detected colorimetrically with alkaline phosphatase conjugated to anti-DIG. Incubating the sections with a suitable substrate such as NBT/BCIP allow for alkaline phosphatase activity which results in the formation of a purple/blue precipitate that can be viewed under light microscope.

The sections were incubated with 100 µl anti-DIG IgG conjugated with alkaline phosphatase diluted in 1:500 1 X blocking solution per slide in a humid chamber for 1 hr

at RT. The slides were rinsed in TBS for 3 minutes (3 changes of 1 minute each) at RT. Thereafter the sections were incubated with 100 µl chromogen NBT/BCIP diluted 1:50 in 1 X detection buffer. 100 µl was added to each slide and left to develop in a dark humid chamber overnight at RT. The reaction was stopped by incubating the slides in 1 X TE buffer for 5 minutes. The slides were then washed in running tab water for 5 minutes at RT. Tissue sections were counterstained with 5 drops of Mayer's Haematoxylin per slide for 5 minutes followed by washing in running tap water for 10 minutes. Thereafter the sections were mounted with glycerine jelly and allowed to dry at RT. Tissue sections were then viewed and images captured using the Zeiss Microscope Camera and Axio software package.

2.3.15.3.2. Fluorescent Detection

Alternatively, DIG-labelled RNA probes hybridized to the target sequence was detected fluorescently with fluorescein isothicyanate (FITC) conjugated to anti-DIG. FITC does not require the presence of a suitable substrate in order to emit a colour precipitate. FITC is excited at 490 nm resulting in the emission apple green colour which can be viewed under a fluorescent microscope.

The slides were washed in briefly in TBS-Tween for 5 minutes followed by incubation in TNB for 30 minutes at 37 ºC. The slides were then incubated in 75 µl of anti-DIG IgG conjugated with FITC diluted 1:500 in TBS-Tween for 30 minutes at 37 ºC. Thereafter the slides were washed in TBS-Tween for 15 minutes (3 changes of 5 minutes each). The slides were then mounted with SlowFade Light Antifade Kit (Molecular Probes) and the

manufacture's instructions were followed. A drop of component C which is an equilibration buffer was placed on the section each section and incubated at RT for 10 minutes or until dry. Then a drop of component A was placed on the each section and covered with a coverslip. The slides were viewed immediately under fluorescent microscope and images captured using Zeiss Microscope Camera and Axio software package.

2.4. Real Time Polymerase Chain Reaction

Real Time Polymerase Chain Reaction (RT-PCR) was developed because of a need to quantitate differences in mRNA expression. It quantitates the initial amount of the template most specifically, sensitively and reproducibly as it monitors the real-time progress of PCR and is a preferable alternative to other forms of quantitative RT-PCR as they detect the amount of final amplified product at the end point (Freeman, 1999). RT-PCR can be used to calculate the number of particles e.g. viral copy in a given amount of blood or the fold difference of a target nucleic acid in an equivalent amount of tests and control samples. These analysis methods are referred to as absolute and relative quantification respectively.

The RT-PCR system is based on the fluorescence reporter. RT-PCR monitors the fluorescence emitted during the reaction as an indicator of amplicon production during each PCR cycle (i.e. Real Time) as opposed to the end point detection (Huguchi, 1993). This signal increases in direct proportion to the amount of PCR product formed after every cycle. Initially fluorescence remains at the background levels and increases in fluorescence are not detectable even though product accumulates exponentially.

Eventually enough amplified product accumulates to yield a detectable fluorescence signal. The cycle at which this occurs is called the threshold cycle (C_T) which is defined as the cycle at which the fluorescence emission exceeds the fixed threshold. The use of threshold cycle (C_T) value makes RT-PCR to be more precise. Fluorescence values are recorded during every cycle and represent the amount of product amplified to that point in the amplification reaction. The more templates present at the beginning of the reaction, the fewer number of cycles it takes to reach a point in which the fluorescent signal is first recorded as statistically significant above background. C_T value measured during the 3-15 cycles indicates the detection of accumulated PCR product. A C_T value of 40 or higher means no amplification and this value cannot be used for calculations.

SYBR Green is one of the fluorescence reporter used in Real Time PCR. Its chemistry provides the simplest format for detecting and quantitating PCR products in real time reactions. SYBR Green is a dye that binds the minor grooves of a double stranded DNA. When SYBR Green dye binds to a double stranded DNA, the intensity of the fluorescence emission increases. As more double stranded amplicons are produced, SYBR Green dye signal will increase. Thus, as a PCR product accumulates, the fluorescence increases.

The disadvantage of SYBR Green dye is that it binds to any double stranded DNA in the reaction including primer-dimers and other non-specific reaction products, which results in the overestimation of the target concentrations. For that reason SYBR green reactions should be optimised to be sensitive and specific. Amplicon size must also be optimised. Shorter amplicons of about 75-200 bp are typically amplified with higher efficiency. Beacon Designer software performs both primer design and amplicon selection. The

efficiency and the reproducibility of a SYBR Green assay can be determined by constructing a standard curve using serial dilutions of known template. The efficiency should be 90-105 %. Coefficient of determination (R^2) can also be used to evaluate whether the RT-PCR is optimised. R^2 value of a standard curve represents how well the experimental data fit the regression line (i.e. how linear the data is). R^2 Value should be greater than 0.980 for quantitative RT-PCR reactions. Melting curves are used to check for the specificity of the primers. Non-specificity of the primers can be detected by multiple picks on the melting curve.

Bio-Rad MJ Mini-Opticon Personal Thermal Cycler (Bio-Rad Laboratories, Hercules, CA, USA) was used to run the quantitative Real Time PCR (qRT-PCR). Primers were designed using Beacon Designer software and sequences are as tabulated in table 2.8. RNA was extracted from MRC5 and A549 cell lines as described in section 2.2.1 and cDNA synthesised using ImProm-II^{TM} Reverse Transcription (Promega Corporation, Madison, WI, USA). Manufacturer's protocol was followed and the reaction carried out as described in section 2.2.3. cDNA was diluted 20 times (1 µl cDNA + 19 µl sdH_2O) and quantified using a spectrophotometer (Amersham Pharmacia Biotech, Picataway, NJ, USA) at 260 nm and the following equation was used to calculate cDNA concentration:

$c = A_{260} \times [A_{260}$ ds DNA$] \times DF$

A_{260} ds DNA = 50 µg/ml

DF = 20

Table 2.8: Primer sequences used for Relative qRT-PCR

Gene	Primer	Sequence (5' to 3')
RPL9	Forward	ttacactgggcttccgttac
	Reverse	gcaacacctggtctcatcc
LIAS	Forward	ttcgtgaggcagatgtagac
	Reverse	tatatgaagaacgcaccaaagg

2.4.1. Optimisation of primers

Temperature gradient was run to optimise the annealing temperature of the primers followed by a melting curve analysis to assess the specificity of the primers.

Table 2.9: Reaction components for primer optimization

Reagent	Volume	Final Concentration
iQ™SYBR Green Mix I (Bio-Rad Laboratories, Hercules, CA,USA)	12.5 µl	1 X
Forward Primer	1 µl	0.4 ρmol/ µl
Reverse Primer	1 µl	0.4 ρmol/ µl
cDNA	*x*	1 µg
sdH_2O	*y*	
Total Volume	25 µl	

x and y - Variable depending on the concentration of the template (cDNA).

Conditions:

Activation: 94 ^{o}C……5 minutes

Amplification: Denaturation: 94 ^{o}C……...30 seconds

Annealing: 55-59 ^{o}C …….30 seconds

} 40 cycles

Extension: 72 ^{o}C…….. 30 seconds

Plate read

Final Extension 72 ^{o}C …….. 10 minutes

Melting temperature analysis: 55-99 ^{o}C – 1 ^{o} increment, hold for 10 seconds at each temperature

2.4.2. Standard curve generation

To assess the amplification efficiency of Quantitative Real Time PCR, serial dilutions of the cDNA were used to generate standard curves. Five fold dilution series of the cDNA were made as tabulated in table 2.10.

Table 2.10: cDNA Dilutions for generating a standard curve.

Dilution	Concentration	Volume cDNA
1 X	1135 ng/µl	1 µl
5 X	227 ng/µl	1 µl 1X + 4 µl sdH_2O
25 X	45.8 ng/µl	1 µl 5X + 4 µl sdH_2O
125 X	9.08 ng/µl	1 µl 25X = 4 µl sdH_2O

Following the serial dilutions qRT-PCR was run. iQ^{TM} SYBR Green I Mix (Bio-Rad Laboratories, Hercules, CA, USA) was used and the reagents components are as in table 2.11.

Table 2.11: Reagent component for the standard curve

Reagent	Volume	Final Concentration
iQ^{TM}SYBR Green Mix I (Bio-Rad Laboratories, Hercules, CA,USA)	12.5 µl	1 X
Forward Primer	1 µl	0.4 ρmol/ µl
Reverse Primer	1 µl	0.4 ρmol/ µl
cDNA (1 X, 5 X, 25 X, 125 X)	1 µl	1135 ng, 227 ng, 45.4 ng, 9.08 ng
sdH_2O	9.5 µl	
Total Volume	25 µl	

Conditions:

Activation: 94 °C……5 minutes

Amplification: Denaturation: 94 °C…….. 30 seconds

Annealing: 57 °C LIAS/… 30 seconds

58 °C RPL9…30 seconds

Extension: 72 °C…….. 30 seconds

Plate read

} 40 cycles

Final Extension 72 °C…….. 10 minutes

Amplification Efficiency (E) of the assay was calculated from slope of the standard curve and converted to % Efficiency using the following formulas:

$E = 10^{-1/slope}$

% E = (E-1) x 100 %

2.4.3. Relative quantitative Real Time Polymerase Chain Reaction

After the efficiency and annealing temperature of the primers were optimised, relative qRT-PCR normalised against the unit mass was carried out. MRC5 was used as a calibrator and A549 as a test.

Table 2.12: Relative qRT-PCR reaction components

Reagent	Volume	Final Concentration
iQ™SYBR Green Mix I (Bio-Rad Laboratories, Hercules, CA,USA)	12.5 µl	1 X
Forward Primer	1 µl	0.4 ρmol/ µl
Reverse Primer	1 µl	0.4 ρmol/ µl
cDNA	*x*	1 µg
sdH_2O	*y* µl	
Total Volume	25 µl	

x and y - Variable depending on the concentration of the template (cDNA).

Conditions:

Activation: 94°C……5 minutes

Amplification: Denaturation: 94 °C…….. 30 seconds

Annealing: 57 °C LIAS/… 30 seconds

58 °C RPL9…30 seconds

Extension: 72 °C…….. 30 seconds

Plate read

} 40 cycles

Final Extension 72 °C…….. 10 minutes

The following equation was used to calculate the ratio of expression of RPL9 and LIAS in lung adernocarcinoma A549 (Test) relative to lung normal fibroblast MRC5 (calibrator)

$$Ratio_{(test/calibrator)} = E^{CT\ (calibrator) - CT(test)TM}$$

2.5. TUNEL

One of the changes that occur during apoptosis is nuclear fragmentation which results in a large number of DNA fragments. These fragments can be detected by labelled 3' OH termini with biotin. The reaction is catalysed by exogenous terminal deoxynucleotide transferase (Tdt). Streptavidin labelled with horse-peroxidase (HRP) is bound to these nucleotides and in the presence of diaminobenzidine (DAB), apoptotic nuclei are stained dark brown.

The Promega DeadEnd^{TM} colorimetric TUNEL system kit (Promega Corporation, Madison, WI, USA) was used. Sections were dewaxed in two changes of xylem for ten minutes each. The sections were then rehydraded in two changes of fresh absolute ethanol for five minutes each. This was followed by a further rehydration in 95 %, 85 %, 70 % and 50 % ethanol for three minutes each. The sections were washed with 0.85 % sodium chloride for five minutes followed by a wash in 1% PBS for five minutes. Sections were fixed in 4 % PFA for 15 minutes followed by three washes in PBS for three minutes each. 100 µl of Proteinase K (Roche diagnostics, Germany) (20µg/µl) diluted 1:500 with PBS was added to each section and incubated for 20 minutes. This was washed off by immersing the sections in PBS for five minutes. The sections were

immersed in 4% PFA for five minutes and then washed in two changes of PBS for five minutes each. 100 µl of equilibration buffer was added to each slide for ten minutes. 1 µl of bionylated mix and 1 µl of Tdt enzyme were added to 98 µl of equilibrated buffer. 100 µl of the mix was added to each slide and incubated fro an hour in a humidity chamber at 37 °C. The sections were then immersed in 2X SSC for 15 minutes followed by three changes of PBS for five minutes each. 100 µl of 0.3 % hydrogen peroxidase was added to each section and incubated for five minutes. The sections were washed in three changes of PBS for five minutes each. 100 µl streptavidin HRP diluted 1:500 in PBS was added to each section and incubated for 30 minutes. After the incubation the sections were immersed in three changes of PBS for five minutes each. 100 µl of the prepared DAB solution was added to each section and incubated until a light brown colour developed. The sections were rinsed in three changes of deionised water followed by dehydration in 50 %, 70 %, 85 % and 95 % ethanol for one minute each. They were further dehydrated in two changes of absolute ethanol for one minute each and immersed in xylene for one minute. The slides were mounted in xylene-based entellan and viewed under a light microscope. The Zeiss camera and Axio software package were used to capture the images.

2.5.1. Controls

For a negative control, Tdt was not added to the sections and for a positive control the sections were treated with DNAse to allow for a fragmentation of the DNA.

2.6. Bioinformatics

To study the interaction of RPL9 and LIAS with other proteins, the Bioinformatics tool BONDplus (Biomolecular Network Database plus) was used. The software interact GENESEQ^{TM} and BINDplus to explain all the relevant biological relationships of the molecule of interest. GENESEQ^{TM} contains high quality easy to understand annotated genetic patented sequences covering genetic discovery. BINDplus contains prominent as well as the latest published low throughput and high throughput interactions documented according to rigorous data curation standards.

Gene Identification (Gene ID) for RPL9 and LIAS were obtained from the National Centre for Biotechnology Information (NCBI) database (http://www.ncbi.nlm.nih.gov). The Gene ID was used on the BONDplus database to search for any interaction discoveries of the two genes.

2.6.1. Gene Conservation

To assess the conservation of RPL9 and LIAS through species, NCBI database was used to retrieve gene homologues of the genes under investigation. Protein sequences in FASTA format of the closest to RPL9 and LIAS by species were retrieved and aligned using CLUSTAL 2.0.3 multiple alignment software.

3. Results

3.1. Expression of LIAS and RPL9 in human lung cancer.

3.1.1. In Situ hybridization

Localization of RPL9 and LIAS RNA was achieved by the fluorescence and colorimetric detection of anti-sense DIG-labelled RNA probes. Anti-DIG conjugated alkaline phosphatase was used for colorimetric detection of the DIG labelled anti-sense probes in the presence of the substrate NBT/BCIP while anti-DIG conjugated FITC was used for fluorescence detection. The enzymatic activity of NBT/BCIP substrate and alkaline phosphatase conjugated anti-DIG results in a purple/blue precipitate. FITC does not require the presence of a substrate; it emits an apple green light when excited at a wavelength of 490nm. The expression of RPL9 and LIAS was determined by comparing tissue sections localised with a DIG-labelled anti-sense probe to those labelled with a DIG labelled sense probes. The following steps were done for in situ hybridization.

3.1.1.1. RNA extraction

Total RNA was extracted using the Trizol^{TM}LS reagent method (section 2.3.1) and the quality of the extracted RNA was analysed on 1% (w/v) formaldehyde agarose gel electrophoresis (section 2.3.2).

3.1.1.2. Polymerase Chain Reaction

RNA obtained was used to synthesis cDNA by reverse transcription PCR as described in section 2.3.3. Synthesised cDNA was used as a template to amplify 165 bp RPL9 and 190 bp LIAS region of interest using gene specific primers (section 2.3.4 and 2.3.5). The

results were analysed on 0.1 % agarose gel electrophoresis (Figure 3-6). RPL9 and LAIS amplified bands were found to be 165 bp (lane 4-7) and 190 bp (lane 8-12) long respectively. cDNA was substituted by nuclease free H_2O in the negative control and the results were positive as no band is observed in negative control lane (lane 2 for RPL9 and lane 3 for LIAS).

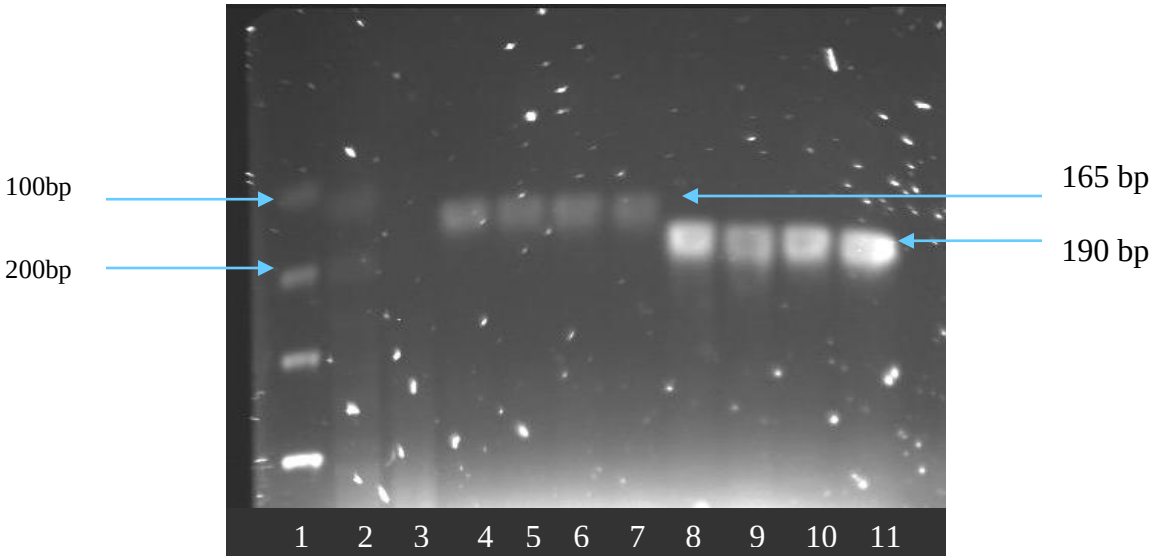

Figure 3-1: Polymerase Chain Reaction

Lane 1 indicates the molecular weight marker. Lane 2 represents the negative control for RPL9 and lane 3 LIAS were cDNA was replaced by nuclease free H_2O. Lane 4-7 represents the amplification of RPL9 while lane 8-12 represents the amplification of LIAS.

3.1.1.3. Cloning of RPL9 and LIAS into p-GEM T Easy

As described in section 2.3.8 PCR products of RPL9 and LIAS were ligated into p-GEM T Easy cloning vector that contains the 3'-T overhangs which allows for easy ligation with Poly (A) Tail of PCR product, the multiple cloning site for restriction digestions and the ampicillin resistant domain used as a selective markers. Ligated clones were transformed into MC1061 *E. coli* competent cell

3.1.1.4. Colony PCR

After cloning positive colonies were selected by colony PCR. Colonies were randomly selected on the ampicillin nutrient agar plates and resuspended in 10µl sdH_2O. The colony mix was used as a template and the region of interest amplified using LIAS and RPL9 specific genes. Results were analysed on 0.8% agarose (Figure 3-7). The insert was present and was found to be the right size for both RPL9 and LIAS, 165 bp and 190 bp long respectively as expected figure.

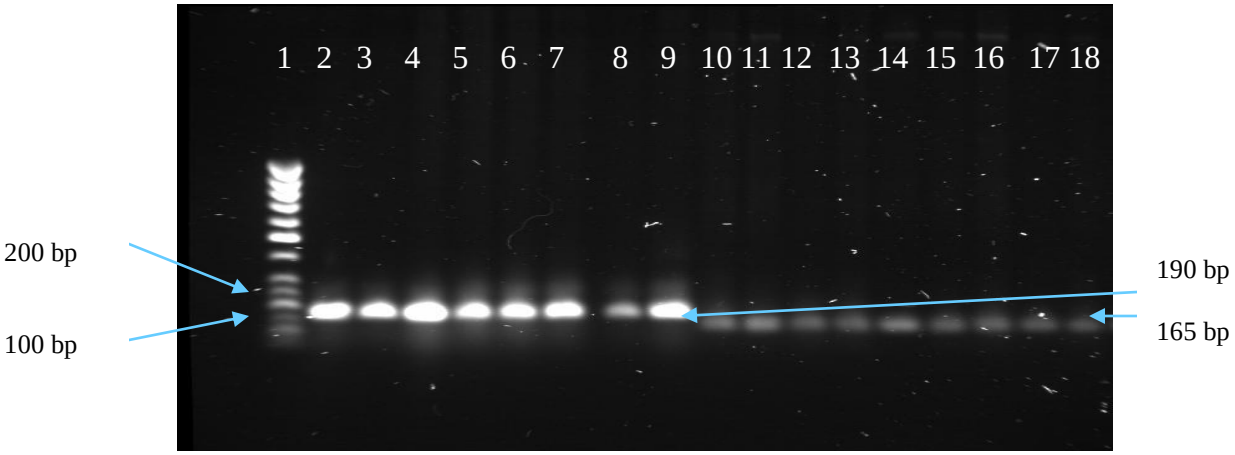

Figure 3-2: Colony Polymerase Chain Reaction

Lane 1 indicate the molecular weight marker. Lane 2-9 shows the presents of LIAS insert from colonies randomly selected from NA-ampicillin plate while lane 10-18 indicates the presents of RPL9 insert.

3.1.1.5. Plasmid DNA extraction and sequencing

Positive colonies which were selected by the presence of the insert by colony PCR were used to inoculate an overnight culture. Plasmid DNA was extracted using the WizardPlus® SV Miniprep Purification System (Promega Corporation, Madison, WI, USA). The purified LIAS and RPL9 recombinant clones were sent to Inqaba biotechnical Industries (RSA) for sequencing to check if the inserts were present, if they were the right sequence and to also check the orientation of the insert. The results showed that the correct insert for both RPL9 and LIAS was present in the recombinant plasmid DNA. This is indicated by the sequence alignment using the reference sequences for RPL9 and LIAS obtained from the National Centre for Biotechnology Information (Figure 3-8). After confirmation of the presence of the correct cloned, the recombinant plasmid DNA was extracted for probe synthesis.

A

```
 Score =  317 bits (165),  Expect = 2e-83
 Identities = 165/165 (100%), Gaps = 0/165 (0%)
 Strand=Plus/Plus

Query  18   CTCCGGGTTGACAAATGGTGGGGTAACAGAAAGGAACTGGCTACCGTTCGGACTATTTGT  77
            ||||||||||||||||||||||||||||||||||||||||||||||||||||||||||||
Sbjct  222  CTCCGGGTTGACAAATGGTGGGGTAACAGAAAGGAACTGGCTACCGTTCGGACTATTTGT  281

Query  78   AGTCATGTACAGAACATGATCAAGGGTGTTACACTGGGCTTCCGTTACAAGATGAGGTCT  137
            ||||||||||||||||||||||||||||||||||||||||||||||||||||||||||||
Sbjct  282  AGTCATGTACAGAACATGATCAAGGGTGTTACACTGGGCTTCCGTTACAAGATGAGGTCT  341

Query  138  GTGTATGCTCACTTCCCCATCAACGTTGTTATCCAGGAGAATGGG  182
            |||||||||||||||||||||||||||||||||||||||||||||
Sbjct  342  GTGTATGCTCACTTCCCCATCAACGTTGTTATCCAGGAGAATGGG  386
```

B

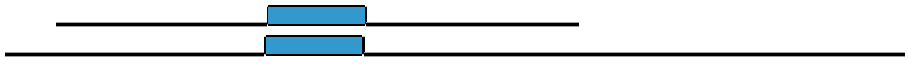

```
 Score =  365 bits (190),  Expect = 8e-98
 Identities = 190/190 (100%), Gaps = 0/190 (0%)
 Strand=Plus/Minus

Query  45   ACAAGGATTTTTGGATTCCTTTCCTTTAAATATGATACGGTCTTTGCAATGTGTTCAGCT  104
            ||||||||||||||||||||||||||||||||||||||||||||||||||||||||||||
Sbjct  699  ACAAGGATTTTTGGATTCCTTTCCTTTAAATATGATACGGTCTTTGCAATGTGTTCAGCT  640

Query  105  CCCCCATCAGGCATATCATCTCGATCCACAGATGTCAGGACAACATAATCCAGACCCCAT  164
            ||||||||||||||||||||||||||||||||||||||||||||||||||||||||||||
Sbjct  639  CCCCCATCAGGCATATCATCTCGATCCACAGATGTCAGGACAACATAATCCAGACCCCAT  580

Query  165  TCTGCAATTGCCTTTGCAGTATTGTAGGGCTCACTGGCATCCAGTGGAGGAGGATTTCTT  224
            ||||||||||||||||||||||||||||||||||||||||||||||||||||||||||||
Sbjct  579  TCTGCAATTGCCTTTGCAGTATTGTAGGGCTCACTGGCATCCAGTGGAGGAGGATTTCTT  520

Query  225  GCAGTCTTAA  234
            ||||||||||
Sbjct  519  GCAGTCTTAA  510
```

Keywords: Query -Reference sequence; Sbjct -Recombinant sequence

Figure 3-3. Sequence alignment of RPL9 and LIAS genes

The clone sequences obtained from Inqaba Biotech was aligned to reference sequences for RPL9 (accession number: BC100285) and LIAS (accession number: BC062751) attained from National Centre for Biomedical Information (NCBI). Both RPL9 (A) and LIAS (B) cloned sequences were found to be 100% identical to their specific reference sequence. The length of the sequences also corresponded with the predicted which was 165bp and 190bp long for RPL9 and LIAS respectively (Table 2.2)

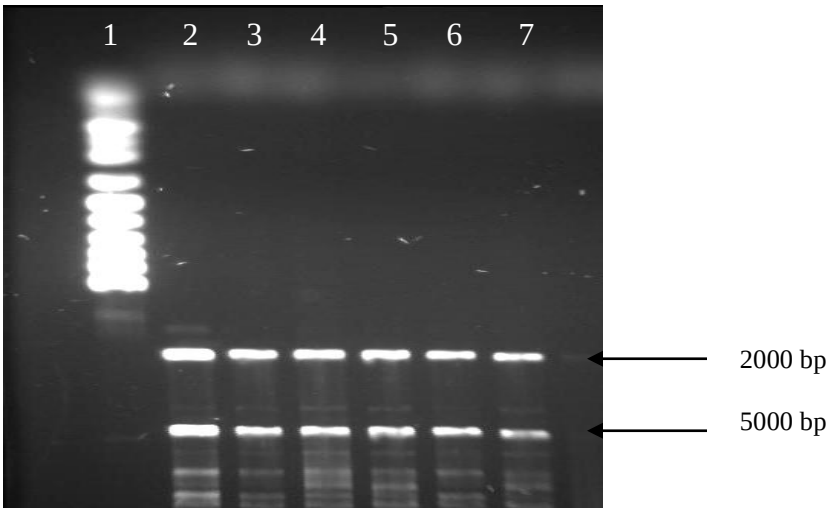

Figure 3-4: Plasmid DNA extraction

Lane 1 indicates molecular weight marker. Lane 2-4 represents a RPL9 clone while lane 5-7 represents LIAS clone. The variable band sizes indicate the different states of the plasmid that varies from tightly coiled to completely relaxed.

3.1.1.6. Linearisation of clones and DIG labeling of probes

The purified clone containing the correct gene and sequence was used as a template for synthesis on DIG labeled probes. PstI was used to generate an anti-sense probe while ApaI was used to generate the sense probe. Figure 3-5 and Figure 3-6 shows the linearization of RPL9 and LIAS clones respectively. The linearised clones (lane 3 and lane 4) were purified from the agarose gel and used as templates for probe synthesis.

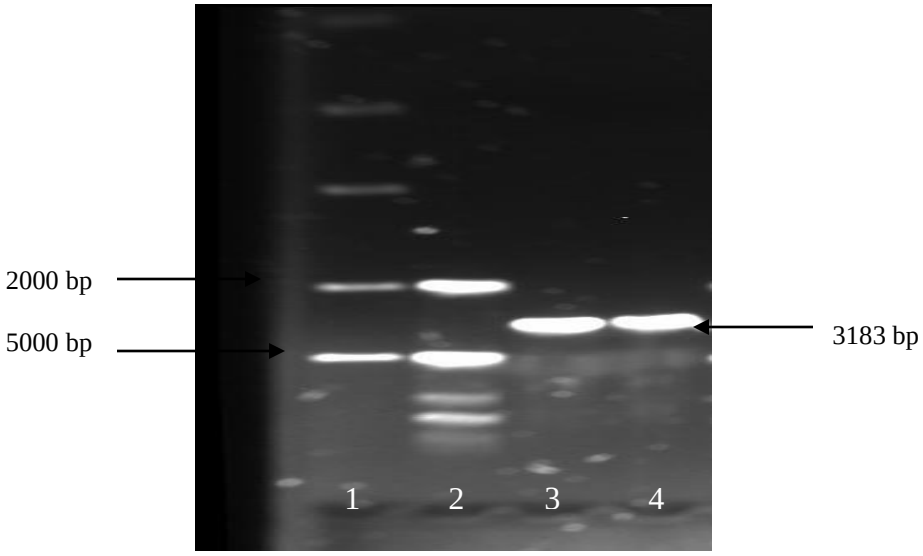

Figure 3-5: Restriction digestion RPL9 clone

Lane 1 shows the DNA molecular weight marker. Lane 2 represents the undigested clone. Lane 3 is the clone digested with Pst1 while in lane 4 is the clone digested with Apa1

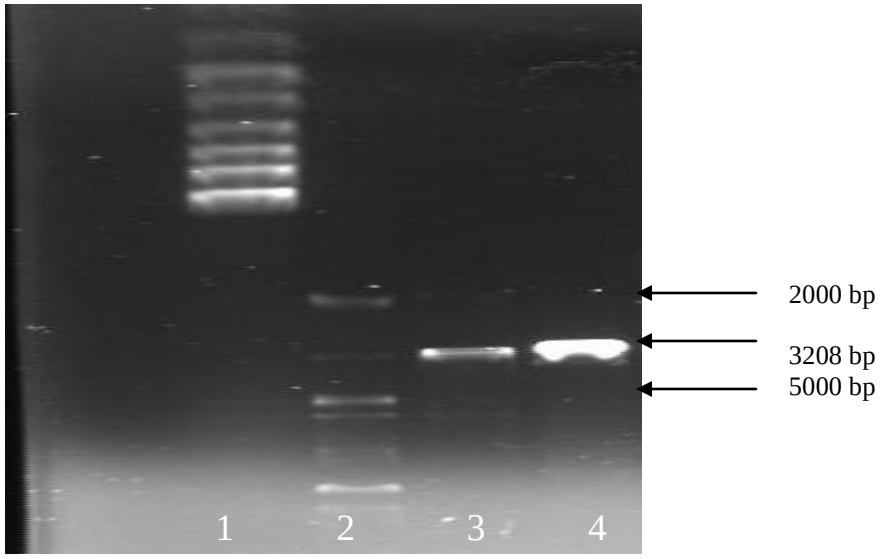

Figure 3-6: Restriction digestion of LIAS clone

Lane 1 represent DNA molecular weight marker. Lane 2 is the undigested clone. Lane 3 is the clone digested with Pst1 while lane 4 is the clone digested with Apa1.

3.1.1.7. Ribosomal Protein L9 and Lipoic Acid Synthetase genes localisation

Localization of RPL9 and LIAS RNA was achieved by the fluorescence and colorimetric detection of an anti-sense DIG-labelled RNA probes. Anti-DIG conjugated alkaline phosphatase was used for colorimetric detection of the DIG labelled anti-sense probes in the presence of the substrate NBT/BCIP while anti-DIG conjugated FICT was used for fluorescence detection. The enzymatic activity of NBT/BCIP substrate and alkaline phosphatase conjugated anti-DIG results in a purple/blue precipitate. FITC does not require the presence of a substrate; it emits an apple green light when excited at a wavelength of 490nm.

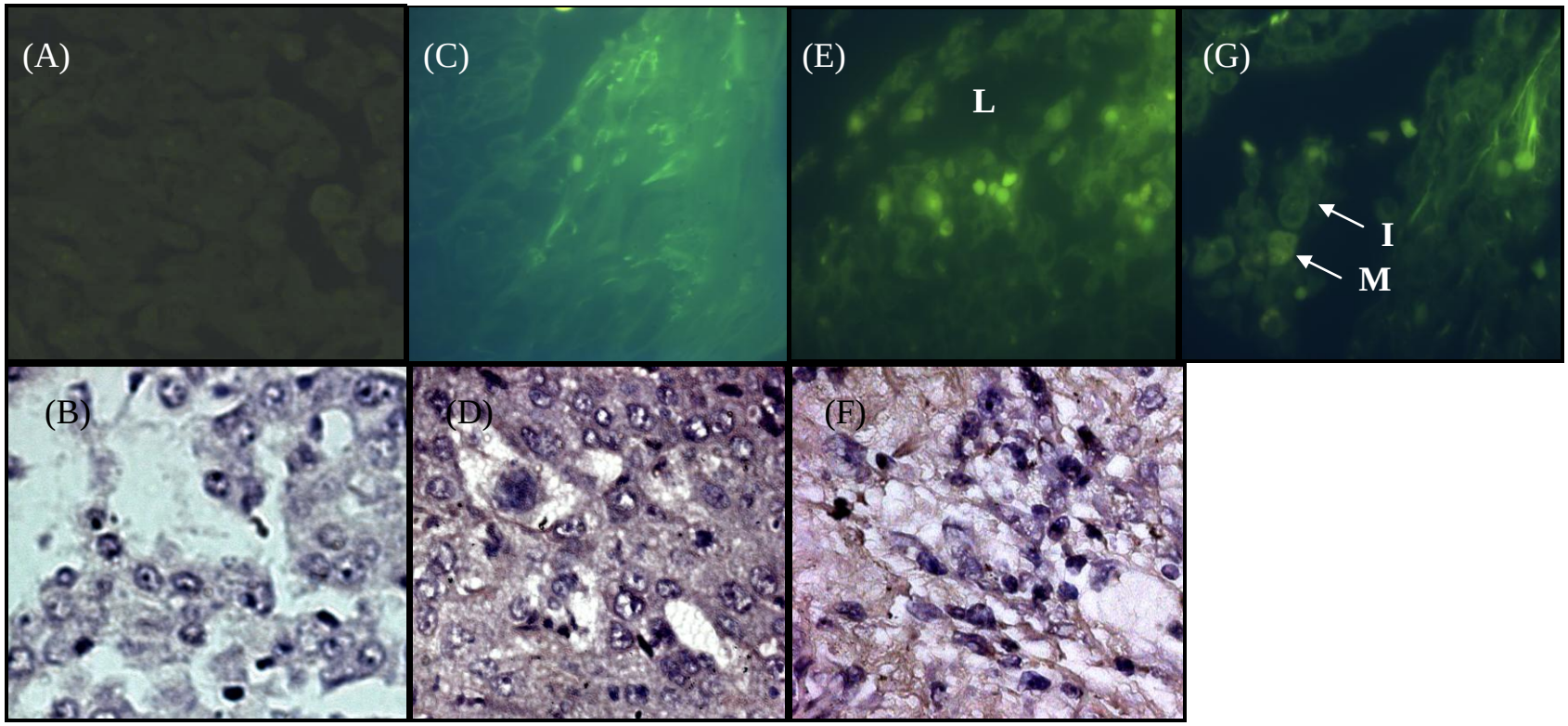

Figure 3-7: Localisation of RPL9 mRNA in Squamous Cell Lung Carcinoma

(A) and (B) represents the negative control, localisation with sense probe which shows no expression of RPL9. In all the three grades of the squamous cell lung carcinoma (C and D, poor differentiated; E and F, moderately differentiated; and G well differentiated) RPL9 mRNA in expressed in the cytoplasm of the type I pneumocytes **(I)**. RPL9 is also expressed in the cytoplasm of the lymphocytes **L** and Macrophages **M**. (Magnification 400X)

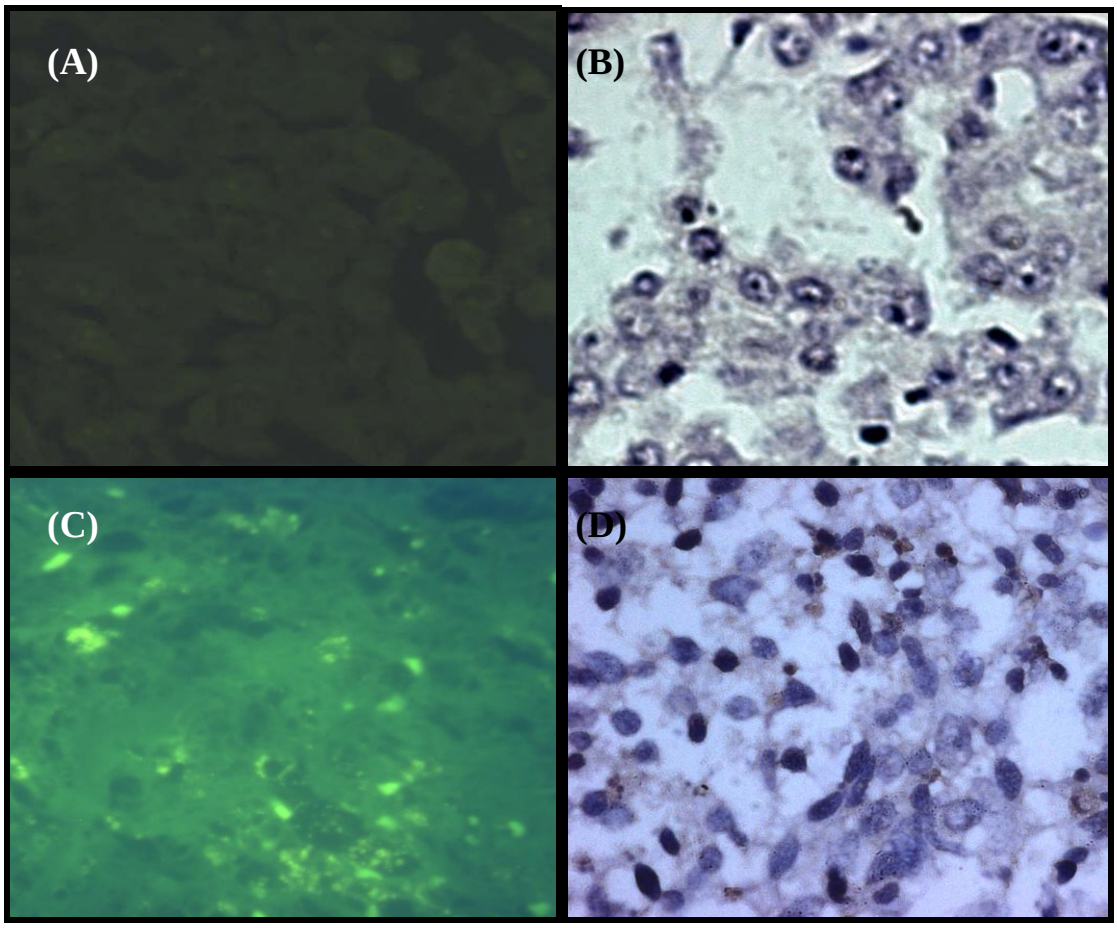

Figure 3-8: Localisation of RPL9 mRNA in Small Cell Lung Carcinoma

(A) and (B) represents the negative control, localisation with sense probe which shows no expression of RPL9. RPL9 is expressed in the cytoplasm of the small cell lung carcinoma tumour cell (C and D) which resembles the lymphocytes. (400X Magnification)

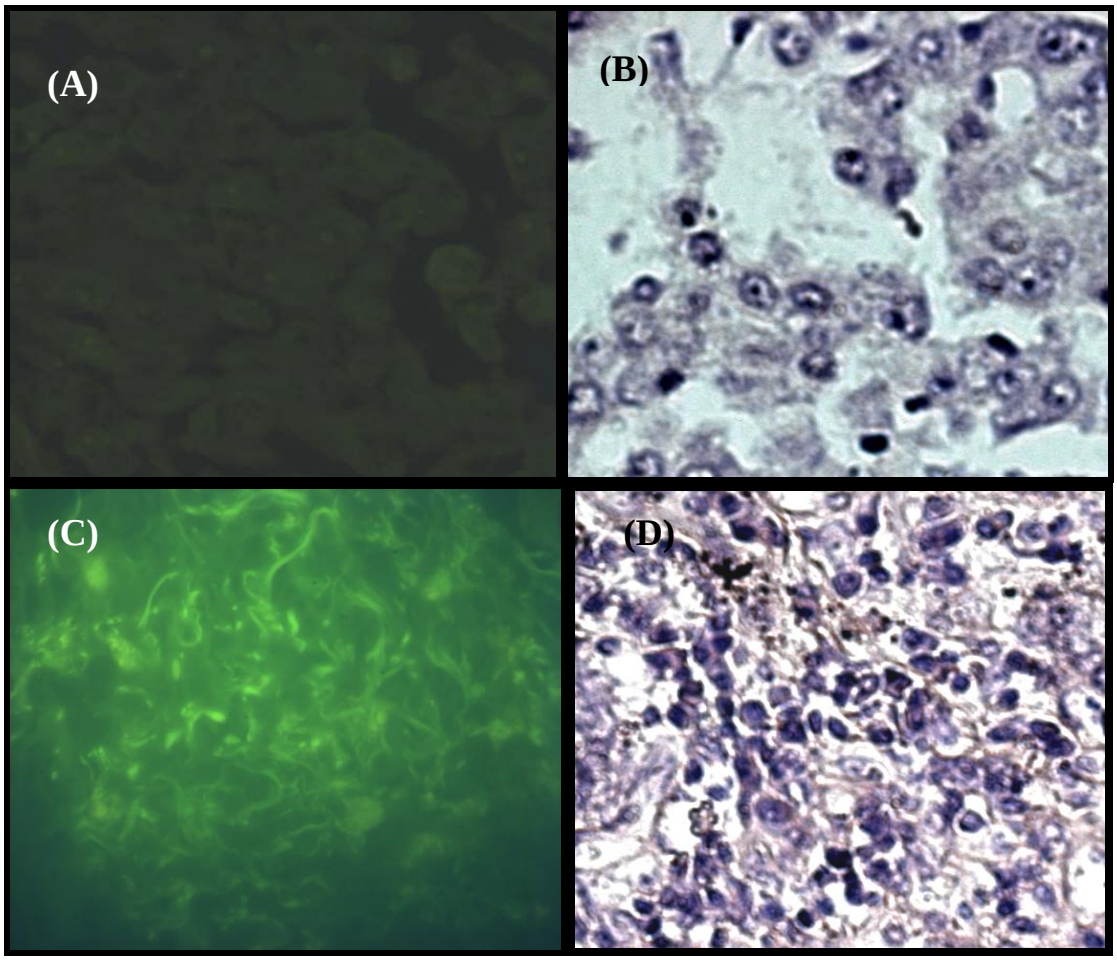

Figure 3-9: Localisation of RPL9 mRNA in Large Cell Lung Carcinoma

(A) and (B) represents the negative control, localisation with sense probe which shows no expression of RPL9. C and D show a high expression of RPL9 in the cytoplasm of the tumour cells and fibres in the surrounding stroma. The cells show no defined pattern between Squamous Cell lung Carcinoma and Lung Adenocarcinoma which is a principle characteristic of Large Cell Lung Carcinoma. (Magnification 400X)

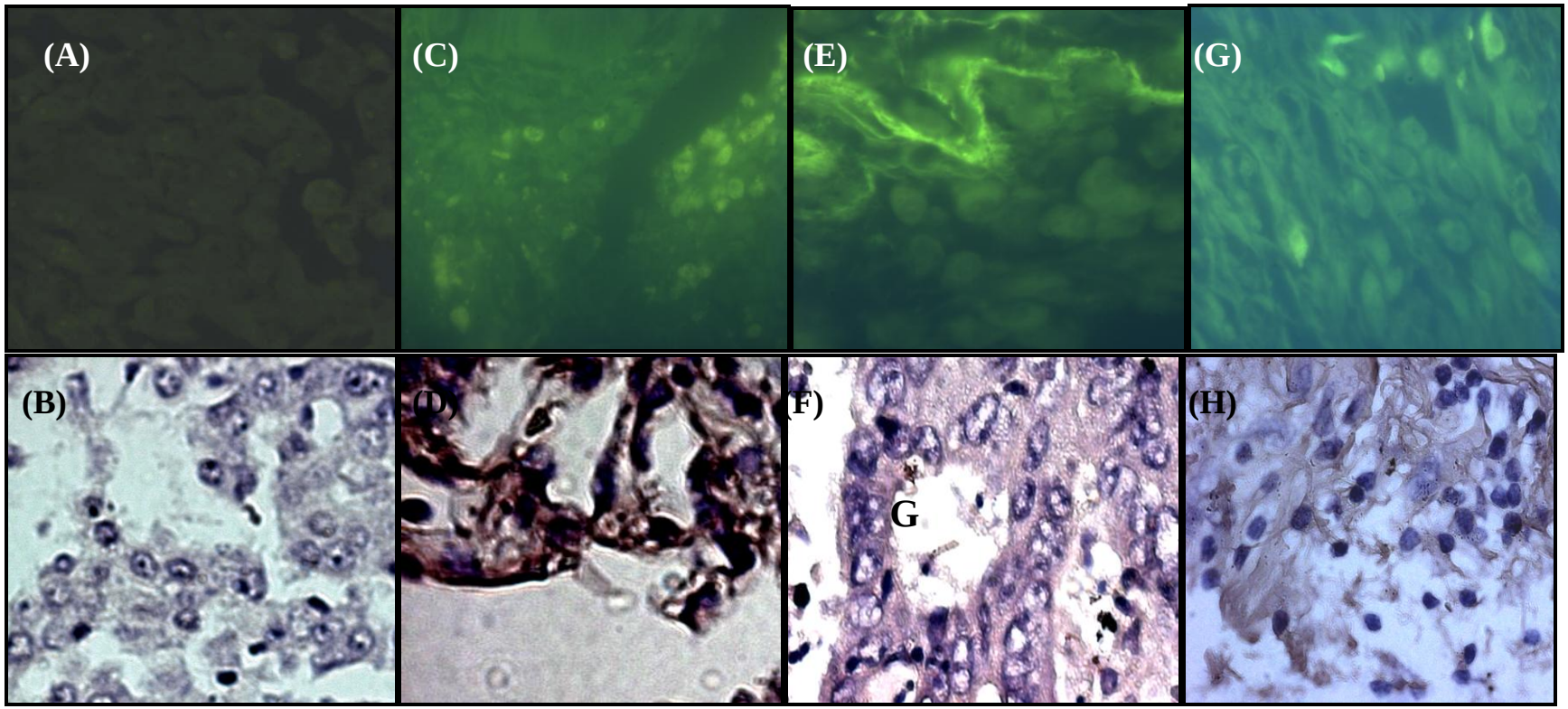

Figure 3-10: Localisation of RPL9 mRNA in Lung Adenocarcinoma

(A and B) represents the negative control, localisation with sense probe which shows no expression of RPL9. RPL9 is localised by a sense probe in the different grades of the tumour tissue. Grade I, poor differentiated (C and D); Grade II, moderately differentiated (E and F) and Grade III, well differentiated (G and H). RPL9 mRNA is expressed in the cytoplasm of the columnar ciliated cells of the bronchial gland **G** which is clearly represented in the moderately differentiated grade (E and F). As the tumour progresses, cells tend to grow in sheets (G and H). (Magnification 400X)

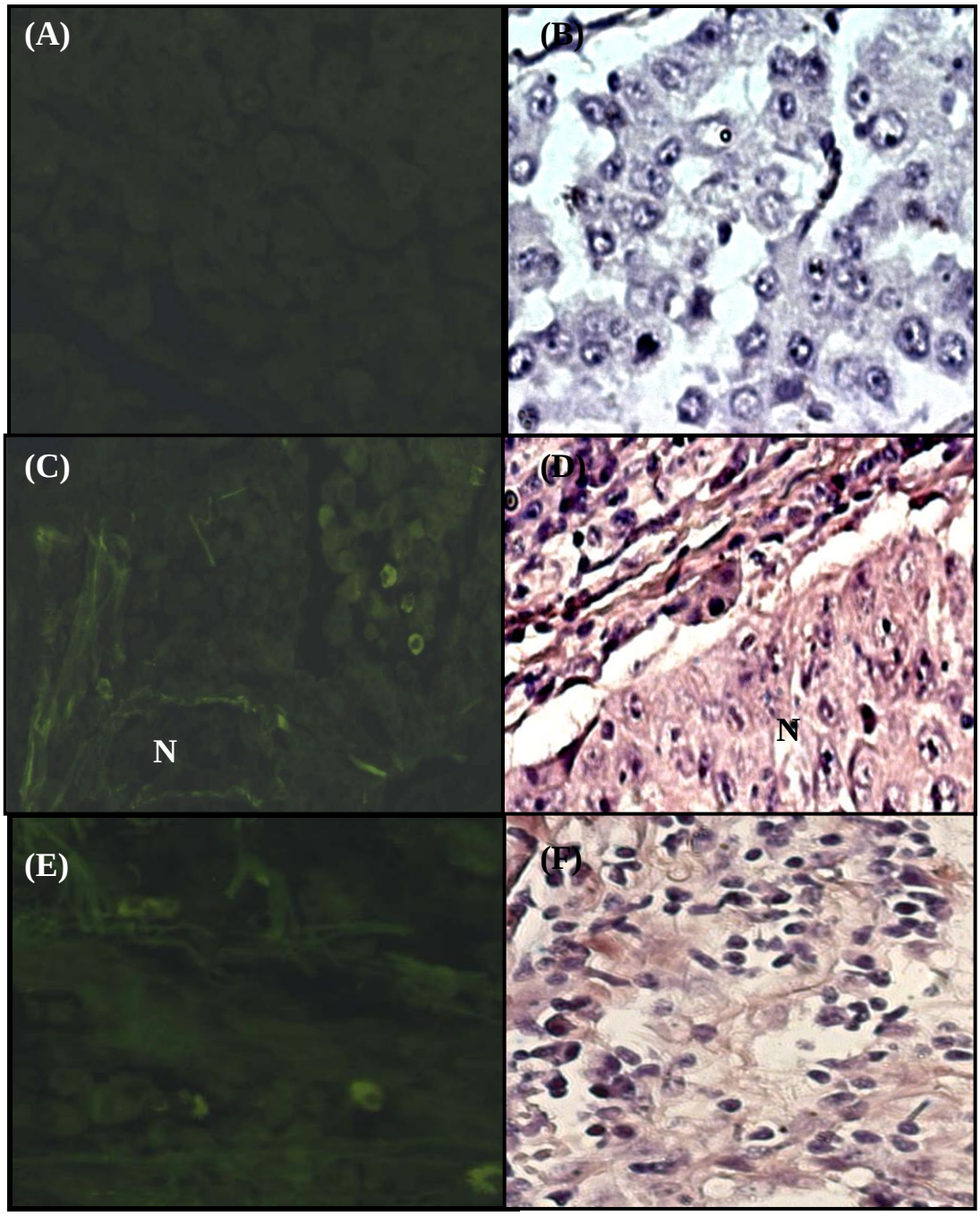

Figure 3-11: Localisation of LIAS in Squamous Cell Lung Carcinoma

(A and B) represents the negative control, localisation with sense probe which shows no expression of RPL9. The results show localisation of LIAS in the cytoplasm of tumour cells. The arrangement of cells in broad sheets and large nests N indicate a major characteristic of squamous cell carcinoma. (Magnification 400X).

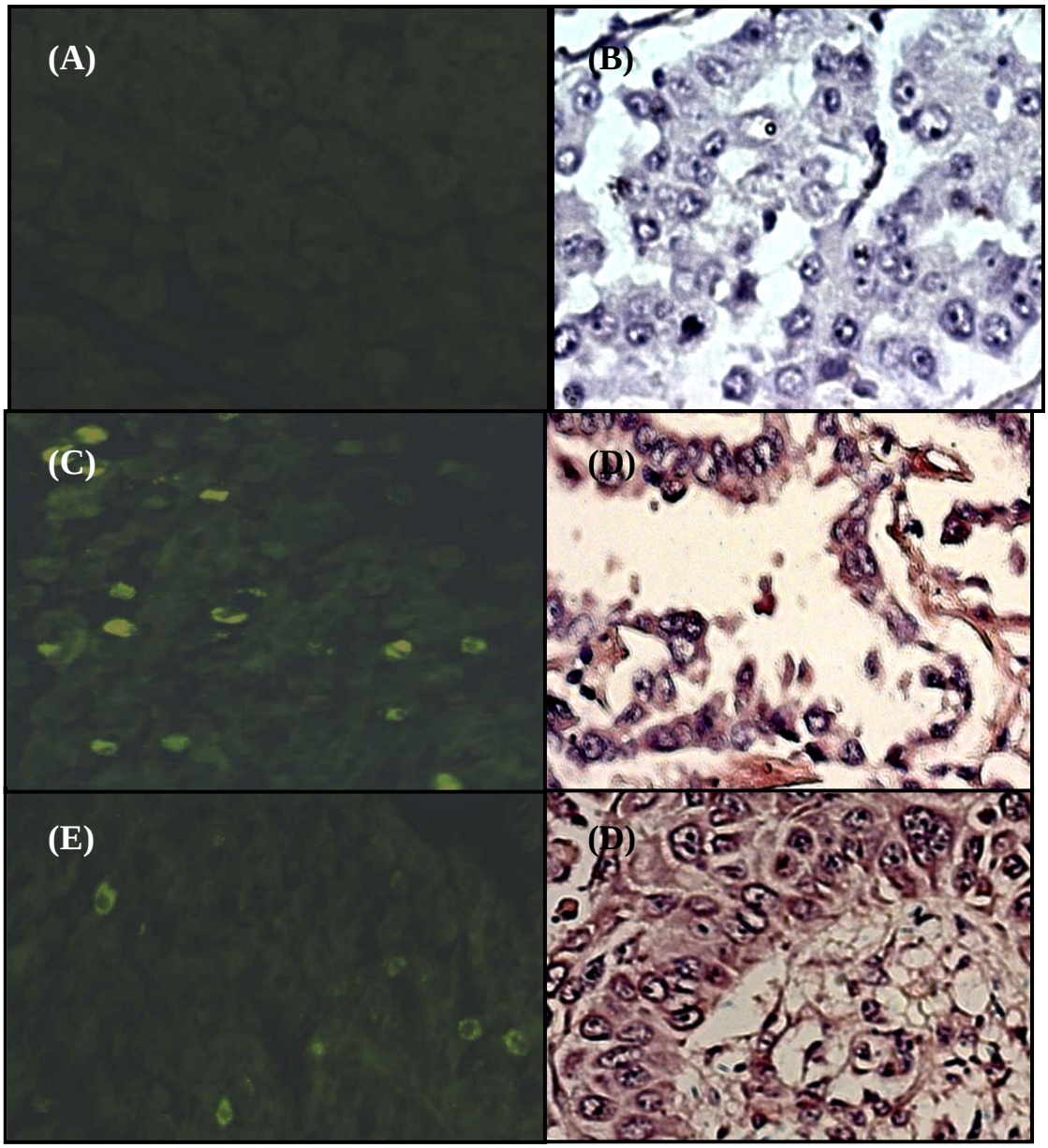

Figure 3-12: Localisation of LIAS mRNA in Lung Adenocarcinoma

A and B represents negative control which is localisation with sense probe. The poorly differentiated (C and D) grade shows a poorly formed glandular structure. The well differentiated (E and F) shows the glands composed of tall columnar epithelium with ample cytoplasm and basally situated nuclei. LIAS mRNA is localised in the cytoplasm of the columnar epithelial cells in the poorly and well differentiated grades. (Magnification 400X)

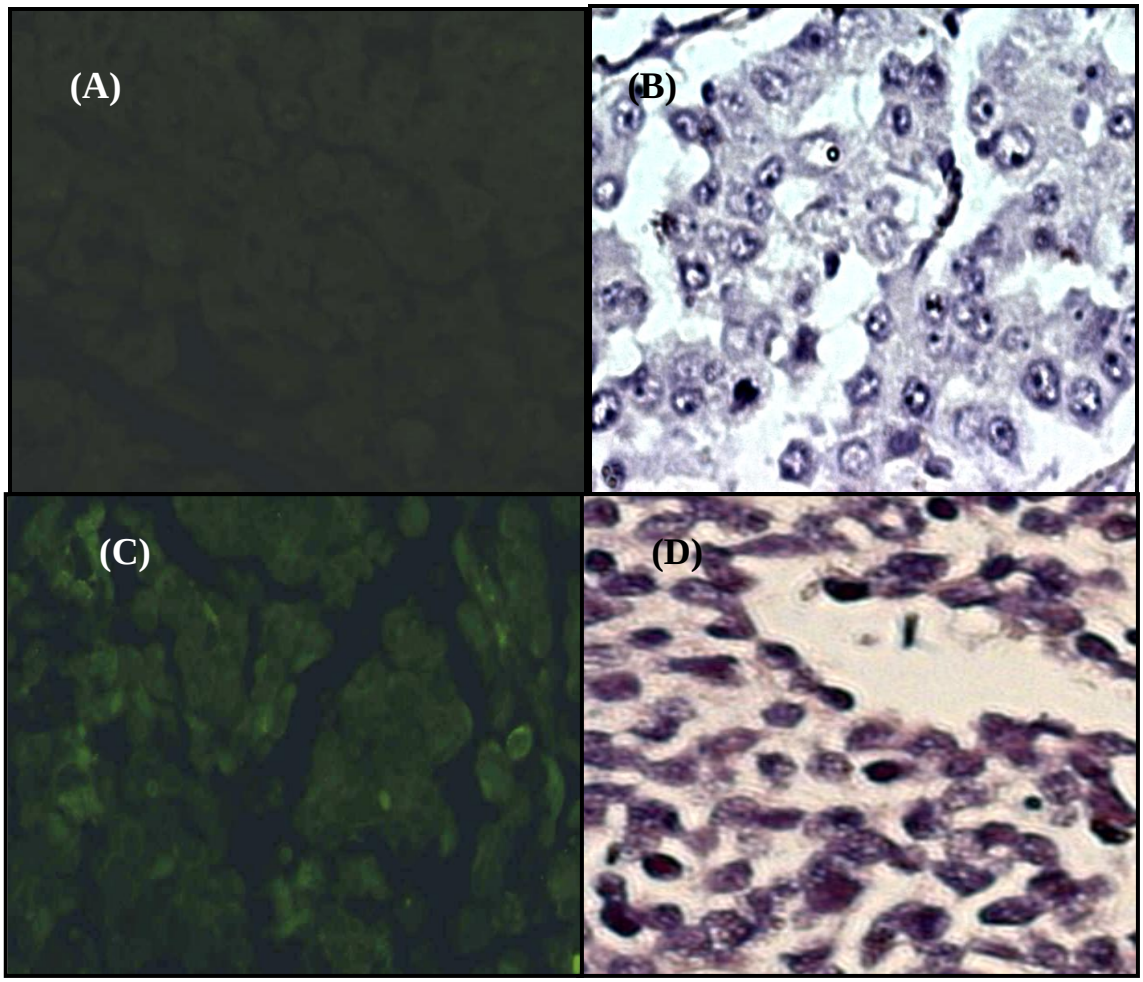

Figure 3-13: Localisation of LIAS mRNA in Small Cell Lung Carcinoma

(A) and (B) represents a negative control, which is a localisation of LIAS mRNA with a sense strand and it shows no expression of LIAS mRNA. In the Small Cell Lung Carcinoma tissue (C and D), LIAS is expressed in the cytoplasm of the tumour cells that resembles lymphocytes. (Magnification 400X)

Summary

The expression of RPL9 and LIAS was done by comparing localisation of RPL9 and LIAS mRNA in lung cancerous and normal tissues with the anti-sense probe to the negative control which is the localisation with the sense probe. Both are expressed in normal and cancerous tissues but the expression is lower in normal tissue compared to cancerous tissue. Observation of the tissue indicated that the expression of RPL9 increases with the progression from poor to well differentiated of the adenocarcinoma and squamous cell carcinoma, figure 3-10 and 3-09 respectively. The expression is the highest in small cell lung carcinoma (figure 3-8) followed by adenocarcinoma, squamous cell lung carcinoma and the lowest in large cell lung carcinoma (figure 3-09). The expression of LIAS increased with the progression of squamous cell lung carcinoma as shown in figure 3-11 and decreased in the progression of adenocarcinoma from poor to well differentiated (figure 3-12). However the expression of LIAS was the highest in adenorcarcinoma, followed by squamous cell carcinoma and the lowest in small cell carcinoma (figure 3-13). The overall expression of RPL9 is relatively higher than LIAS in lung normal tissue and lung cancer.

3.2. Real Time Polymerase Chain Reaction

Real Time PCR was used to quantify the expression level of RPL9 and LIAS in lung cancer. RNA was extracted from lung adenocarcinoma (A549) and lung normal fribroblast (MRC5) cell lines. mRNA from both cell lines was reverse transcribed into cDNA using reverse transcriptase and oligo-(dT)15 primers. cDNA was used as a template for the Real Time PCR using SYBR Green I and the gene specific primers. Standard curves, melting curves and quantitation curves were used to analyse the results using the Opticon 3.1 software.

3.2.1. Assessment of assay efficiency and optimisation using standard curves

In order to assess the efficiency of the assay, standard curves for the genes under investigation were constructed using serial dilutions of template DNA. The standard curves were constructed by plotting the log of the starting template concentration against the threshold cycle (C_T) obtained from the amplification of each dilution. Amplification efficiency was calculated using the slope obtained from the standard curve using the following formula:

$$E \text{ (Efficiency)} = 10^{-1/\text{slope}}$$

Amplification efficiency can also be converted into percentage efficiency by using the formula:

$$\% \text{ Efficiency} = (E-1) \times 100\%$$

Five fold dilution series of the cDNA was used as a standard template.

***Calculation*:**

LIAS

Slope = -3.38

E = $10^{-1/slope}$

=1.97

%Efficiency = (E-1) x 100%

= 97%

RPL9

Slope = -3.35

E = $10^{-1/slope}$

= 1.98

%Efficiency = (E-1) x 100%

= 98%

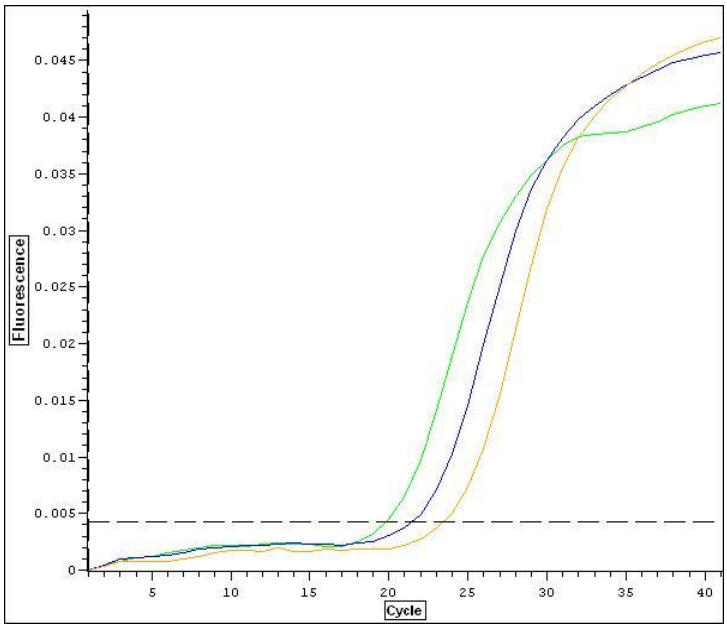

Concentrations

- 227 ng
- 45.4 ng
- 9.08 ng

A

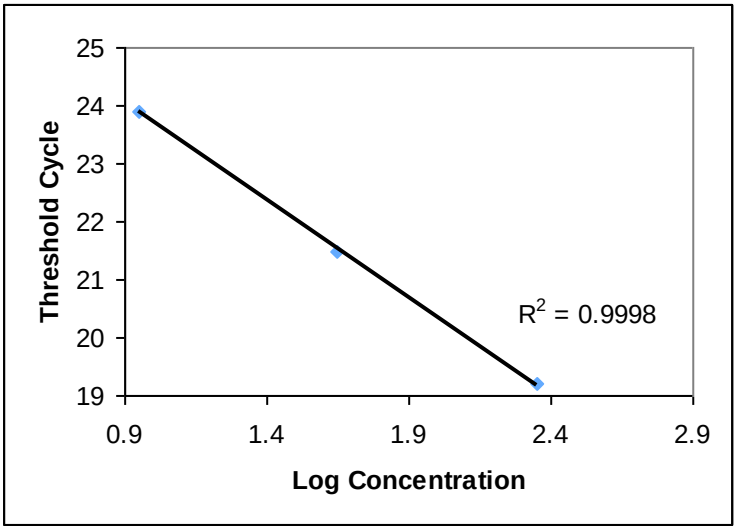

Log []	Threshold Cycle
2.35	19.2
1.65	21.5
0.95	23.9

B

Slope = -3.35, PCR efficiency: 98%

Figure 3-14: RPL9 standard curve to assess the efficiency of the reaction assay. Amplification curve (**A**) for RPL9 gene using SYBR Green I dye illustrate equidistance between the five fold dilution series of the DNA extracted from MRC5 cell line. Standard curve C_T values obtained from the amplification curve plotted against the Log concentration of the template starting quantity for each dilution. The slope of the curve was found to be -3.35 and the efficiency was 98%

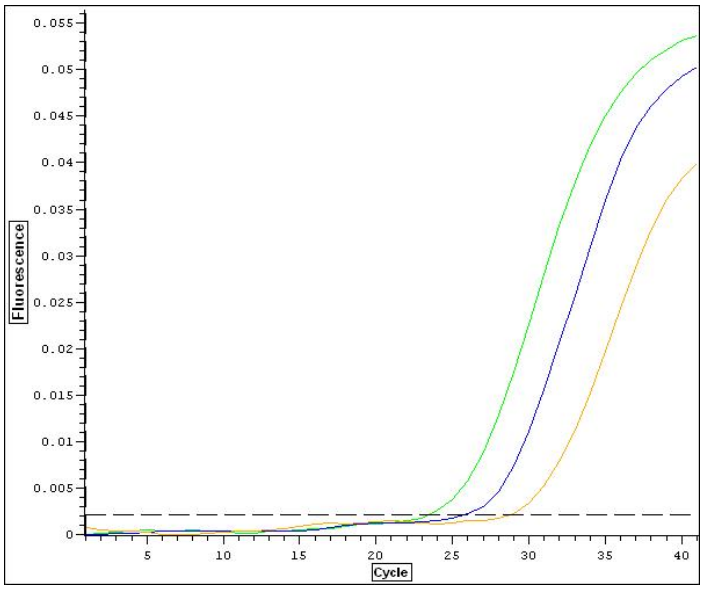

Concentrations

- 1135 ng
- 227 ng
- 45.4 ng

A

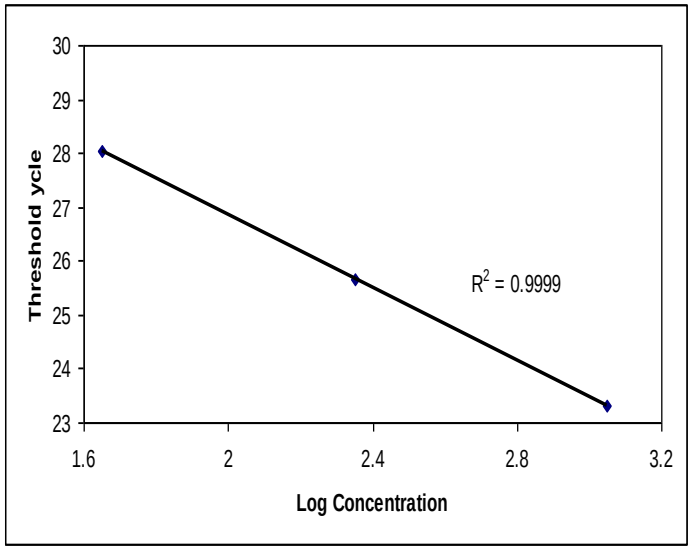

Log []	Threshold Cycle
3.05	23.32
2.35	25.65
1.65	28.05

B

Slope : -3.38; PCR efficiency: 97%

Figure 3-15: LIAS standard curve generated to assess the efficiency of the reaction assay. Amplification curve (A) for LIAS gene using SYBR Green I dye illustrate equidistance between five fold dilution of the starting quantity of the template cDNA. C_T values obtained from the amplification curve were plotted against the Log concentrations for all the dilutions to generate a standard curve. The calculated PCR efficiency using the slope (-3.38) of the curve was 97%

3.2.2. Melting curves for RPL9 and LIAS

Melting curves were plotted and used to assess for the presence of multi-products due to the presence of contaminating DNA, presence of primer dimers or the non-specificity of the primers. The quantified product was allowed to melt at a constant increase in temperature of 1°C and allowed to hold for 30 seconds from 55 °C to 99°C. The presence of single peak signifies the presence of single identical product. The presence of multi-products will be indicated by multi peaks and same applies with primer dimmers. Since elimination of primer dimers is very crucial for the accuracy of real time PCR using SYBR Green dye, melting curves presents a very useful tool for gene expression analysis.

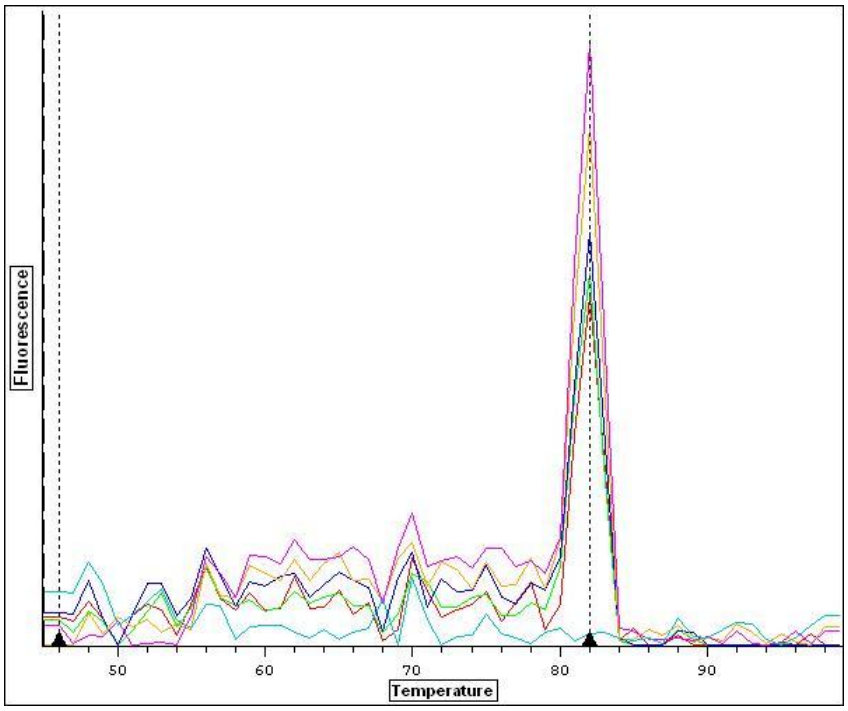

Figure 3-16: Annealing temperature optimization and melting curve to analyse the specificity of RPL9 primers

In order to optimise the annealing temperature of the primers, a temperature gradient (52 – 59 ^{o}C) with replicates of concentrations was run. The primers showed to be optimum at 58 ^{o}C (_). The curve shows the specificity of the primers which is observed by a single peak with a melting temperature of 81°C in all the replicates. The blank (_) shows no primer dimmers or contamination with foreign DNA as no peak is observed.

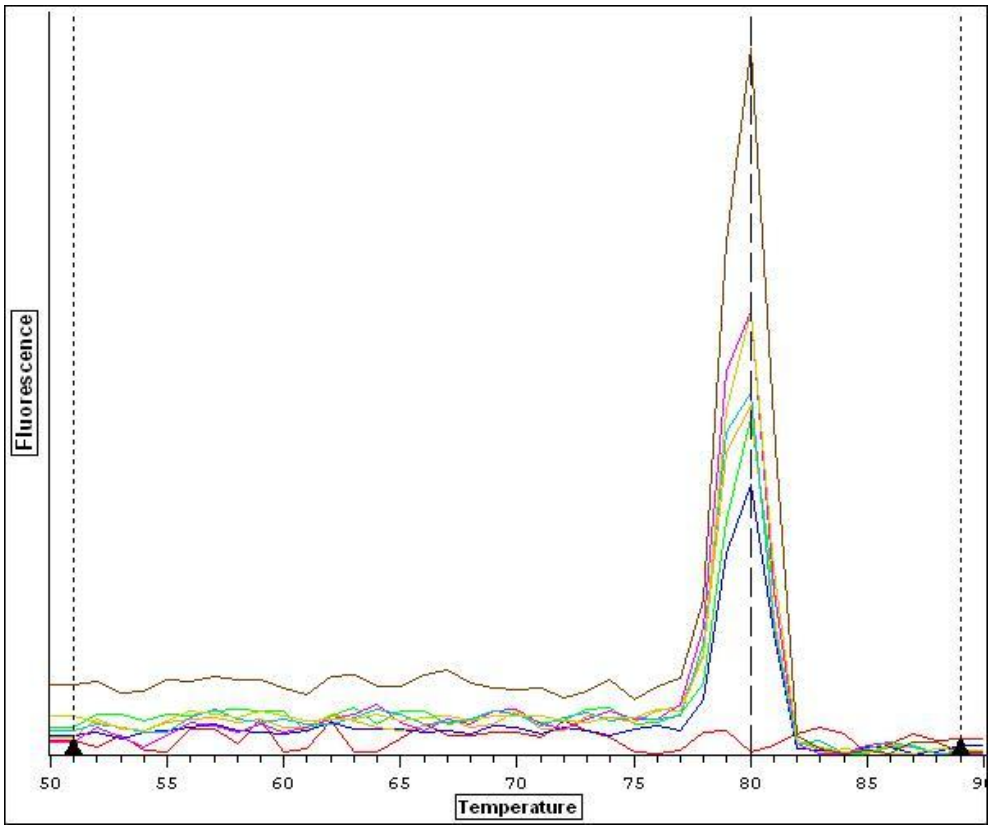

Figure 3-17: Annealing temperature optimization and melting curve to analyse the specificity of LIAS primers

A temperature gradient (52-59^{o}C) was run and LIAS primers are optimum at 57^{o}C ( ). The curve shows the specificity of the primers which is observed by a single peak with a melting temperature of 80°C in all concentration replicates. The blank ( ) shows no contamination with foreign DNA or primer dimmers as no peak is observed.

3.2.3. Relative Quantitative Real Time Polymerase reaction of RPL9 and LIAS expression normalised against unit mass

Relative quantification is used to compare an expression level of a gene between a test and calibrator, e.g. cancerous and normal cells of the same tissue as opposed to absolute quantification that measures the number of particles in a given amount of sample. The system monitors the fluorescence emitted during the reaction as an indicator of amplicon production during each cycle. The threshold cycle (C_T) is recorded as the cycle at which fluorescence emission exceeds the fixed threshold. The lower the C_T value of the test (cancerous cells) relative to the calibrator (normal cells) the higher the templates present at the beginning of the reaction and the higher the C_T value the lower the template (Section 2.4). When running relative qRT-PCR that is normalised against unit mass, quantity/ concentration of the starting template must be equal. cDNA was synthesized using RNA extracted from MRC5 and A549 cell lines. cDNA was quantified using a spectrophotometer at A_{260} and 1µg MRC5 and 1µg A549 cDNA was used as a starting material.

MRC5:

A_{260} = 1.494

DF = 20

A_{260} ds DNA = 50 µg/ ml

[MRC5] = A_{260} x[A260 ds DNA] xDF

= 1.494 µg/ µl

A549:

A_{260} = 1.787

DF = 20

A_{260} ds DNA = 50 µg/ ml

[A549] = A_{260} x [A_{260} ds DNA] x DF

= 1.787µg/ µl

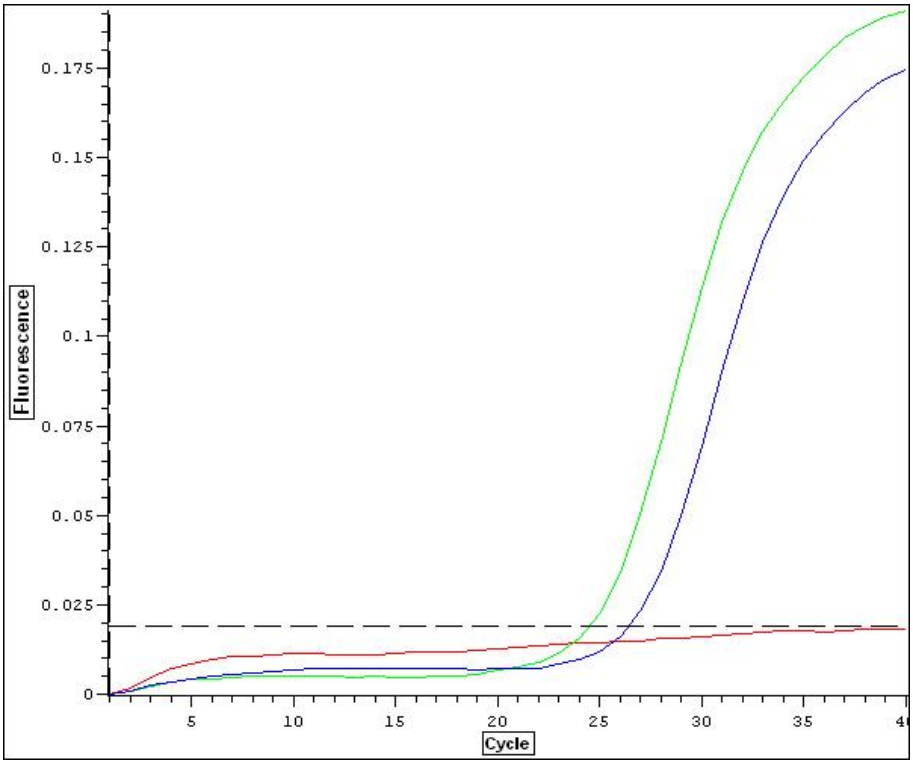

Figure 3-18: Quantification curve for LIAS

The above figure illustrate the expression level of LIAS in lung adernocarcinoma A549 (■) relative to lung normal fibroblast MRC5 (■). C_T values for A549 and MRC5 is 24.4 and 26.5 respectively. Using the ratio equation described in section 2.4.3 with the amplification efficiency of 1.97, the expression of LIAS is 4 fold upregulated in A549 than in MRC5. In the blank (■) template was replaced with sdH_2O.

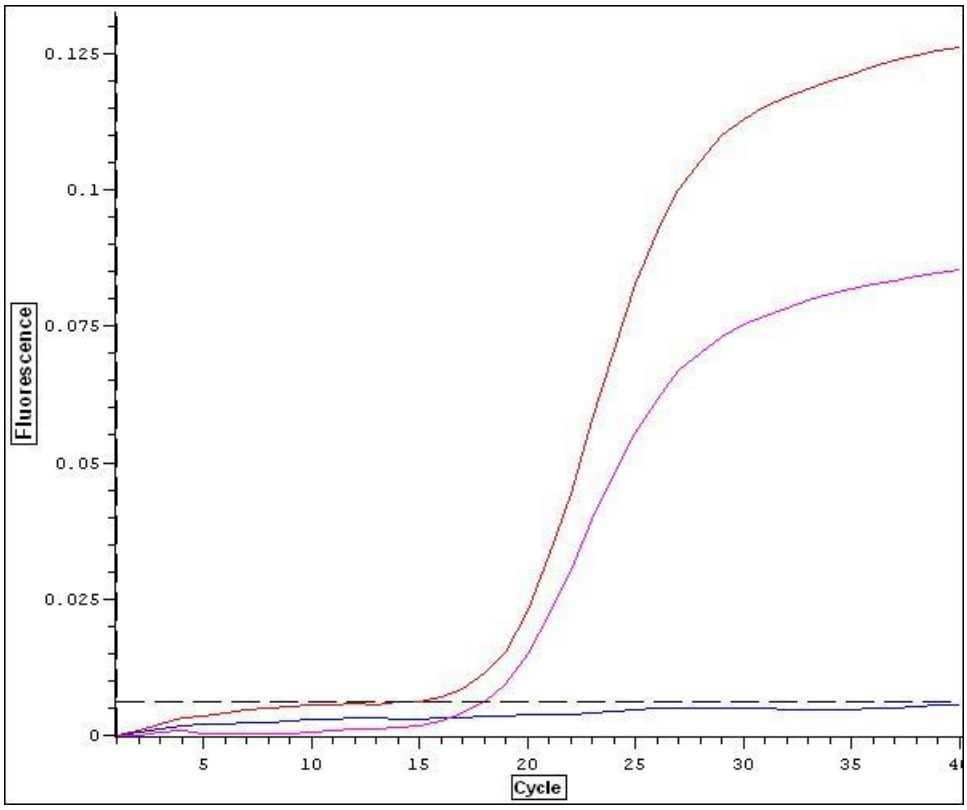

Figure 3-19: Quantification curve for RPL9

The figure above illustrate the expression level of RPL9 in lung adernocarcinoma A549 (■) relative to lung normal fibroblast MRC5 (■) normalised against a unit mass. C_T values for A549 and MRC5 is 15.05 and 18.07 respectively. Using amplification efficiency of 1.98, the expression of RPL9 is 8 fold upregulated in A549 than in MRC5. In the blank (■) template was replaced with sdH_2O and it doesn't show any trace of contaminating DNA .

Summary

RPL9 and LIAS gene specific primers designed with the Beacon Designer Software showed to be highly efficient which was demonstrated by the standard curves. The efficiency of LIAS and RPL9 were calculated to be 97% and 98% respectively (Figure 3-14 and Figure 3-15) which is within the accepted range of primer efficiency of 90-105%. The efficiencies demonstrate that for every cycle of the real time PCR, the starting amount of template is doubled which is the main principle behind every PCR protocol.

Melting curves were utilised to analyse the specificity of the primers and this is observed by the peaks on the curve. The results are represented as a graph of relative fluorescence over time ($-dT/dT_{max}$) versus temperature. Melting curves for both genes under investigation showed specificity of the primers which was observed by a single peak. Melting temperature for LIAS and RPL9 was $80^{o}C$ and $81^{o}C$ respectively as indicated in Figure 3-16 and Figure 3-17.

Using a unit mass as a normaliser RPL9 and LIAS were quantified. RNA was extracted from fresh MRC5 and A549 cell lines. RNA was used to make up cDNA by reverse transcription and quantified by spectrophotometer. One µg of the cDNA was used as a template for real time PCR.

Using the equation: $Ratio_{(test/calibrator)} = E^{\,CT\ (calibrator)\ -\ CT(test)}$ the ratio of expression of RPL9 and LIAS in lung adenocarcinoma relative to normal lung was determined. LIAS was found to be 4 fold up-regulated in lung adenocarcinoma while RPL9 was found to be 8 fold up-regulated (Figure 3-18 and Figure 3-19).

3.3. TUNEL

The terminal deoxynucleotide transferase-mediated deoxyuridine triphosphate biotin nick-end labeling (TUNEL) was applied to visualize where in the tissue apoptosis was occurring. During apoptosis, one of the morphological changes observed in the nuclei of apoptotic cells is the formation of DNA fragmnets in the region of 180 to 200 base pairs. The DeadEnd^{TM} colorimetric TUNEL system adds biotinylated deoxyuridine at the 3' – OH DNA ends of each fragment by the nontemplate-dependent DNA polymerase, Terminal deoxynucleotidyl Transferase (TdT). Horseradish-peroxidase-labelled streptavidin binds to the biotinylated nucleotides and a subsequent addition of peroxidase substrate, hydrogen peroxide and diaminobenzidine (DAB) chromogen result in apoptotic nuclei staining dark brown.

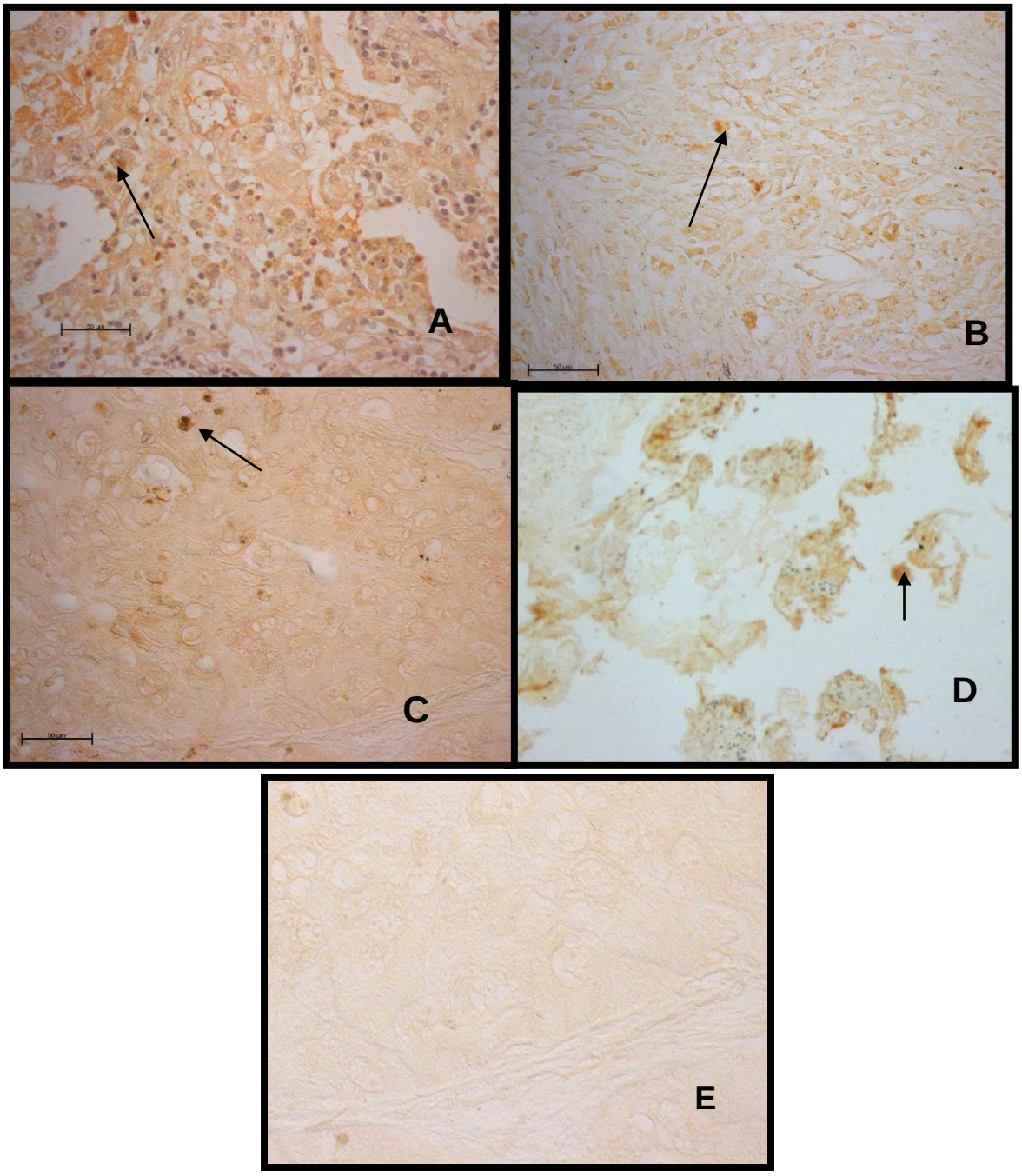

Figure 3-20: Apoptosis detection by TUNEL in lung cancer

TUNEL representation in (A) adenocarcinoma, (B) large cell carcinoma, (C) squamous cell carcinoma and (D) Mesothilia. E represents a negative control. Magnification 400X.

Summary

The TUNEL method labels DNA fragments and is therefore an effective technique for apoptosis detection. Fragmentation of the DNA was observed in the cytoplasm and is the highest in adenocarcinoma. By comparing the results obtained from In situ Hybridization and Real Time PCR it can be concluded that apoptosis occurs in the same regions and the same pattern as the expression level of RPL9 mRNA. Localisation of RPL9 mRNA was the highest in adenocarcinoma, followed by squamous cell carcinoma and then large cell carcinoma. The pattern of apoptosis is observed in lung cancer. This association is the same with LIAS expression.

3.4. Bioinformatics

3.4.1. Gene Conservation

For gene conservation through species, NCBI was used to check for human RPL9 and LIAS gene homologues. The amino acid sequences of the closest species to that of human were retrieved from NCBI and pair-wise alignment done using CLUSTALW 2.0.3 multiple sequence alignment software. The search results were as shown below

3.4.1.1. Lipoic Acid Synthetase CLUSTALW 2.0.3 multiple sequence alignment

The results are presented as scores that indicate percentage similarities between two sequences. Human (*Homo sapiens*) LIAS is most identical to that of Rat (*Rattus norvegicus*) with a percentage similarity score of 91. This is followed by mouse (*Mus musculus*) with 90% score similarity. Human LIAS is least similar to Drosophila with a 61% score similarity.

```
Sequence 1: gi|37577166|ref|NP_006850.2|     372 aa (Homo sapiens)
Sequence 2: gi|13277380|ref|NP_077791.1|     373 aa (Mus musculus)
Sequence 3: gi|58865650|ref|NP_001012037.1   373 aa (Rattus norvegicus)
Sequence 4: gi|17737685|ref|NP_524183.1|     380 aa (Drosophila)

Pair-wise alignment

Sequences (1:2) Aligned. Score:  90
Sequences (1:3) Aligned. Score:  91
Sequences (1:4) Aligned. Score:  61
Sequences (2:3) Aligned. Score:  95
Sequences (2:4) Aligned. Score:  61
Sequences (3:4) Aligned. Score:  61
```

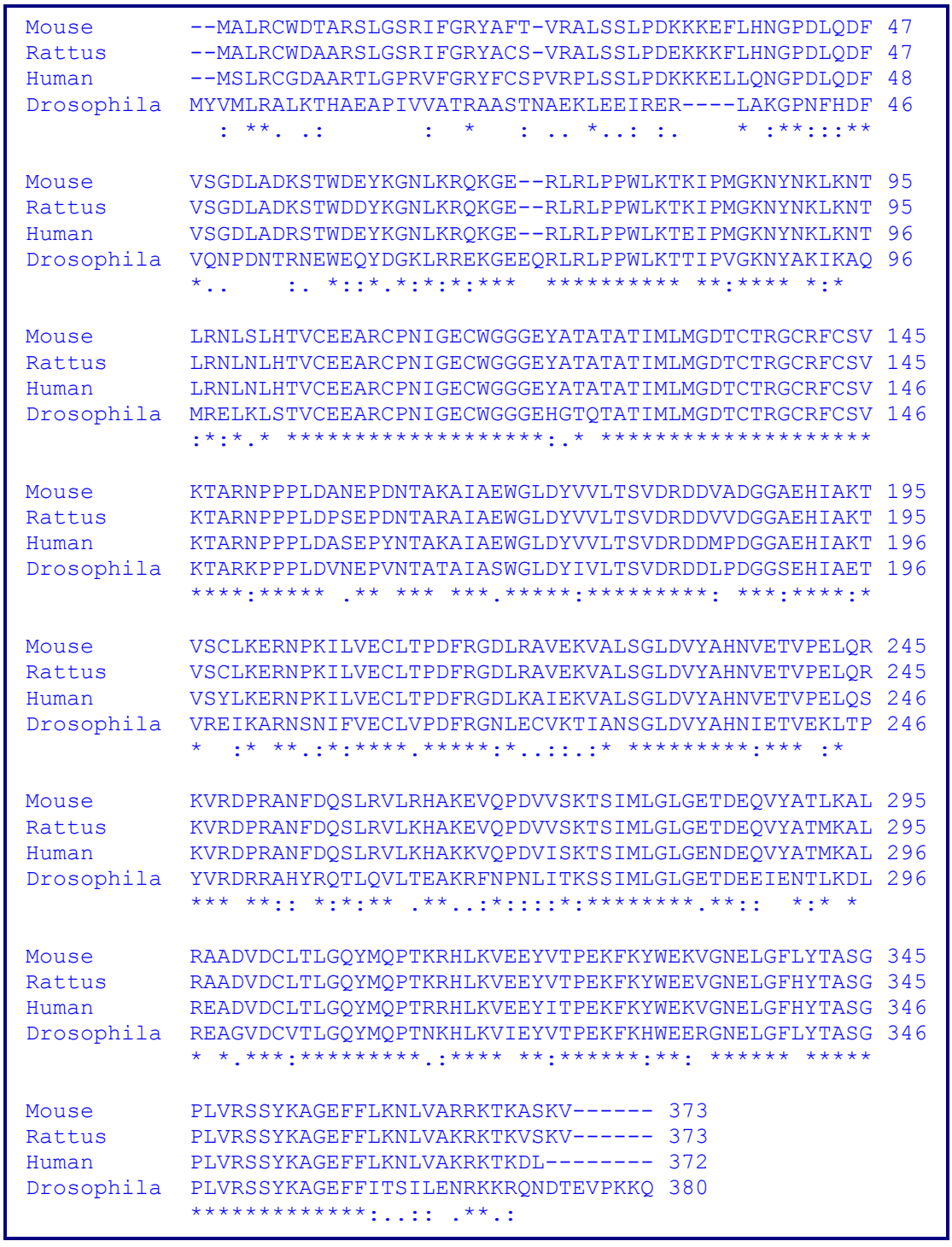

Figure 3-21: CLUSTALW 2.0.3 multiple sequence alignment for LIAS

Overall LIAS showed a poor conservation among species through evolution. The highest similarity for LIAS was found between Rat and Mouse with a score of 95. Human LIAS had the highest similarity to Mouse and Rat with a score of 90 and 91 respectively. Other species have a poor similarity to human

3.4.1.2. Ribosomal Protein L9 CLUSTALW 2.0.3 multiple sequence alignment

RPL9 was found to be highly conserved. *Homo sapiens* (Human), *Pan troglodytes* (Chimpanzee) and *Canis lupus* (Timber Wolf) were found to be 100 % identical. The mouse (*Mus musculus*) amino acid sequence was found to be 98 % identical to human RPL9 amino acid sequence. Rat (*Rattus norvegicus*) amino acid sequence was discovered to be 93 % identical to human RPL9 sequence and this is due to the longer rat amino acid sequence, 17 amino acids longer.

```
Sequence 1: gi|15431303|ref|NP_000652.2|     192 aa (Homo sapiens)
Sequence 2: gi|114593631|ref|XP_001141738.   192 aa (Pan troglodytes)
Sequence 3: gi|57048082|ref|XP_536256.1|     192 aa (Canis familiaris)
Sequence 4: gi|119904384|ref|XP_001256310.   192 aa (Bos taurus)
Sequence 5: gi|149249821|ref|XP_001474169.   192 aa (Mus musculus)
Sequence 6: gi|109503459|ref|XP_224924.3|    209 aa (Rattus norvegicus)

Pair-wise alignment

Sequences (1:2) Aligned. Score:  100
Sequences (1:3) Aligned. Score:  100
Sequences (1:4) Aligned. Score:  98
Sequences (1:5) Aligned. Score:  98
Sequences (1:6) Aligned. Score:  93
Sequences (2:3) Aligned. Score:  100
Sequences (2:4) Aligned. Score:  98
Sequences (2:5) Aligned. Score:  98
Sequences (2:6) Aligned. Score:  93
Sequences (3:4) Aligned. Score:  98
Sequences (3:5) Aligned. Score:  98
Sequences (3:6) Aligned. Score:  93
Sequences (4:5) Aligned. Score:  97
Sequences (4:6) Aligned. Score:  92
Sequences (5:6) Aligned. Score:  93
```

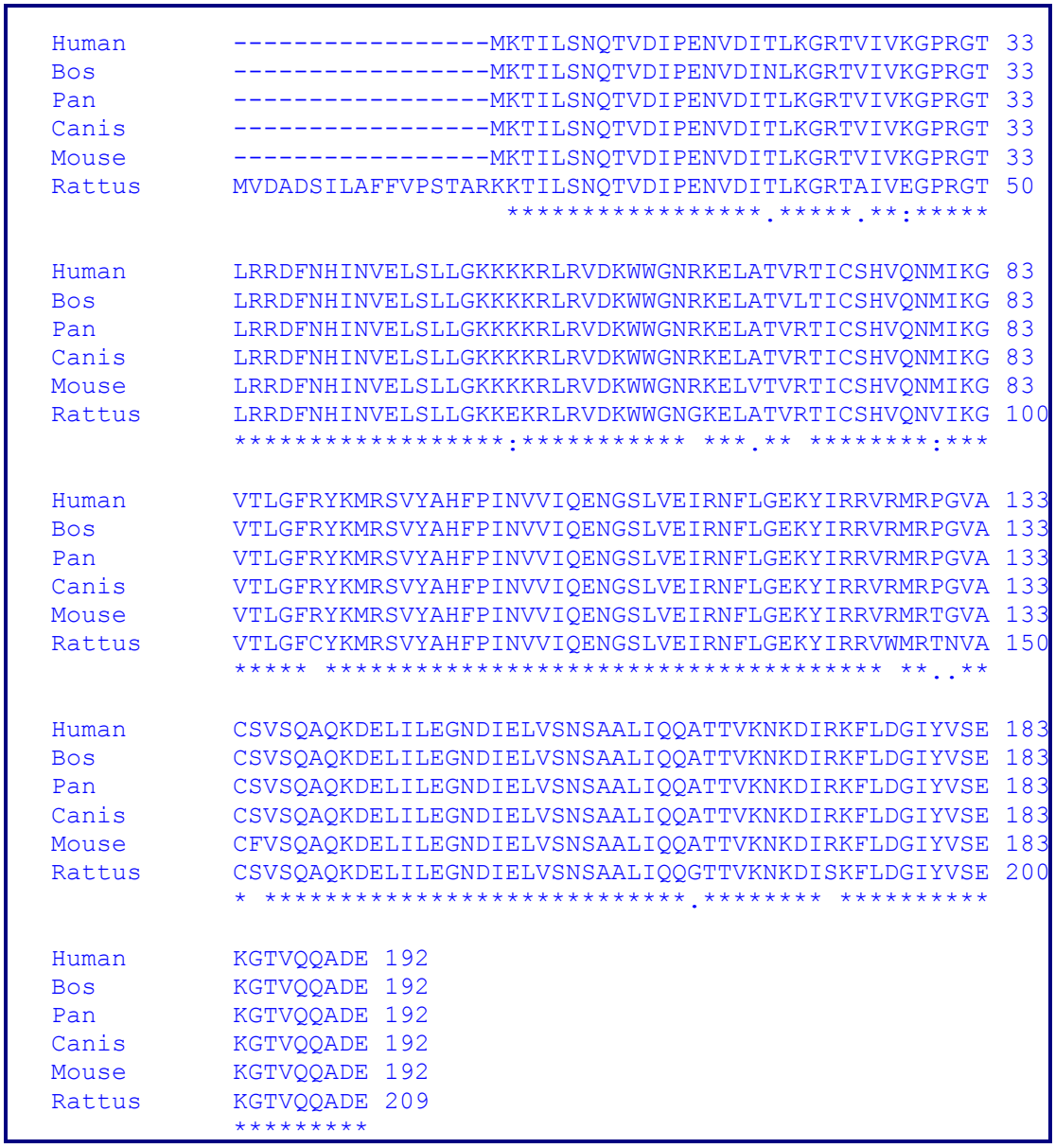

Figure 3-22: CLUSTALW 2.0.3 multiple sequence alignment for RPL9

RPL9 showed a strong conservation through evolution. A 100 % similarity was found between Human, Chimpanzee and Timber Wolf.

3.4.2. Bioinformatics gene Interaction

BONDplus database was used to find any reported interactions of LIAS and RPL9 with other genes or gene products. No interaction of LIAS with other genes was reported thus far. Li *et.al*., 2003 reported interaction of c-myc, max, polII and TafII250 with RPL9 promoter region. The ratio of expression of RPL9 against c-myc, max and TafII250 was found to be 3.56, 3.59 and 4.95 respectively. Among other genes promoter regions reported to interact with c-myc were tumour suppressor gene p53, pro-apoptotic Bax and anti-apoptotic Bcl2 with a ratio of expression to c-myc of 2.42, 1.16 and 0.77 respectively.

Summary

Biologists estimate that there are about 5 to 100 million species of organisms living on Earth today. Evidence from morphological, biochemical, and gene sequence data suggests that all organisms on Earth are genetically related. RPL9 was found to be highly conserved, and this could be because of its function in protein synthesis. NCBI was used to obtain the gene homologues for human RPL9 and LIAS. The protein sequences for genes with highest similarity to human were used to do a multiple sequence alignments using CLUSTAL 2.0.3 tool. *Homo sapiens* (Human), *Pan troglodytes* (Chimpanzee) and *Canis lupus* (Timber Wolf) were found to be 100 % similar (figure 3-22). Lipoic acid synthetase was found to be less conserved through the species. Sequence alignment showed a 90%, 91 % and 61 % similarity to Mus musculus (mouse), Rattus norvegicus (rat) and Drosophilla respectively (figure 3-21).

No interaction with other genes was reported for LIAS on the BONDplus database. c-Myc, max, polII, TafII250 were reported to interact with RPL9 promoter region (Li *et.al*., 2003) suggesting that the expression of RPL9 is controlled by transcription factor c-myc.

4. Discussion

4.1. Lung cancer

Lung cancer is the most important leading cause of death due to cancer. Although lung cancer has a lower incident rate than other types of cancers (breast, colon, prostate and cervical), it is very lethal and the 5 years survival rate is less than 5 %. About 60 % of the people diagnosed with lung cancer die within one year and nearly 75 % die within two years and the figures have not improved in the past decade (American Cancer Society, 2006). In South Africa, lung cancer constitutes 6.7% of all cancers in men and 2.8% of all cancers in women from all age groups. Breaking down these figures into race groups, the coloured and white males combined constitute 42.4% of all male lung cancer cases and black men constitute 55% of lung cancer cases which is the highest incidence rates among the male population (Sitas, *et al*., 1998).

Most cytotoxic drugs kill tumour cells by apoptosis. Defects in apoptosis signaling have a great contribution to resistance of tumour cells to chemotherapy. One of the characteristic features for lung cancer is resistance to apoptosis which suggest that the sensitization to apoptosis of lung tumour cells is very crucial in the attempt to treat lung cancer (Nachmais *et al*., 2004). Discovery of anti-apoptotic and pro-apoptotic genes is very essential in the discovery of novel therapeutic drugs directed at eradicating tumour cells by targeting apoptosis not only in lung cancer but cancer in general.

4.2. In Situ Hybridization

In Situ Hybridization was used to localize as well as to assess the expression of RPL9 and LIAS at tissue level in normal and lung cancer using anti-sense probes. Down or up-regulation of RPL9 and LIAS was determined by comparing the intensity of the labeling by both colorimetric and fluorescence detection. RPL9 localised in the cytoplasm of both normal and cancerous tissue but the expression was higher in the cancer than the normal. The expression increased with the progression of the cancer from poor to well differentiated of lung adenocarcinoma and squamous cell lung carcinoma. The expression was the highest in small cell lung carcinoma followed by adenocarcinoma and then squamous cell lung carcinoma. RPL9 was least expressed in large cell carcinoma. LIAS also localised in the cytoplasm. Literature indicates that LIAS is expressed in the mitochondrion which is located in the cytoplasm. This would have been observed if a high resolution and magnification microscope such as an electron microscope was used. Using the intensity of the labelling to quantify the expression, LIAS expression increased with the progression of squamous cell lung carcinoma and adenocarcinoma from poor to well differentiated. However the expression of LIAS was the highest in adenorcarcinoma, followed by squamous cell carcinoma and the lowest in small cell carcinoma. The overall expression of RPL9 is relatively higher than LIAS in lung normal tissue and lung cancer.

Over-expression and loss of function of a number of genes such as tumour suppressor genes (p53 and Rb) and proto-oncogenes (c-myc) has been associated with different types of cancer including lung cancer (Kohno and Yokota, 1999; Sherr and McCormick, 2002). Tumour cells over-express these genes in the attempt to induce apoptosis with no success. This could mainly be due to the fact that apoptosis is a molecular mechanism that involve

a couple of genes among which some are usually mutated in cancer. But the gene products will still accumulate in the cell.

Over-expression of RPL9 and LIAS further suggests that either RPL9 or LIAS or both could be directly or indirectly associated with apoptosis. Quantitative Real-time PCR and Bioinformatics tools were used for further analyses.

4.3. Real Time Polymerase Chain Reaction

Real Time PCR is a technique used in gene expression analyses. It uses the principle of polymerase chain reaction but unlike the conventional method which determines the amount of product formed at the end of the reaction, Real Time polymerase chain reaction measures the amount of product real time that is after every cycle. With good set of primers and under optimum conditions, polymerase chain reaction is exponential, that is the product doubles after every cycle. With modern technology that allows measurement of product after every cycle this has proved to be a very useful tool in gene expression analyses. Different indicators are included in the reaction depending on the objective of the experiment. The most common are DNA binding fluorescence dyes such as SYBR green. The dye binds exclusively to double stranded DNA and fluoresces at a specific wavelength.

Expression of RPL9 and LIAS was relatively quantified in lung cancer using lung normal fibroblast as a reference. Lung adenocarcinoma A549 and lung normal MRC5 fibroblast cell lines were used. The choice of A549 as a representative for lung cancer was motivated by the fact that, lung adenocarcinoma is the most common type of all lung

cancers, mainly because of high prevalence of tobacco smoking. RNA extracted from A549 and MRC5 cultured cell lines was used to synthesize cDNA by reverse transcription using oligo-$(dT)_{15}$ primers. cDNA was quantified and the same amount for cancer and normal used for real time PCR using gene specific primers. The efficiency of RPL9 primer was optimized to 98 % and 97 % for LIAS by using standard curves. Specificity of the reaction for both genes was determined and optimized by melting curves. Non-specificity and contamination of primers can be demonstrated by multiple picks on the melting curve with a different melting temperature to that of the expected product. Because SYBR binds to any double stranded DNA, designing primers that do not form dimers is very crucial. Because of the high sensitivity of this technique, primer dimers can be detected even at very low quantities and this can be demonstrated as picks with low melting temperature because of their relatively smaller size. Using the same amount of cDNA and running the reactions at optimum conditions ensures that any variation in the amount of the product formed signified the difference in expression level of the gene in lung cancer relative to the normal lung.

Taking the ratio of the threshold cycle of the test (cancer) to that of the calibrator (normal) the expression level of RPL9 was found to be 8-fold up-regulated in lung adenocarcinoma relative to the normal counterpart. These results imply that RPL9 is expressed in lung adenocarcinoma 8 times more than in the normal lung. LIAS was found to be 4-fold up-regulated in lung cancer relative to normal lung.

The relatively high difference in expression level of RPL9 and LIAS in adenocarcinoma to normal lung, together with the resistance to apoptosis of CHO cell line with mutated RPL9 and LIAS suggests that one of the two genes or both may be very crucial in

mammalian apoptotic pathway. As it is well known that failure to undergo apoptosis by cells can lead to development of cancer, any molecular maker that can assist in early detection of cancer is very important. These can also lead to improved treatment of not only lung cancer but also other types of cancer.

4.4. Bioinformatics

BONDplus database was used to search for any reported interaction discoveries of RPL9 and LIAS. Gene IDs were obtained from NCBI and no interaction discoveries for LIAS were reported. For RPL9, the search returned a discovery by Li *et al* (2003) that was aiming at determining the transcriptional regulatory role of c-myc. The study reported the interaction of c-Myc, Max, PolII and TAFII250 proteins with RPL9 promoter region in the Daudi cells. Daudi cells, is an established cell line originally derived from Burkitt's lymphoma patients. These cells express a high level of c-myc and have been used extensively as an experimental system to study the role of c-myc.

The c-myc gene is a proto-oncogene that was discovered over 20 years ago as the cellular homolog of the retroviral v-myc oncogene (Bishop, 1982; Bister and Jansen 1986). Later on the c-myc proto-oncogene was found to be activated in various animal and human tumours (Cole, 1986). c-Myc protein contains a transactivation domain within its N-terminal 140 aa (Kato *et al.*, 1990). The c-myc binds to and transactivates through consensus 5'-CACGTG-3' sequences (Dang, 1999). Major roles of c-myc include regulation of the cell cycle, differentiation and apoptosis. The search for c-myc partner resulted in the discovery of Max protein. Max (myc associated factor X) is a transcription factor that functions as a homodimer or heterodime with Mad, Mxi1 and Myc. In contrast

to Myc, Max does not contain a transcription protein. Myc/Max heterodimewrs bind to target sites to transactivate genes via the myc transactivation domain. Max homodimers are thought to counter the function of the Myc/Max heterodimers through competitive binding to target DNA sites.

A study on the 32D.3 myeloid progenitor cell line further support the role of c-myc in apoptosis. The cell line is dependent on interleukin-3 (IL-3) for myc expression and growth showed the continuous drive of cells into S-phase and accelerated rate of apoptosis under the enforced c-myc expression and in the absence of IL-3. Serum deprived Rat1 fibroblasts overexpressing c-myc undergo dramatic apoptosis that is dependent on the wild type p53. The regions of c-myc required for transcriptional regulation and cellular transformation are also required for serum deprived-induced apoptosis. Therefore it is summarized that c-myc protein affects the transcription of genes that participate in apoptosis and because of frequent association of c-myc oncogene with human malignancies, identification of c-myc interacting genes might help in the fight against human malignancies.

PNAS supporting data for the study by Li *et al.,* 2003 showed an up-regulation of RPL9 and other genes that were up-regulated is apoptotic genes p53 and Bax. An anti-apoptotic gene Bcl-2 was down-regulated. The ratio of expression of RPL9 was relatively higher than most well characterized genes. The high expression of RPL9 was also discovered by quantitative real time PCR and in situ hybridization.

CLUSTALW 2.0.3 Multiple sequence alignment was employed to further analyse the biological role of RPL9 and LIAS. The results showed a less conservation of LIAS amino acid through evolution. The highest similarity was obtained between Human (*Homo*

sapiens) and Rat (*Rattus norvegicus*) LIAS with a similarity score of 91 %. Contrary to LIAS, RPL9 has been highly conserved through evolution. Human *(Homo sapiens)* RPL9 amino acid sequence was found to be 100 % identical to *Pan troglodytes* (Chimpanzee) and *Canis lupus* (Timber Wolf) and 98 % identical to the mouse (*Mus musculus*) amino acid sequence. The high conservation of RPL9 through evolution could be an indication of its biological function in apoptosis. The same pattern of conservation is observed among other crucial genes such as p53.

Paul *et al* (Paul *et al.,* 1995) reported high level of antigenic activity in ribosomes isolated from mouse UV induced 6132A PRO tumour cells. Reintroduction of the lost wild type L9 allele into 6132A-PRO variant suppressed the growth of tumour cells in vivo. This study support the preliminary finding by Prof D.J.G Rees that discovered resistance to apoptosis by the CHO cell line following promoter trap mutagenesis, resulting in mutation in LIAS and RPL9.

High expression of RPL9 in cancer cell line and tissue section coupled with high conservation through evolution, as well as supporting literature showing an interaction of RPL9 with c-myc and antigen activity from cell lines with mutations on the RPL9 allele strongly suggest that RPL9 may play a crucial role in apoptosis as a pro-apototic gene.

4.5. TUNEL

One of the characteristics of apoptosis is the degradation of DNA after the activation endonucleases. This DNA cleavage leads to strand breaks within the DNA. The TUNEL method identifies apoptotic cells in situ by using terminal deoxynucleotidyl transferase (TdT) to transfer biotin-dUTP to these strand breaks of cleaved DNA. The

biotin-labeled cleavage sites are then detected by reaction with HRP conjugated streptavidin and visualized by DAB showing brown color.

Fragmentation of the DNA was observed in the cytoplasm. The highest fragmentation is the highest in adenocarcinoma and by comparing the results obtained from In situ Hybridization and Real Time PCR it can be concluded that apoptosis occurs in the same regions and the same pattern as the expression level of RPL9 mRNA. Localisation of RPL9 mRNA was the highest in adenocarcinoma, followed by squamous cell carcinoma and then large cell carcinoma. This association is also the same with LIAS expression.

5. Conclusion

In situ hybridization showed localization of RPL9 and LIAS in the cytoplasm of both normal and cancerous lung tissue sections. The intensity of localization was greater in cancer than in normal tissue. The expression of RPL9 was greater in small cell lung carcinoma, followed by adenocarcinoma, squamous cell lung carcinoma and then large cell lung carcinoma. However the expression of LIAS was the highest in adenorcarcinoma, followed by squamous cell carcinoma and the lowest in small cell carcinoma. The overall expression of RPL9 was relatively higher than LIAS. Quantitative real time PCR confirmed the up-regulation of RPL9 and LIAS in lung cancer relative to its normal counterpart. It also confirmed the relatively high expression of RPL9 compared to LIAS. The fragmentation of DNA was measured by TUNEL. The DNA fragmentation was observed in the cytoplasm and is the highest in adenocarcinoma. Comparing TUNEL and In situ hybridization results, LIAS and RPL9 mRNA localises in the cytoplasm which is the side where DNA fragmentation was observed. This pattern further serves as an evidence of the involvement of RPL9 and LIAS in apoptosis.

Bio-informatics tool, CLUSTAL 2.0.3 revealed that LIAS is less conserved through evolution. A high conservation was revealed with RPL9. Human RPL9 was found to be 100 % similar to that of Timber Wolf and Chimpanzee and 98 % to mouse L9. BOND*plus* database reported an interaction of c-myc proto-oncogene, max, polII and TAFII250 transcription factor with RPL9 promoter region. Major roles of c-myc and TAFII250 include regulation of the cell cycle, differentiation and induction of apoptosis. The ratio of expression of RPL9 to c-myc was high which indicates a strong interaction. This strongly suggests that RPL9 is involved in the induction of apoptosis

All these discoveries coupled with resistance to apoptosis of CHO cell line in which RPL9 and LIAS were found to be mutated following promoter-trap mutagenesis, strongly suggests that RPL9 might be playing a role in cell cycle and apoptosis and the elevated expression of RPL9 can be used a molecular marker for cancer diagnosis.

This study showed preliminary results presenting a vital direction to future studies to investigate the molecular functions of these two genes.

6. References

1. Adams, P. (2001) Regulation of the Retinoblastoma Tumor Suppressor Protein by Cyclin/Cdks, *BBA-Reviews on Cancer 1471*, 123-133.
2. Albain, K.S., Crowley, J.J. and LeBlanc, M. (1991). Survival determinants in extensive-stage non-small-cell lung cancer: the Southwest Oncology Group experience. *Journal of Clinical Oncology*. 9(9): 1618-1626.
3. Amato, A., Lentini, L., Schillaci, T., Iovino, F., and Di Leonardo, A. (2009) Rnai Mediated Acute Depletion of Retinoblastoma Protein (Prb) Promotes Aneuploidy in Human Primary Cells Via Micronuclei Formation, *BMC Cell Biol 10*, 79.
4. Ames, B.N., Shigenaga, M.K., and Gold, L.S. (1993). DNA lesions, inducible DNA repair, and cell division: three key factors in mutagenesis and carcinogenesis. *Environ Health Perspect*. 5:35-44.
5. Ashkenazi, A. and Dixit, V.M. (1998). Death receptor: Signaling and modulation. *Science.* 281, 1305-1308.
6. Ashkenazi, A., Pai, R.C., Fong, S., Leung, S., Lawrence, D.A., Marsters, S.A., Blackie, C., Chang, L., McMurtrey, A.E., Hebert, A., Deforge, L., Koumenis, I.L., Lewis, D., Harris, L., Bussiere, J., Koeppen, H., Shahrokh, Z., and Schwall, R.H. (1999). Safety and antitumor activity of recombinant soluble Apo2 ligand. *J Clin Invest.*104 (2):155-62.
7. Ashkenazi, A., and Herbst, R. (2008) To Kill a Tumor Cell: The Potential of Proapoptotic Receptor Agonists, *The Journal of Clinical Investigation 118*, 1979.
8. Baehrecke, E.H. (2002). Hoe Death shapes life during development. *Nat Rev Mol Cel Biol*. 3:779-787.

9. Beckett, W.S. (1993). Epidemiology and etiology of lung cancer. *Clin Chest Med*. 14:1-15.

10. Benjamin, D.R. and Daniel, S.P. (2006). KLF4, p21 and context-dependent opposing forces in cancer. *Nature Reviews Cancer* **6**, 11-23.

11. Bishop, J.M. (1982). Retroviruses and cancer genes. *Advanced Cancer Research*. 37: 1-32.

12. Bister, K., and Jansen, H.W. (1986). Oncogenes in retroviruses and cells biochemistry and molecular genetics. *Advanced Cancer Research*. 47: 99-188.

13. Brabender et al. (2001). Epidermal growth factor receptor and HER-neu mRNA expression in non-small cell lung cancer is correlated with survival. *Clin cancer*. 7, 1850-1855

14. Brambilla, C., Fievet, F., Jeanmart, M., de Fraipont, F., Lantuejoul, S., Frappat, V., Ferretti, G., Brichon, P.Y., and Moro-Sibilot, D. (2003). Early detection of lung cancer: role of biomakers. *Eur. Respir. J*. 39, 36S-44S.

15. Busby, R.W., Schelvis, J.P.M., Yu, D.S., Babcock, G.T. and Marletta, M.A. (1999). Lipoic Acid Biosynthesis: LipA Is an Iron-Sulfur Protein**.** *J. Am Chem Soc*. 121: 19, 4706-4707

16. Christopher, D.M. Fletcher (2000). Diagnostic histophathology of tumours, 2nd edition. Churchill Livingstone, China. 171-98.

17. Cole, M.D. (1986). The myc oncogene: its role in transformation and differentiation. *Annual Rev Genetics*. 20: 361-384.

18. Damjanov, I (1996). Histopathology: A color atlas and textbook, 1st edition. Williams and Wilkins, USA. 127-128.

19. Dang, C.V. (1999). c-Myc target genes involved in cell growth, apoptosis, and metabolism. Molecular and Cellular Biology. 19: 1-11.
20. Debatin, K.M. and Krammer, P.M. (2004). Death receptors in chemotherapy and cancer. *Oncogene* 23, 2950-2966.
21. Denissenko, M.F., Pao, A., Tany, M., and Pfeifer, G.P. (1996). Preferential formation of benzo[a]pyrene adducts at lung cancer mutational hotspots in p53. *Science*. 274: 430-432.
22. De Stefani, E., Boffetta, P., Ronco, A.L., Brennan, P., Correa, P., Deneo-Pellegrini, H., Gutierrez, P. and Mendilaharsu, M. (2005). Squamous and small cell carcinomas of the lung: similarities and differences concerning the role of tobacco smoking. *Lung Cancer*. 4, 1-8.
23. Doll, R. (1998). The first reports on smoking and lung cancer. *Clio Med*. 46, 130-142.
24. Doll, R. and Hill, A.B (1950). Smoking and carcinoma of the lung. Preliminary report. *Br Med J.* 2, 739.
25. Franklin, W.A. (2000). Diagnosis of lung cancer – pathology of invasive and preinvasive neoplasia. *Chest*. 117, 80S-89S.
26. Frederik, H.I., and Peter, H.K. (2002). Immune escape of tumors: apoptosis resistance and tumor counterattack. *Journal of Leukocyte Biology*. 71:907-920
27. Friedman, M., Mikhail, J.R., and Bhoola, K.D. (1965) Cushing's syndrome associated with carcinoma of the bronchus in a patient with normal plasma electrolytes. *BMJ*. 5426: 27-9

28. Gottlieb, T.M., and Oren, M. (1996). p53 in growth control and neoplasis, *Biochem. Biophys. Acta.* 1287, 77-102.

29. Gupta, A., and Raina, V.. (2010). Geftinib. *J Cancer Res Ther*. 6(3):249-54.

30. Higashiyama, M., Doi, O., Kodama, K., Yokouchi, H., Nakamori, S., and Tateishi, R. (1997). Bcl-2 oncoprotein in surgically resected non-small cell lung cancer: possibly favorable prognostic factor in association with low incidence of distant metastasis. *J Surg Oncol.* 64(1):48-54

31. Hainaut, P., and Pfeifer, G.P. (2001). Patterns of p53 G->T transversions in lung cancer reflected the primary mutagenic signature of DNA damage by tobacco smoke. *Carcinogenesis*. 22, 367-374.

32. Harris, C.C., and Hollstein, M. (1993). Clinical implications of the p53 tumour suppressor gene. *N Engl J Med*. 329: 1318-1327.

33. Harbour, J.W., Luo, R.X., Dei Santi, A., Postigo, A.A., Dean D.C. (1999). Cdk phosphorylation triggers sequential intramolecular interactions that progressively block Rb functions as cells move through G1. *Cell*. 17;98(6):859-69.

34. Harbour, J.W., Lai, S.L., Whang-Peng, J., Gazdar, A.F., Minna, J.D. and Kaye, F.J. (1988). Abnormalities in structure and expression pattern of retinoblastoma gene in human SCLC.

35. Hibi, K., Takahashi, T., Yamakawas, K., Ueda, R., Sekido, Y., Ariyoshi, Y., Suyama, M., Takagi, H., Nakamura, Y. and Takahashi, T. (1992). Three distinct regions involved ii 3p deletions human lung cancer. *Oncogene.* 7: 445-449.

36. Hockenbery, D.M. (2010). Targeting mitochondria for cancer therapy. *Environ Mol Mutagen.* 51(5):476-89.

37. Igney, F.GH. and Krammer, P.H. (2002). Death and anti-death: tumour resistance to apoptosis. *Nat Rev Cancer*. 2, 277-288.

38. Ihde, D.C. (1991). Non-small lung cancer: I. Biology, diagnosis and staging. *Curr Probl Cancer*. 15:65-103.

39. Israels, L.G., and Israels E.D. (1999). Apoptosis. *Stem Cells*. 17, 306-313.

40. Iwahashi, T., Koh, C.S., Inoue, A. and Yanagisawa, N. (1997). Tumor necrosis factor-alpha and transforming growth factor-beta production by isolated mononuclear cells from the spinal cords of Lewis rats with experimental autoimmune encephalomyelitis. *J. Exp. Med.* 183(2): 123-33

41. Jiang, S., Sato, Y., Kuwao, S., and Kameya, T. (1995). Expression of bcl-2 oncogene protein is prevalent in small cell lung carcinomas. *The Journal of Pathology*. 177 (2): 135 – 138

42. Johnson, B.E., and Kelley, M.J. (1993). Overview of genetic and molecular events in the pathogenesis of lung cancer. *Chest*. 103, 1S-3S.

43. Johnson, B.E., Russell, E., Simmons, A.M., Phelps, R., Steinberg, S.M., Ihde, D.C., Gazdar, A.F. (1996). Myc DNA amplification in 126 tumour cell lines from patients with small cell lung carcinoma. *J.Cell Biochem. Suppl*. 24, 210-217.

44. Joseph, B., Ekedahl, J., Sirzen, F., Lewensohn, R., and Zhivotovsky, B. (1999). Differences in Expression of pro-caspases in small cell and non-small cell lung carcinoma. *Biochem.Biophys. Res*. 262: 381-387

45. Kaiser, U., Hofmann, J., Schilli, M., Wegmann, B., Klotz, U., Wedel, S., Virmani, A.K., Wollmer, E., Branscheid, D., Gazdar, A.F., and Havemann, K. (1996).

Steroid-hormone receptors in cell lines and tumor biopsies of human lung cancer. *Int J Cancer*. 67(3):357-64

46. Kammouni, W., Ramakrishna, G., Sithanandam, G., Smith, G.T., Fornwald, L.W., Masuda, A., Takahashi, T. and Anderson, L.M. (2002). Increased K-Ras Protein and Activity in Mouse and Human Lung Epithelial Cells at Confluence. *Cell Growth & Differentiation.* 13: 441-448.
47. Kato, G.J., Barrett. J., Villa-Garcia, M., and Dang. C.V. (1990). An amino terminal c-myc domain required for neoplastic transformation activates transcription. *Molecular and Cellular Biology*. 10:5914-5920.
48. Kawasaki, M., Kuwano, K., Nakanishi, Y., Hagimoto, N., Takayama, K., Pei, X.H., Maeyama, T., Yoshimi, M., and Hara, N. (2000). Analysis of Fas and Fas ligand expression and function in lung cancer cell lines. *Eur J Cancer*. 36(5):656-63
49. Kerr, J.F., Wyllie, A.H., and Currie, A.R. (1972). Apoptosis: A basis biological phenomenon with wide- ranging implications in tissue genetics. *J Cancer* 26, 239-257.
50. Kiechle, F.L., and Zhang, X. (2002). Apoptosis: biochemical aspects and clinical implications. *Clin. Chem. Acta.* 326: 27-45
51. Kischkel, F.C., Lawrence, D.A., Chuntharapai, A., Schow, P., Kim, K.J. and Ashkenazi A. (2000). Apo2L/TRAIL-dependent recruitment of endogenous FADD and caspase-8 to death receptors 4 and 5. *Immunity.* 12(6):611-20.
52. Kischkel, F.C., Lawrence, D.A., Chuntharapai, A., Schow, P., Kim, K.J. and Ashkenazi A. (2000). Apo2L/TRAIL-dependent recruitment of endogenous FADD and caspase-8 to death receptors 4 and 5. *Immunity.* 12(6):611-20.

53. Kitaura, H., Nagata, N., Fujimura, Y., Hotokezaka, H., Yoshida, N. and Nakayama, K. (2002). Effect of IL-12 on TNF-alpha-mediated osteoclast formation in bone marrow cells: apoptosis mediated by Fas/Fas ligand interaction. *J. Immunology*. 169(9):4732-8

54. Kischkel, F.C., Hellbardt, S., Behrmann, I., Germer, M., Pawlita, M., Krammer, P.H., and Peter, M.E. (1995). Cytotoxicity-dependent APO-1 (Fas/CD95)-associated proteins form a death-inducing signaling complex (DISC) with the receptor. *EMBO J.* 14, 5579-5588.

55. Kiyohara, C., Otsu, A., Shirakawa, T., Fuduka, S., and Hopkin, J.M. (2002). Genetic polymorphisms and lung cancer susceptibility. *Lung cancer.* 37: 241-256.

56. Kohno, T and Yokota, J. (1999). How many tumour suppressor genes are involved in human lung carcinogenesis? *Carcinigenesis.* 20: 1403-4110.

57. Kroemer, G., Galluzzi, L., Vandenabeele, P., Abrams, J., Alnemri, E.S., Baehrecke, E.H., Blagosklonny, M.V., El-Deiry, W.S., and Golstein, P. (2009). Classification of cell death. *Cell Death Differ*. 16(1):3-11.

58. Lai, S.L., Perng, R.P., and Hwang, J. (2000). p53 gene status modulates the chemosensitivity of non-small cell lung cancer cells. *J. Biomed. Sci*. 7: 64-70.

59. Li, Z., Van Calcar, S., Qu, C., Cavenee, W.K., Zhang, M.Q., and Ren, B. (2003). A global transcriptional regulatory role for c-myc in Burkitt's lymphoma cells. PNAS. 100: 8164-8169.

60. Liddell, F.D. (2001). The interaction of asbestos and smoking in lung cancer. *The Annals Of Occupational Hygiene*. 45: 341-356.

61. Li-Feng, L., Chia-Hua, L., Li-Yen, S., Wei-Ling, L., Chih-Chao, L. and Kou-Wha, K. (2004). Action of solamargine on human lung cancer cells-enhancement of the susceptibility of cancer cells to TNFs. *FEBS Letters*. 577: 67-74.
62. Lockshin, R.A., and Zakeri, Z. (2001). Programmed cell death and apoptosis: origins of the theory. *Nat Rev Mol Cell Biol*. 2: 545-50.
63. Manna, S.K. and Aggarwal, B.B. (2000). All-trans-retinoic acid upregulates TNF receptors and potentiates TNF-induced activation of nuclear factor-kappaB, activated protein-1 and apoptosis in human lung cancer cells. *Oncogene*. 17: 2110-2119.
64. Mantovani, G., Maccio, A., Madeddu, C., Mura, L., Gramignano, G., Lusso, M.R., Massa, E., Mocci, M. and Serpe, R. (2003). Antioxidant agents are effective in lymphocyte progression through cell cycle in advanced cancer patients. *J. Mol. Med.* 81(10): 664-73.
65. Manuel, A. and Sergio, M. (1997). Regulation of Cdk/Cyclin complexes during the cell cycle. *Int. J. Biochem. Cell Biol*. 29: 559-573
66. Martin, S.J., Reuteliagsperge, C.P., cGahon, A.J., Rader, J.A., van Schie, R.C., Laface, D.M. and Green, D,R. (1995). Early redistribution of plasma membrane phosphatidylserine is a general feature of apoptotis regardless of the initiating stimulus: inhibition by overexpression of Bcl-2 and Ab1. *J Exp Med* 182: 1549-1556.
67. Mazuruk, M., Schoen, J., Chader, G.J., Iwata, T.,Rodrigues, I.R. (1996). Structural organization and chromosomal localization of the human ribosomal

protein L9 gene. *Biochimica et Biophysica Acta (BBA)- Gene structure and expression*. 1305: 151-162.

68. McCabe, M.L., and Dlamini, L. (2005). The molecular mechanisms of oesophageal cancer. *International immunopharmacology.* 7-8: 1113-30.
69. Mendelsohn, J., and Baselga, J. (2000). The EGF receptor family as a target for cancer therapy. *Oncogene*. 19: 6550-6565
70. Mountain, CF (1997). Revisions in the international system for staging lung cancer. *Chest.* 111:1710-1717
71. Morabia, A., and Wynder, E.L. (1992). Relation ob bronchiolalveolar carcinoma. *BMJ.* 304: 541-543.
72. Nachmias, B., Ashhab, Y. and Ben-Yehuda, D. (2004). The inhibitor of apoptosis protein family (IAPs): as emerging therapeutic target in cancer. *Semin Cancer Biol*. 14: 21-243.
73. Nagata, S. (1997). Apoptosis by death factor. *Cell*. 88: 355-365.
74. Nigg, E. (1995). Cyclin-dependent protein kinases. Key regulators of the eukaryotic cell cycle. *Bioessays*. 17: 147-480.
75. Nurse, P. (1994). Ordering the S phase and M phase in the cell cycle. *Cell.* 79: 547- 550
76. Ohmori, T., Podack, E.R., Nishio, K., Takahashi, M., Miyahara, Y., Takeda, Y., Kubota, N., Funayama, Y., Ogasawara, H., and Ohira, T. (2003). Apoptosis of lung cancer cells caused by some anti-cancer agents (MMC, CPT-11, ADM) is inhibited by bcl-2. *Biochem Biophys Res Commun*. 192(1):30-6

77. Omar, L., Moulay, A.M., and Thomas, W.R. (1999). TNM Staging of Lung Cancer. *Chest.* 115:233-235.

78. Parisi, T., Bronson, R., and Lees, J. (2008) Inhibition of Pituitary Tumors in Rb Mutant Chimeras through E2f4 Loss Reveals a Key Suppressive Role for the Prb|[Sol]| E2f Pathway in Urothelium and Ganglionic Carcinogenesis, *Oncogene*.

79. Parkin, D.M., Bray, F., Ferlay, J., Pisani, P. (2005). Global cancer statistics, 2002. *CA Cancer J Clin*. 55:74-108

80. Paul, A., Monach, S.C., Meredith, C.T., and Hans, S. (1991). A unigue tumour antigen produced by a single amino acid substitution. *Immunity*: 2: 45-59.

81. Richardson, G.E., and Johnson, B.E. (1993). The biology of lung cancer. *Semin. Oncol*. 20: 105-127.

82. Rusan, N., and Peifer, M. (2008) Original Cin: Reviewing Roles for Apc in Chromosome Instability, *The Journal of Cell Biology 181*, 719.

83. Salveses, G.S., Dixit, V.M. (1999). Caspase activation: The induced-proximity model. *Proc Natl Acad Sci*. 96: 10964-7.

84. Saelens, X., Pestjens, N., Vande Walle, L., van Gurp, M., van Loo, G. and Vandenabeele, P. (2004). Toxic protein released from mitochondria in cell death. *Oncogene* 23: 2861-2874.

85. Sherr, C.J. and McCormick, F. (2002). The Rb and p53 pathway in cancer. *Cancer Cell*. 2: 103-112

86. Sitas, F., Madhoo, J. and Wessie, J. (1998). Incidence of Histology Diagnosed Cancer in South Africa, 1993-1995. National Cancer Registry of South Africa, SA institude for Medical Research, South Africa.

87. Slebos, R.J., Hruban, R.H., Dalesio, O., Mooi, W.J., Offerhaus, G.J., and Rodenhuis, S. (1991). Relation between K-ras oncogene activation and smoking in adenocarcinoma of the human lung. *J. Natl. Cancer Inst.* 83: 1024-1027.

88. Sozzi, G., Sard, L., De Gregorio, L., Marchetti, A., Musso, K., Buttitta, F., Tornielli, S., Pellegrini, S., Veronese, M.L., Manenti, G., Incarbone, M., Chella, A., Angeletti, C.A., Pastorino, U., Huebner, K., Bevilaqua, G., Pilotti, S., Croce, C.M., and Pierotti, M.A. (1997). Association between cigarette smoking and FHIT gene alterations in lung cancer. *Cancer Res*. 57(11):2121-3

89. Tammemagi, M.C., McLaughlin, J.R., and Bull, S.B. (1999). Meta-analysis of p53 tumour suppressor gene alterations and clinocopathological features in resected lung cancers. *Cancer Epidemiol. Biomakers Pre*. 8: 625-634.

90. Tommasi, S., Pilato, B., Pinto, R., Monaco, A., Bruno, M., Campana, M., Digennaro, M., Schittulli, F., Lacalamita, R., and Paradiso, A. (2008) Molecular and in Silico Analysis of Brca1 and Brca2 Variants, *Mutation Research-Fundamental and Molecular Mechanisms of Mutagenesis*.

91. Van de Mark, K., Chen, J.S., Steliou, K., Perrine, S.P. and Faller, D.V. (2003). Alpha-lipoic acid induces p27Kip-dependent cell cycle arrest in non-transformed cell lines and apoptosis in tumor cell lines. *J Cell Physiol*. 194: 325-40.

92. Volm, M., and Rittgen,W. (2000). Cellular predictive factors for the drg response of lung cancer. *Anticancer research*. 20(5B): 3449-3458

93. Watabe, Y., Nazuka, N., Tezuka, M., and S, S. (2010) Aryl Hydrocarbon Receptor Functions as a Potent Coactivator of E2f1-Dependent Transcription Activity. *Biol Pharm Bull 33*, 389-3997

94. Weintraub, SJ., Chow, K.N., Luo, R.S., Zhang, S.H., He, S., and Dean, D.C. (1995). Mechanism of active transcriptional repression by the retinoblastoma protein. *Nature.* 29; 375(6534):812-5.

95. West, I.C. (2000). Radicals and oxidative stress in diabetes. *Diabetic Medicine.* 17, 171-180(10)

96. Whang-Peng, J., Kao-Shan, C.S., Lee, E.C., Bunn, P.A., Carney, D.N., Gazdar, A.F. and Minna, J.D. (1982). Specific chromosome defect associated with human small-cell lung cancer; deletion 3p(14-23). *Science*. 8: 215:181-2.

97. Williams, M.E and Sussex, I.M. (1995). Developmental regulation of ribosomal protein L16 genes in *Arabidopsis thaliana*. *The Plant J* 8: 65-76.

98. Wingo, P.A., Tong, T. and Bolden, S. (1995). Cancer statistics. *CA Cancer J Clin*. 45: 8-30.

99. Wynder, E.L. and Graham, E.A. (1950). Tobacco smoking as a possible etiologic factor in bronchogenic carcinoma. *J Am Med Assoc*. 143: 329-36

100. Xiao, B., Spencer, J., Clements, A., Ali-Khan, N., Mittnacht, S., Brocen~ o, C., Burghammer, M., Perrakis, A., Marmorstein, R., and Gamblin, S. (2003) Crystal Structure of the Retinoblastoma Tumor Suppressor Protein Bound to E2f and the Molecular Basis of Its Regulation, *Proceedings of the National Academy of Sciences 100*, 2363-2368.

101. Yasuno R. and Wada H. (2002). The biosynthetic pathway for lipoic acid is present in plastids and mitochondria in Arabidopsis thaliana. *FEBS letters.* 517(1): 110-114

102. Yanase, N., Hata, K., Shimo, K., Hayashida, M., Evers, B., and Mizuguchi, J. (2005). Requirement of c-jun NH2-terminal kinase activation in interferon-alpha-induced apoptosis through upregulation of tumor necrosis factor-related apoptosis-inducing ligand (TRAIL) in Daudi B lymphoma cells. *Exp. Cell. Res*. 310:10-21

103. Yuseke, K., Kohki, K., and Shigekazu, N. (2010). Interferon-induced TRAIL-independent cell death in DNAase II embryos. *Eur. J. Immunol*. 40:2590-2598.

104. Zhang, W., Li, J., Kanginakudru, S., Zhao, W., Yu, X., and Chen, J. J. (2010a) The Human Papillomavirus Type 58 E7 Oncoprotein Modulates Cell Cycle Regulatory Proteins and Abrogates Cell Cycle Checkpoints, *Virology 397*, 139-144.

Appendix 1: Reagents and Solutions

Tfb1	30nM KAc (Fluka Chemie GmbH, Sigma-Aldrich Chemie, GmbH, Steinheim, Switzerland) 50 mM $MnCL_2$ (Riedel-de-Haën, Sigma-Aldrich Laborchemikalie GmbH, Seelze) 10mM $CaCl_2$ (Riedel-de-Haën, Sigma-Aldrich Laborchemikalie GmbH, Seelze) 100mM $MnCl_2$ (Riedel-de-Haën, Sigma-Aldrich Laborchemikalie GmbH, Seelze) 15% (v/v) Glycerol (Merck Chemicals (Pty) Ltd, Gauteng, South Africa) Solution was sterilized by filtration
Tfb2	10 mM MOPS, pH 7.0 (Fluka Chemie GmbH, Sigma-Aldrich Chemie, GmbH, Steinheim, Switzerland) 75 mM $CaCl_2$ (Riedel-de-Haën, Sigma-Aldrich Laborchemikalie GmbH, Seelze)

	10 mM KCI (Riedel-de-Haën, Sigma-Aldrich Laborchemikalie GmbH, Seelze) 15 % (v/v) Glycerol (Merck Chemicals (Pty) Ltd, Gauteng, South Africa) Solution sterilized by filtration
TYM Broth	2.0 % Bacto-Tryptone (Merck Chemicals (Pty) Ltd, Gauteng, South Africa) 0.5 % Bacto-Yeast Extract (Merck Chemicals (Pty) Ltd, Gauteng, South Africa) 0.1 M NaCl (Merck Chemicals (Pty) Ltd, Gauteng, South Africa) 10 mM $MgCl_2$ (Merck Chemicals (Pty) Ltd, Gauteng, South Africa) pH to 7.0 with NaOH. Autoclave
1.0 M NaOH	Dissolve 36.9 g NaOH (Merck Chemicals (Pty) Ltd, Gauteng, South Africa) in 100 ml dH_2O
70 % Ethanol	70 ml 100 % Ethanol and make up 100 ml with dH_2O
0.1 % (v/v) DEPC H_2O	1 ml DEPC (Sigma-Aldrich Chemie GmbH, Steinheim, Switzerland) in 1 L dH_2O Shake a 37°C overnight and autoclave
	100 mM Tris

10 X Reaction Buffer, pH 8.3	500mM KCl
dNTP Mix	10 mM dATP 10 mM dCTP 10 mM dTTP 10 mM dGTP
Luria Broth	1 % Bacto-Tryptone (w/w) 0.5 % Bacto-Yeast Extract (w/w) 1 % NaCl (w/w) Bring to 1 litre with dH_2O
Agar plates	14g Nutrient Agar (w/w) 500 ml distilled water Boil to dissolve and autoclave Pour agar in Petri dishes, wrap in foil and store at 4°C
100 mg/ ml Ampicillin	Dissolve 0.1g Ampicillin (Roche Diagnostics GmbH, Mannehein, Germany) in 1 ml sdH_2O
100 µg/ L Ampicillin Agar Plates	Dissolve 50 µl 100 mg/ ml Ampicillin to slightly cooled Luria Agar and swirl to mix. Pour agar in Petri dishes and store at 4 °C
4 % PFA	Dissolve 2.5 g PFA (Merck Chemicals (Pty) Ltd, Gauteng, South Africa) in 25 ml 200 mM Phosphate Buffer by slow heating to 60 °C until solution becomes clear
200 mM Phosphate	4.3 g Disodium Hydrogen-Orthophosphate (Na_2HPO_4)

Buffer, pH 7.4	Anhydrous (Merck Chemicals (Pty) Ltd, Gauteng, South Africa) 3.1 g Sodium Dihydrogen Phosphate (NaH_2PO_4) (Riedel-de-Haën, Sigma-Aldrich Laborchemikalie GmbH, Seelze) Add 250 ml DEPC-treated H_2O and autoclave
0.1 M HCl	Dilute 10 ml 9M (32 % HCI (v/v) with 990 ml DEPC-treated H_2O)
10 X TBS	50 ml 1 M Tris, pH 7.5 30 ml 5 M NaCl Make up to 1 L with DEPC Treated H_2O
1 M Tris, pH 7.5	Dissolve 6.1 g Tris in 50 ml dH2O Adjust pH to 7.5 with 1 M HCl. Autoclave
5 M NaCl	Dissolve 73.05 g NaCl in 250 ml dH_2O. Autoclave
0.5 % Acetic Anhydride	Add 0.25 ml 100% Acetic Anhydride (v/v) (Merck Chemicals (Pty) Ltd, Gauteng, South Africa) to 5 ml 1 M Tris, pH 7.5 and make up to 50 ml with DEPC treated H_2O
20 X SSC	Dissolve 175.3 g NaCl, 88.2 g Tri-Sodium Citrate (Merck Chemicals (Pty) Ltd, Gauteng, South Africa) in 800 ml DEPC-treated H_2O. Adjust to pH 7.0 with 0.1 M HCl and make up to 1 L with DEPC-treated H_2O
40 % Dextran (v/v)	Add 40 g Dextran Sulphate Sodium Salt (Sigma-Aldrich,

	Germany) to 70 ml DEPC-treated H_2O. Dissolve by heating at 68 °C for 3-4 hours. Make up to 100 ml with DEPC-treated H_2O. Store at 4 °C
10 % SDS	Dissolve 10 g SDS (Roche Diagnostics, Germany) in 100 ml DEPC-treated H_2O
50 % Formamide	Add 12.5 ml Formamide to 12.5 ml DEPC-treated H_2O
0.8 % (w/v) agarose gel	Dissolve 0.8 g agarose in 100ml 1 X TBE buffer. Allow to cool to 50 °C and add 1 µl of 100 µl/ ml ethidium bromide. Allowed to set in a gel-casting tray
37 % (v/v) formaldehyde	Add 3.7 ml 100 % Formaldehyde (Riedel-de-Haën, Sigma Aldrich Laborchemikalien GmbH, Seelze) to 6.3 ml DEPC-treated H_2O
10 X TBE buffer	108 g Tris 55 g Boric acid 9.3 g EDTA (Saarchem Merck, Gauteng, South Africa) Dissolve and make final volume to 1l, adjust pH to 8.3
10 X TE buffer	12.11 g Tris-Cl (Sigma, Steinheim, Germany) 5.72 g EDTA (Saarchem Merck, Gauteng, South Africa) 700 ml distilled water Adjust pH to 7.5, make final volume to 1 l, autoclave
1 % (w/v) formaldehyde agarose gel	Dissolve 1 g agarose in 10 X MOPS and 84.6 ml DEPC-treated H_2O. Allow the gel to cool to 50 °C prior to addition of 5.4 ml 37

	% (v/v) formaldehyde and 4 µl of 100 µg/ml ethidium bromide
Formaldehyde Gel Loading Buffer	720 µl Formamide 160 µl 10 X MOPS Buffer 260 µl 37 % Formaldehyde (v/v) 100 µl DEPC-treated H_2O 10 mg/ ml Ethidium Bromide 80 µl Bromophenol Blue (Riedel-de-Haën, Sigma Aldrich Laborchemikalien GmbH, Seelze)
10 X MOPS	41.86 g MOPS 3.72 g EDTA 4.1 g Sodium Acetate Make up to 1 l with distilled water, wrap bottle in foil
4 M LiCl	Dissolve 8.478 g LiCl (Sigma Aldrich, Germany) in 50 ml sdH_2O.
TNB	2 ml Maleic Acid 2.5 ml Blocking buffer 45 ml 1 X TBS
10 X PBS	Dissolve in 800 ml of sdH_2O: 8 g NaCl 0.2 g KCl 1.44 g $Na_2HPO_4 \cdot 12H_2O$ and 0.24 g KH_2PO_4.

	Adjust the pH to 7.4 with HCl. Add sdH_2O to 1 L
0.5 M EDTA, pH 8.0	Dissolve 18.62 g EDTA (Merck Chemicals (Pty) Ltd, Gauteng, South Africa) in 50 ml sdH_2O. Adjust pH with 1 M NaOH until pH 8.0 and make up to 100 ml with DEPC H_2O
10 X Maleic Acid (Roche Diagnostics, Germany)	0.1 M Tris-HCl 0.15 M NaCl Adjust to pH 7.5 with NaOH
20 X TBS-Tween	5 ml Tween 20 (Sigma –Aldrich, Germany) to the final volume of 1L with 1 X TBS
1 X Blocking buffer	5 ml 10 X Maleic Acid 5 ml 10 X blocking buffer 40 ml Sterile distilled water
1 X Detection buffer	5 ml 10 X detection duffer 45 ml sterile distilled water